COOLING FAN AND SYSTEM PERFORMANCE AND EFFICIENCY IMPROVEMENTS

Final Report

Reporting Period Start Date: 06/01/2002
Reporting Period End Date: 07/31/2005

Authors:
Ronald Dupree (Caterpillar)

September 2005

DOE Award: DE-FC04-02AL68081

Caterpillar Inc
Technical Center Building E Div 852
PO Box 1875
Peoria, Illinois 61656-1875

COOLING FAN AND SYSTEM PERFORMANCE AND EFFICIENCY IMPROVEMENTS

Final Report

Abstract

Upcoming emissions regulations (Tiers 3, 4a and 4b) are imposing significantly higher heat loads on the cooling system than lesser regulated machines. This work was a suite of tasks aimed at reducing the parasitic losses of the cooling system, or improving the design process through six distinct tasks:

1. **Develop an axial fan that will provide more airflow, with less input power and less noise**. The initial plan was to use Genetic Algorithms to do an automated fan design, incorporating forward sweep for low noise. First and second generation concepts could not meet either performance or sound goals. An experienced turbomachinery designer, using a specialized CFD analysis program has taken over the design and has been able to demonstrate a 5% flow improvement (vs 10% goal) and 10% efficiency improvement (vs 10% goal) using blade twist only.
2. **Fan shroud developments, using an 'aeroshroud' concept developed at Michigan State University**. Performance testing at Michigan State University showed the design is capable of meeting the goal of a 10% increase in flow, but over a very narrow operating range of fan performance. The goal of 10% increase in fan efficiency was not met. Fan noise was reduced from 0 to 2dB, vs. a goal of 5dB at constant airflow. The narrow range of fan operating conditions affected by the aeroshroud makes this concept unattractive for further development at this time
3. **Improved axial fan system modeling is needed to accommodate the numbers of cooling systems to be redesigned to meet lower emissions requirements.** A CFD fan system modeling guide has been completed and transferred to design engineers. Current, uncontrolled modeling practices produce flow estimates in some cases within 5% of measured values, and in some cases within 25% of measured values. The techniques in the modeling guide reduced variability to the goal of $\pm$ 5% for the case under study.
4. **Demonstrate the performance and design versatility of a high performance fan.** A "swept blade mixed flow" fan was rapid prototyped from cast aluminum for a performance demonstration on a small construction machine. The fan was mounted directly in place of the conventional fan (relatively close to the engine). The goal was to provide equal airflow at constant fan speed, with 75% of the input power and 5 dB quieter than the conventional fan. The result was a significant loss in flow with the prototype due to its sensitivity to downstream blockage. This sensitivity to downstream blockage affects flow, efficiency, and noise all negatively, and further development was terminated.
5. **Develop a high efficiency variable speed fan drive to replace existing slipping clutch style fan drives.** The goal for this task was to provide a continuously variable speed fan drive with an efficiency of 95%+ at max speed, and losses no greater than at max speed as the fan speed would vary throughout its entire speed range. The process developed to quantify the fuel savings potential of a variable speed fan drive has produced a simple tool to predict the fuel savings of a variable speed drive, and has sparked significant interest in the use of variable speed fan drive for Tier 3 emissions compliant machines. The proposed dual ratio slipping clutch variable speed fan drive can provide a more

efficient system than a conventional single ratio slipping clutch fan drive, but could not meet the established performance goals of this task, so this task was halted in a gate review prior to the start of detailed design.

6. **Develop a cooling system air filtration device to allow the use of automotive style high performance heat exchangers currently in off road machines.** The goal of this task was to provide a radiator air filtration system that could allow high fin density, louvered radiators to operate in a find dust application with the same resistance to fouling as a current production off-road radiator design. Initial sensitivity testing demonstrated that fan speed has a significant impact on the fouling of radiator cores due to fine dusts, so machines equipped with continuously variable speed fan drives would be expected to have more radiator debris fouling problems than a machine with a constant speed fan. Filtration concepts looked at a wide range of filtration technologies, but the combination of pressure drop constraints and the small size of the debris to be filtered made this a futile exercise. The most successful technologies evaluated all incorporate some way to increase the Reynolds number inside the heat exchanger air flow path. A form of an "air knife" concept has emerged as the most promising technology to pursue.

Table of contents

Executive Summary

Task 1 - Develop an axial fan that will provide more airflow, with less input power and less noise. The initial plan was to use Genetic Algorithms to do an automated fan design, incorporating forward sweep for low noise. The Genetic Algorithms would control design variables that would be then be evaluated by a CFD program to predict the fan performance. The output of the CFD program would be reviewed by the GA software. The GA software would then revise one or more variables, and return the inputs to the CFD program. To make the plan work, a simplified CFD code was needed that could predict fan performance with a limited number of defined points on the blade surface. Two generations of fans were designed using GA's to optimize aerodynamic performance, and forward sweep to minimize noise. Neither generation of fan design was close to our needed performance, so the direction of design was changed to a more classical design method, using a full CFD design code, and fully identified fan surfaces. This design method has been able to demonstrate a 5% flow improvement (vs 10% goal) and 10% efficiency improvement (vs 10% goal) using a combination of blade twist an blade root treatment.

Task 2 – Develop for machine use, an 'aeroshroud' concept developed at Michigan State University. This concept utilizes the Coanda effect, injecting air around the entire circumference of the shroud along the blade tip/shroud interface. Performance development at Michigan State University showed the design is capable of meeting performance goals relative to flow, but over a very narrow operating range of fan performance. Fan noise was affected in the same region of fan performance as the flow. In the area where the shroud improved flow, the fan noise was reduced by 2dB at constant flow. This shroud concept is somewhat unique, in that it could significantly affect the performance of the fan at its stall point, but the narrow range of improvement makes this concept unattractive for further development at this time

Task 3 – Improve the axial fan system modeling process accuracy to accommodate the numbers of cooling systems to be redesigned to meet lower emissions requirements. Any engine developments to reduce emissions that result in an increase of heat rejection will generally require some form of cooling system redesign. CFD is one of the tools used by engineers to predict the performance of the redesigned cooling system. Current practice (in 2002) for CFD analyses resulted in cooling system airflow estimates from less than 5% to more than 25% deviation from measured values. To be successful in redesigning cooling systems, the CFD airflow analysis results must be consistently within 5% of the measured value. A cooling system mockup, that allowed low restriction, high restriction, and a side by side cooling system configuration to be evaluated, was constructed and evaluated at MSU's automotive cooling fan development facility, with detailed measurements of flow rate and localized flow measurements around the fan shroud area.

Task 4 - Demonstrate the performance and design versatility of a high performance fan. Lab test data showed that a Caterpillar designed SBMF fan match the flow and pressure capabilities of a typical conventional low noise axial fan at the same speed, but would require only approximately 80% of the input power, and would be approximately 6dB quieter. The designers of an off-road construction machine were utilized to design the SBMF fan installation to replace their existing fan, and a fan was rapid prototyped in cast aluminum for a back to back performance comparison against two commercially available axial fans. The result was that the SBMF fan provided only about 60% of the flow of the commercial fans at constant rpm, and was approximately 1dB louder at constant airflow. Lab testing was then conducted to determine the cause of the loss of flow. The fan was developed in a 'free outlet' system, where there is nothing to block the airflow coming from the fan. On the machine, the fan is located very near the front of the engine. Controlled lab tests confirmed that a conventional axial fan lost less than 5% of its airflow going from no engine behind the fan, to a simulated engine located close behind the fan. The SBMF fan lost 25% of its airflow during the same tests. The flow sensitivity to objects mounted close behind the fan make this concept unattractive for further development at this time.

Task 5 - Develop a high efficiency variable speed fan drive to replace existing slipping clutch style fan drives. This can provide both significant sound reductions and fuel savings versus a typical fixed speed ratio fan drive. A process, based on weather history from the Department of Energy, was developed to quantify the fuel savings potential of a variable speed fan drive. Potential fuel savings, based on methods developed as part of this task, showed fuel savings of 13% for a large off-road machine operating 24 hours/day in the Midwest U. S. with an engine load factor of 68%, and fuel savings of 14.4% for the dual ratio design (higher load factors naturally provided less fuel savings). The dual ratio concept was developed to the point of preparing for detailed component design, but was not pursued further due to the limited additional fuel savings available, and due to the need for a high pressure oil control source that would not be available on many stationary power applications.

Task 6 – Develop a cooling system air filtration device to allow the use of automotive style high performance heat exchangers currently in off road machines. Initial sensitivity testing demonstrated that fan speed has a significant impact on the fouling of radiator cores due to fine dusts, so machines equipped with continuously variable speed fan drives would be expected to have more radiator debris fouling problems than a machine with a constant speed fan. Filtration concepts looked at a wide range of filtration technologies, but the combination of pressure drop constraints and the small size of the debris to be filtered make filtration unpractical. The most successful technologies evaluated all incorporate some way to increase the Reynolds number inside the heat exchanger air flow path. A form of "air knife" concept has emerged as the most promising technology and will be pursued in further development.

Fuel savings

Potential fuel savings discussed at start of program

Overall assumptions-
The off-highway market is very diverse and covers a wide variety of markets, so a series of assumptions must be made:
Fan input power of a typical Tier 3 machine-

- A typical Tier 1 emissions legal, off-highway cooling fan requires 5% to 8% of the rated engine output power at rated fan speed. If we assume 6.5% to the fan, at 60% load factor, the fan consumes 11% of the total machine fuel consumption.
- A typical Tier 2 emissions legal off-highway cooling fan requires 8% to 12% of the rated engine output power at rated fan speed.
- Tier 3 engines are expected to have 20% higher jacket water heat rejection than their Tier 2 counterparts This would increase the cooling system heat load by 10%. If heat exchanger type and size, and allowable temperatures are kept constant, then the fan airflow (and speed) would have to increase by 15%. Fan input power is a cubic function of speed, so fan input power would increase by 1.15^3, or 52% above Tier 2. This would increase fan input power to 12% to 18% of engine rated output power. We will assume the fan input power, on the average increases to 15% of the engine output power.
- If the machine is operating at a load factor of 60%, the fan input power represents 25% of the total fuel consumed by the machine

Task 1 goal - Reduce fan power consumption by 10% at constant flow in a typical cooling system.
Task 2 goal – Reduce fan power consumption by 10% at constant flow in a typical cooling system.
Task 3 goal – This task impacts the development time required to put a new machine into production. This would have a very small impact on total U. S. fuel consumption.
Task 4 goal – Provide the same air flow and pressure rise at less than 75% of the input power required for a conventional fan design.
Task 5 goal – The fan should be at least 95% efficient at maximum drive ratio. As the fan speed varies over its entire operating speed range, the clutch power transmission losses should not exceed 5% of rated input power.
Task 6 goal – A 10% improvement in heat exchanger performance at constant fan input power would allow a tier 3 machine to be cooled at the same cooling system fuel consumption as a Tier 2 machine.

Demonstrated fuel savings

Overall assumptions-

A review of actual machine designs for tier 3 emissions configurations shows that combinations of engine developments, and heat exchanger performance improvements have been able to provide acceptable cooling with Tier 2 emissions legal fan input power, so the overall assumptions can be rewritten as follows-

Fan input power of a typical Tier 3 machine-

- A typical Tier 1 emissions legal, off-highway cooling fan requires 5% to 8% of the rated engine output power at rated fan speed. If we assume 6.5% to the fan, at 60% load factor, the fan consumes 11% of the total machine fuel consumption.
- A typical Tier 2 or Tier 3 emissions legal off-highway cooling fan requires 8% to 12% of the rated engine output power at rated fan speed.
- If the machine is operating at a load factor of 60%, and the fan input power represents 12% of rated power, the fan represents 20% of the total fuel consumed by the machine.

Task 1 demonstrated - Reduce fan power consumption by 5% at constant flow in a typical cooling system. This should equate to a 1.7% machine fuel consumption reduction.
Task 2 demonstrated – No reduction in fan power consumption.
Task 3 – This task impacts the development time required to put a new machine into production. This would have a very small impact on total U. S. fuel consumption.
Task 4 demonstrated – In an unobstructed system, the same air flow and pressure rise was provided at less than 75% of the input power required for a conventional fan design. The development was stopped due to performance losses with a significant downstream obstruction. If this technology could be used on machines without significant downstream restrictions, the fuel savings would be 5% of the machine total fuel consumption.
Task 5 demonstrated – Peak losses will not be significantly different than with a single ratio clutch. Machine fuel consumption savings prediction for machine operating in Midwest (Peoria, Il.) would be 5.9% for single ratio clutch vs. fixed ratio, and 6.7% for dual ratio slipping clutch vs. fixed ratio fan.
Task 6 goal – A 10% improvement in heat exchanger performance at constant fan input power would provide cooling equivalent to a 15% fan speed increase, or a 50% fan input power increase. This would be an avoidance of a 10% machine fuel consumption increase.

Fuel consumption estimates from Oak Ridge National Labs[1]

PROJECTED OFF-HIGHWAY FUEL USE IN 2005
Using the growth rate from 1997 to 2001, by sector and fuel type, a projection was calculated for the year 2005 which indicates that the total fuel use off-highway will be almost 20.5 billion gallons. The results of the projection are shown in the following table:

Projection of off-highway fuel consumption in the year 2005 (millions of gallons)

Sector	Gasoline	Diesel	Other	Total
Agriculture	357	3,753	4	4,114
Industrial-commercial	1,705	2,039	2,398	6,143
Construction	259	5,998	21	6,278
Personal-recreational	3,626	47	7	3,680
Other	2	76	3	81
Totals	5,949	11,914	2,433	20,296

The total fuel consumption for all off-road applications in 2005 was projected to be 20,296 million gallons or 76.8 billion liters. The following technologies are all additive, with the exception of task 5. In other words, fan blading improvements could be combined with fan shroud improvements for a total reduction of losses from baseline of 20%, vs. the individual gains of 10% each.

Demonstrated Potential Fuel Consumption Savings
Fuel Consumption Due to Cooling System Changes Only

Technology	Machine Annual Fuel Consumption Change from Baseline	% Total fuel consumption to cooling system	Fuel consumed by cooling system Billions of liters	Fuel savings Billions of liters
Tier 3 system, belt drive fan (no technology)-baseline	Baseline	20%	15.4	Baseline
Task 1 fan blading improvements	-1.7%	18.7%	14.1	1.3
Task 4 high performance fan	-5%	15.9%	11.6	3.8
Task 5 fan clutch (high performance technology)	-6.7%	13.6%	10.3	5.1
Task 6 radiator air filtration	10% fuel consumption increase aviodance	27.3%	23.0	7.6

Combining fuel savings of the individual tasks

Two tasks were devoted to fan developments, Task 1 was aimed at larger diameter fans (>1 meter in diameter) and Task 4 was aimed at smaller diameter fans (<0.75 meter diameter). The results from these two tasks cannot be added. The fuel savings value of the fan in Task 4 is much higher than the value of the more conventional fan design of Task 1.

The value of fan improvements (Task 1 and 4) cannot be directly added to the fan clutch (Task 5), since the fan clutch is saving fuel by running the fan at reduced speeds.

The fuel savings potential of the radiator air filtration (Task 6) should be additive to the fuel savings potential of EITHER the fan developments (Task 1 or Task 4) OR the fan clutch (Task 5).

Maximum combined fuel savings should be based on the combination of the dual ratio fan clutch (Task 5) and radiator filtration (Task 6). The combined fuel savings of the two technologies could represent a combined fuel savings and fuel consumption avoidance of 12.7 billion liters, for a cumulative fuel savings of the two technologies of 15% of the total fuel consumed in off-road applications. This represents a 'best case' scenario, where all machines are initially equipped with a belt driven constant ratio cooling fan, and no machines are currently able to take advantage of high performance, louvered fin radiator cores due to dust plugging problems.

Experimental

Task 1- **Fan performance data** was acquired using ANSI/AMCA Standard 210-99, "Laboratory Methods Of Testing Fans for Aerodynamic Performance Rating", using figure 11 'Outlet Chamber Setup-Nozzle on End of Chamber'. In place of the nozzle, a laminar flow element may be used, depending on the test location.
Fan sound data was acquired by constructing a mockup cooling system with variable restriction, then testing using the methods outlined in European Union Directive 2000/14/EC to measure the fan sound power.

Task 2 – **Fan performance data** was acquired at MSU as described in SAE technical paper 971784 'The Automotive Cooling Fan Research and Development Facility" by S. C. Morris, Michigan State Univ., J. F. Foss Michigan State Univ., and J. E. Pakkala Capital Machine Design
Fan performance and sound data at Caterpillar was acquired using the same methods as Task 1

Task 3 – **Fan performance data** was acquired at MSU as described in SAE technical paper 2001-01-1701 "Evaluating CFD Models of Axial Fans by Comparisons with Phase-Averaged Experimental Data" by J. Foss and D. Neal Michigan State University and M. Henner and S. Moreau Valeo Motors and Actuators

Task 4 – **Fan performance and sound data** was acquired using the same methods as Task 1

Task 6 – **Radiator debris fouling** test methods were developed from the methods described in SAE technical paper 80102 "Airside Fouling of Internal Combustion Engine Radiators" by T. Cowell and D. A. Cross of COVRAD, Ltd. with some significant modifications. The fouling media (dust) in both cases was intended to duplicate 'air cleaner test dust' as described in either BS1701 or the fine grade of test dust as described in SAE standard J726. In both cases, commercially available products were used that matches the size range of the air cleaner test dust, but is much less expensive. In the case of this testing, US Silica's SilCoSil 53 fine ground silica sand was used. The US silica product size distribution is shown below:

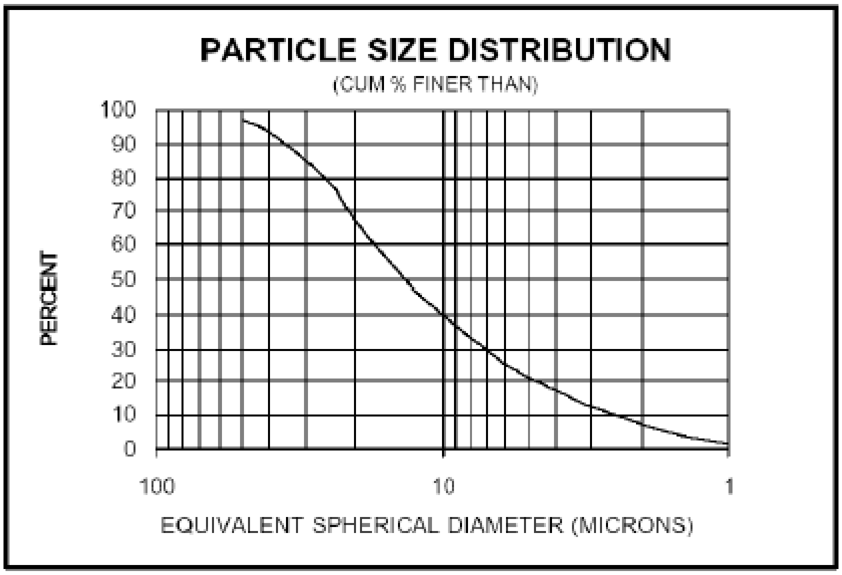

Versus the size distribution for the SAE fine air cleaner test dust:

Size µm	Maximum Volume Fraction A2 Fine
1	2.5 to 3.5
2	10.5 to 12.5
3	18.5 to 22.0
4	25.5 to 29.5
5	31 to 36
7	41 to 46
10	51 to 54
20	70 to 74
40	88 to 91
80	99.5 to 100
120	100
>120	none

Since the test dust was finely ground silica, the operator was specially trained, appropriate respiration protection was provided, and the test facility was equipped with special filtration equipment to control the silica dust.

The COVRAD test facility was designed as a single pass test:

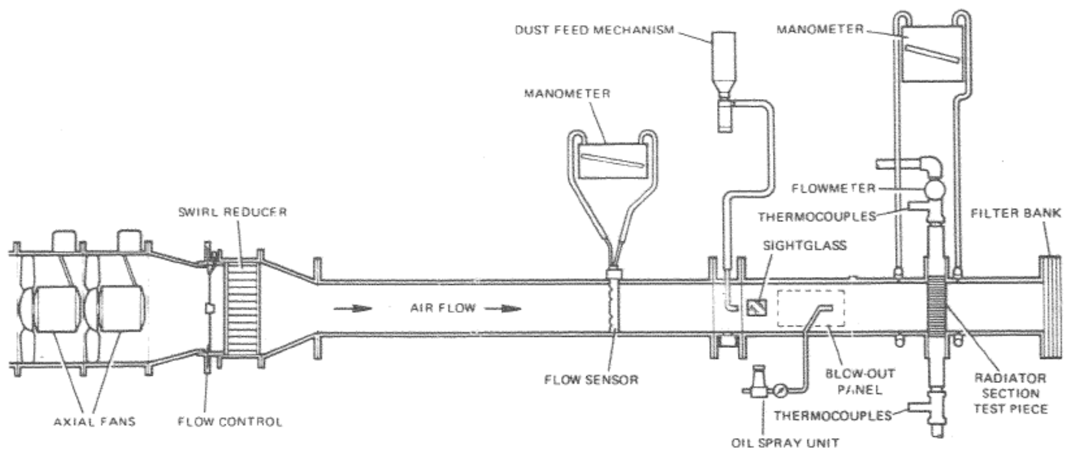

The Caterpillar facility was built as a multi-pass test facility, capable of keeping the fine debris particles in suspension:

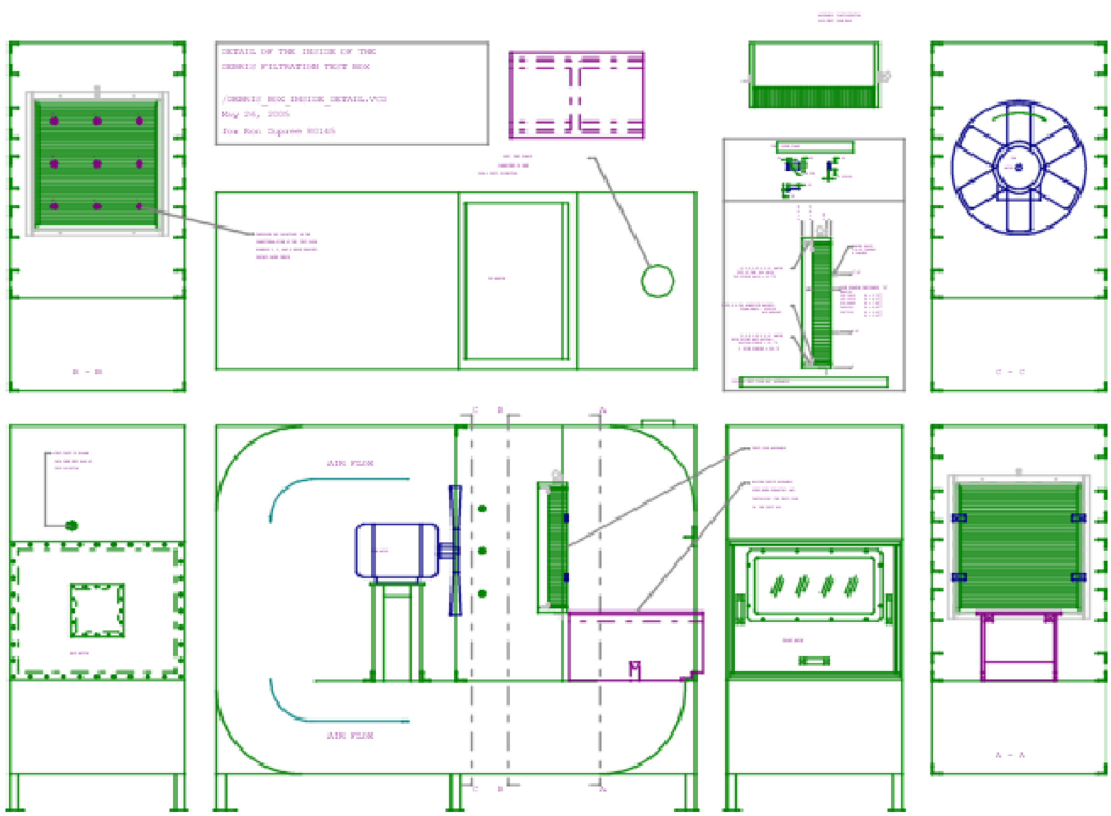

Part of the test procedure was to determine an appropriate fan speed and debris feed rate on a baseline core, before testing a candidate core. Fouling was observed with a combination of pressure drop measurements, as well as photographs, but it was found that photos taken at regular intervals provided some of the best documentation of the fouling of a given core. Fouling testing was done by injecting dust at a constant rate while monitoring core air side pressure drop, and documenting fouling with photographs. Once established, the fan speed and dust injection rate were maintained constant throughout the tests. Once tested, a radiator could be reused by thoroughly washing with a pressure washer, then completely drying before installing in the test facility for evaluation.

Results and Discussion

Task 1 - Develop an axial fan that will provide more airflow, with less input power and less noise

Detailed task goals and development plan- Fan design is an art of tradeoffs. It is virtually impossible to design a new fan that will have improved performance at all operating conditions than state of the art designs, but it is possible to design a fan that optimizes its performance over a portion of the fan operating range. Based on expectations of future cooling system development, the range of fan specific diameters from 1.5 to 1.8 was deemed to be the range of interest for future fan developments. The baseline fan for performance comparison is a sheet metal design, 711mm od, with 6 blades at a chord angle of 26°, operating in a knife edge shroud with 8 mm radial tip clearance.

Initial development methods-

Genetic algorithms have been successfully used in many applications that have multiple variables. The GA's can very successfully find a global optimum IF the GA can be tied to an automatic solver, so that as the GA generates a new design based on the knowledge it has captured, the new input data can be sent to the solver for another iteration. This places some restrictions on the way the problem is handled, for example: the solver and the GA program must be able to 'talk' together without a human interface, and a large number of potential solutions must be evaluated as we seek the global optimum solution. These constraints meant that we needed to use a simplified CFD analysis tool to determine the performance of the design, and the blade surface design needed to be based on a limited number of points in space. To simplify the problem, the fan would derive its low noise characteristics from the use of a pre-determined leading edge profile, and the shape of the blade surface would be determined by the location of six points in space. Once an optimum blade was designed by this process, a prototype would be built to measure the flow, power, and noise before using classical CFD design tools to further refine the design.

Initial results –

The GA solution method provided the fan design as shown in this photo:

The first generation design did not meet design goals, so a revised second generation fan was designed and built using the same methods. This second generation design had better performance than the initial design, but still did not meet the performance goals for flow, efficiency, or noise levels as shown in this comparison:

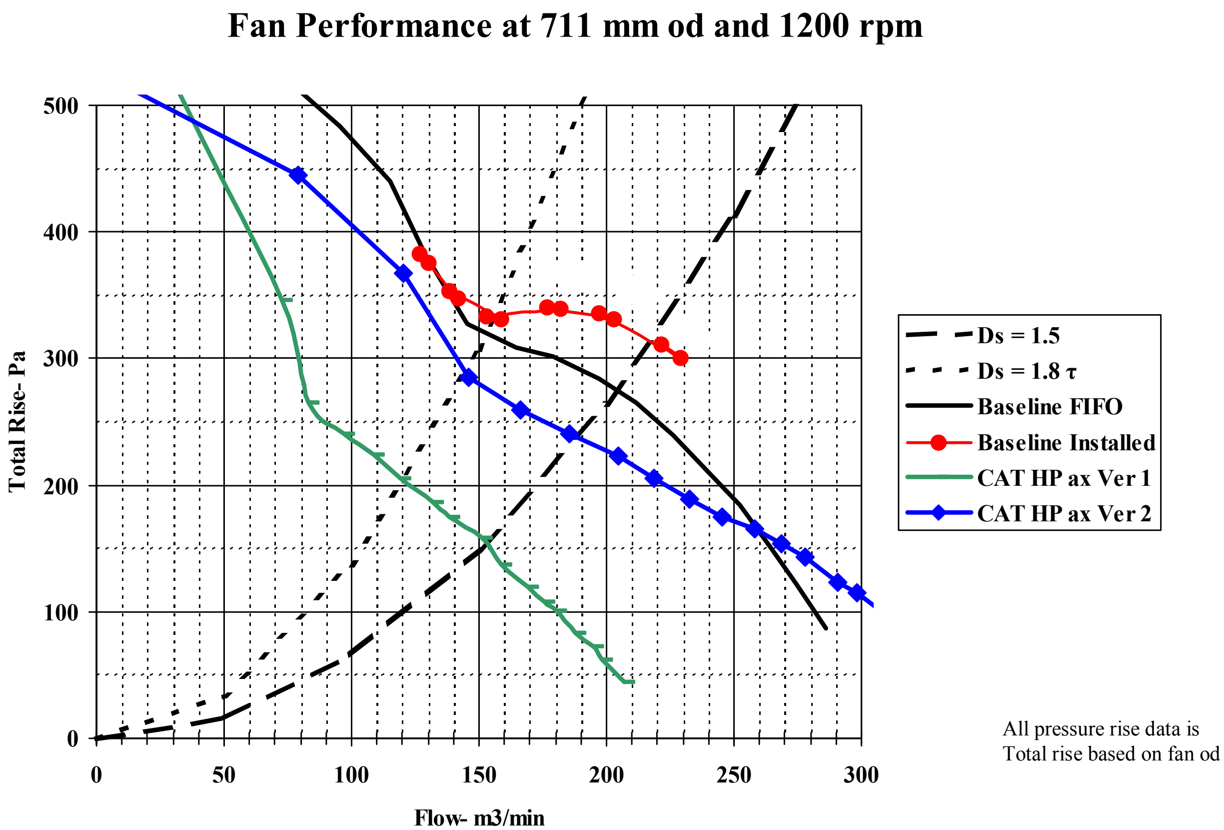

In addition, the prototype fan noise at constant rpm was no lower with the high performance design than the baseline fan, so that at constant airflow in a given system, the noise level of the high performance design was significantly louder than the baseline design.

Based on the demonstrated performance of the Genetic Algorithm designed fans, work was halted on this method, and a more conventional methodology was used to generate a third generation fan design.

Later design method-

The third generation fan was designed using 'conventional' CFD analysis techniques, guided by the experiences of an experienced CFD analyst, using commercial codes. Analysis was completed on the third generation fan, as shown in this drawing:

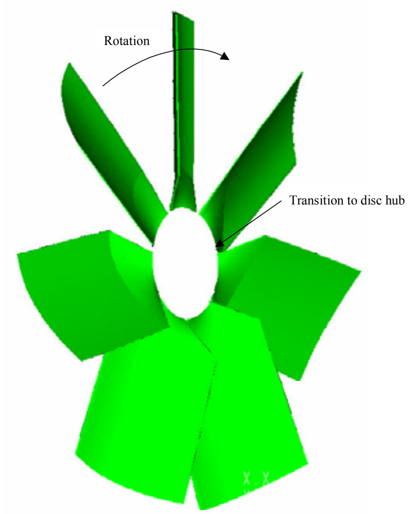

With the following predicted performance-

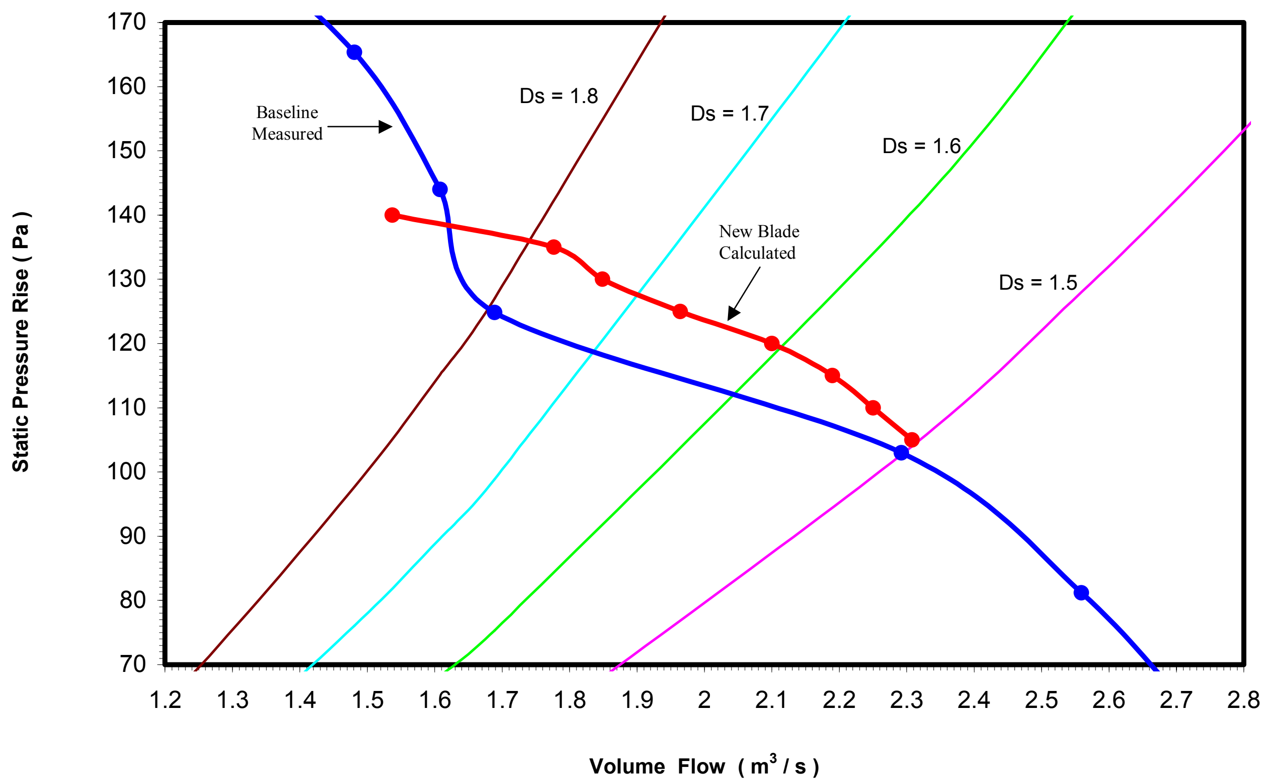

And predicted efficiency-

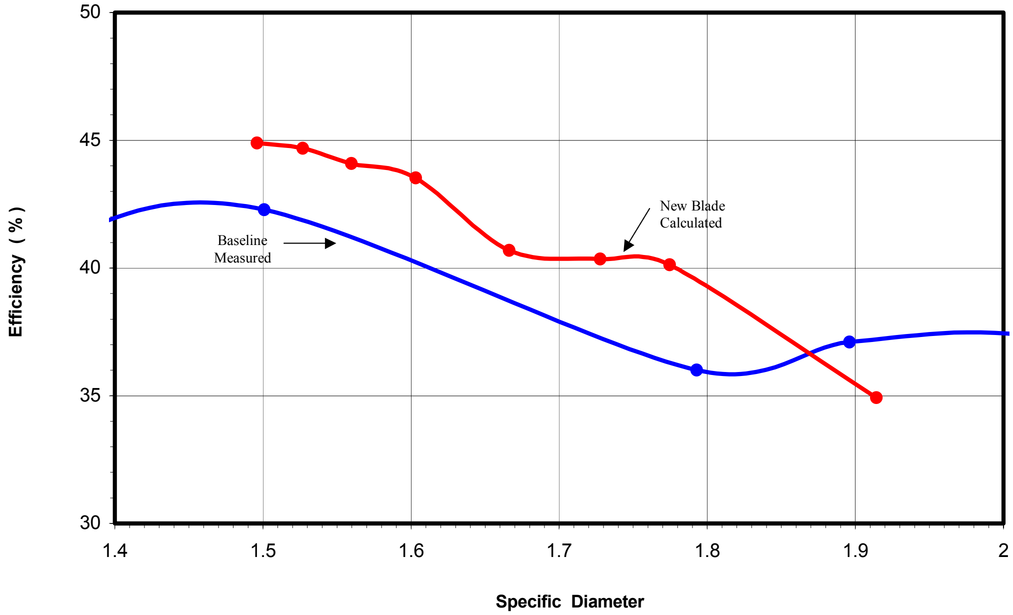

This data (all with knife edge fan shrouds) implies a 4% flow increase and an 8% input power reduction. Time constraints did not allow a prototype to be built and tested to validate these results within this project. A prototype fan was constructed, however, and evaluated with a demonstrated flow increase of 14%, and a power reduction of 21% from our baseline. The prototype fan was equipped with a venturi shroud for these evaluations, vs. a knife edge shroud for the baseline fan.

Six vs. seven blades value for sound reduction-

The baseline fan has six blades, but the prototype fan of the same diameter uses seven blades. New machine designs often have side by side cooling systems, with a lower restriction radiator mounted in parallel with a higher restriction radiator. Will a system with a side by side cooling configuration, and an even number of blades in the fan be inherently louder than a system with an odd number? To answer the question, a fan supplier provided three different fans for evaluation, each designed to provide the same airflow at the same speed. Fan 1 had six blades, fan 2 had seven blades evenly spaced, and fan 3 had seven blades with unequal spacing as shown on the photo below-

The sound was measured at two speeds in a cooling system mockup with the following results-

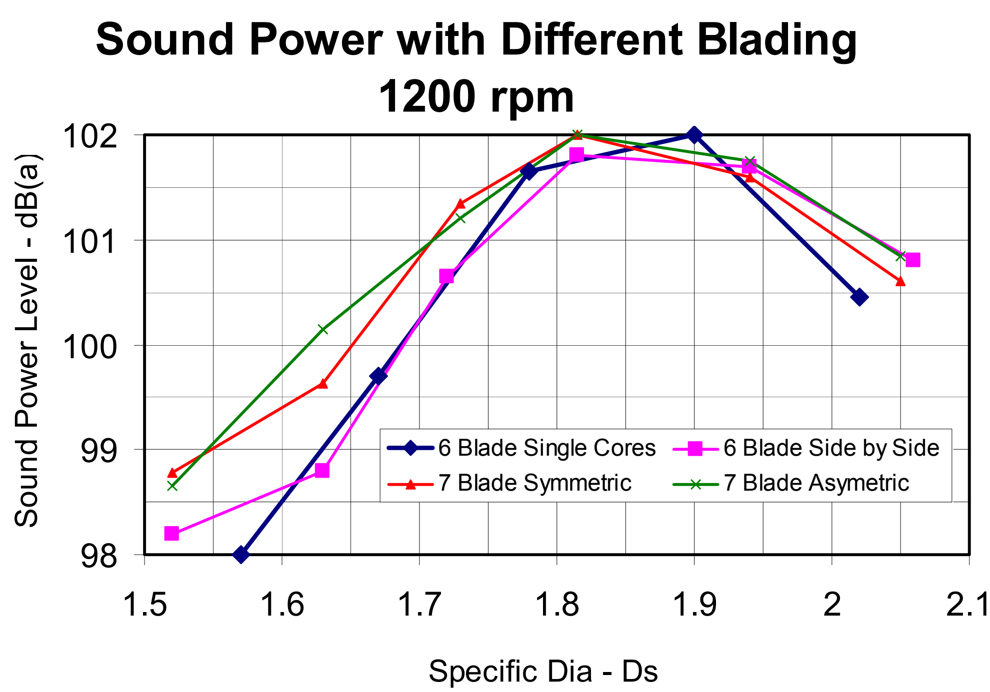

The quietest fan, by 1 to 2dB(a) was the six blade fan vs. either of the seven blade designs. The presence of a full across radiator, or a split radiator with a significant difference in the restriction between the two sides had no effect on the noise level of the six blade fan. One aspect that was noted during the testing was that the seven blade asymmetric fan design produced a pronounced low frequency rumbling sound, which was much more objectionable to the listener, even though the noise level was the same as the symmetric fan designs.

Task 2 – Develop for machine use, an 'aeroshroud' concept developed at Michigan State University

Background of aeroshroud concept

The original development of the aerodynamic shroud was motivated by the relatively large tip clearance of cooling fans in light and medium duty trucks. The large tip clearance is necessary because of the large relative motions between the engine mounted cooling fan and the chassis mounted shroud and radiator[2] (Morris 1997). Morris was the first to investigate the efficacy of the aerodynamic shroud on an automotive cooling fan with a diameter of 457 mm and a tip clearance of 25 mm. Integral flow measurements such as fan input power and volume flow rate were acquired in addition detailed velocity measurements in the wake of the fan. These data demonstrated that the aerodynamic shroud increased performance at higher flow rates but decreased performance at lower flow rates. Because of this result, it was concluded that system resistance, characterized by the fan grill, radiator, and air-conditioning condenser in an automobile, plays an important role in determining the efficiency of the aerodynamic shroud and fan combination. In particular, a large system resistance lessens the efficiency and a smaller system resistance allows the aerodynamic shroud to increase the efficiency of the fan. Furthermore, qualitative observations using a tuft in the wake of the fan showed that the high momentum annular jet changed the reverse flow in the tip clearance area to a positive axial flow providing an additional contribution to the net flow rate through the fan.

In the original investigation by Morris (1997), the cooling fan was partially immersed in the shroud. In particular, the shroud covered only the upper portion of the fan blades and had a sharp edge outlet. The partially shrouded configuration allowed the fan to produce static pressures even throughout the stall range, which is characterized by strong radial flow. However, when the aerodynamic shroud was used, it forced the flow in an axial direction explaining the decrease in performance at the lower flow rates. In a later study[3] (Morris and Foss, 2001), the authors used a rounded outlet that accommodated this radial flow and found that the enhanced performance of the fan with the aerodynamic shroud was extended into even lower flow rates.

Aeroshroud concept evaluation

This is the design of aeroshroud as presented by Morris and Foss:

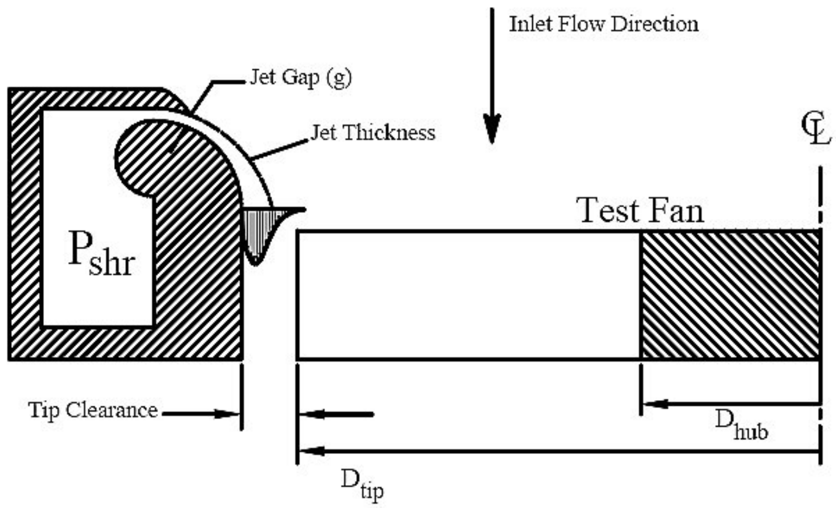

The shroud, on the left side of the picture, is a pressure vessel that contains air pressurized by an external source. The air escapes via a Jet Gap that extends 360 degrees around the shroud. The escaping air remains attached to the surface of the shroud due to the Coanda effect, to provide the performance benefits of the shroud.

The shroud built for this evaluation followed utilized a rounded inlet/rounded outlet as shown below:

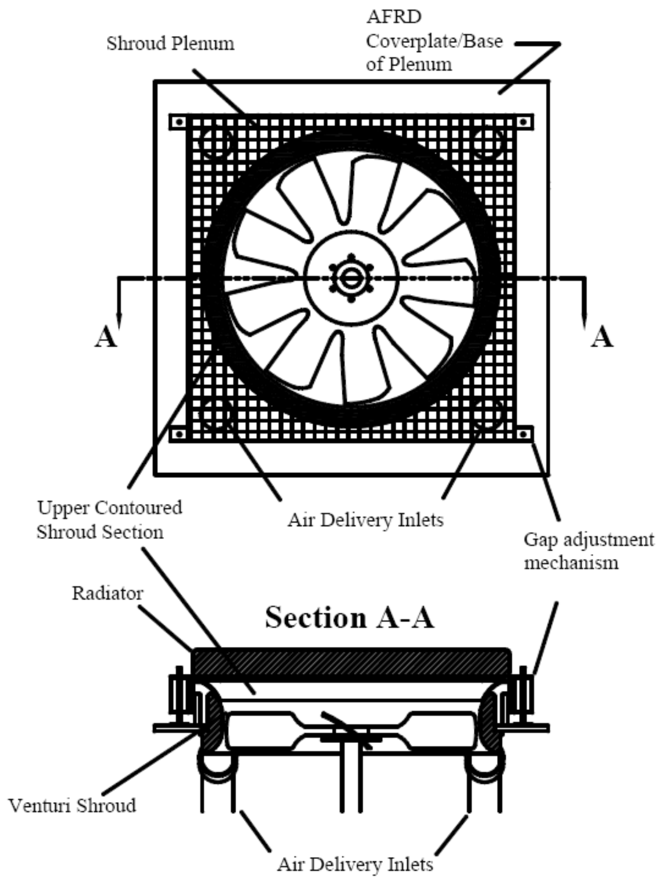

There was a concern about the interaction of the fan and shroud, so a fan was chosen that was thought to most nearly represent a potential high performance axial fan that might be designed as part of task 1:

The following chart captures the performance of the fan as a function of flow through the aeroshroud, where fl represents the flow through the shroud (as indicated by internal shroud pressure. Higher pressure means higher shroud air flow).[9] Ds, of 1.5 to 1.8 represents the range of system restriction of interest for this project.

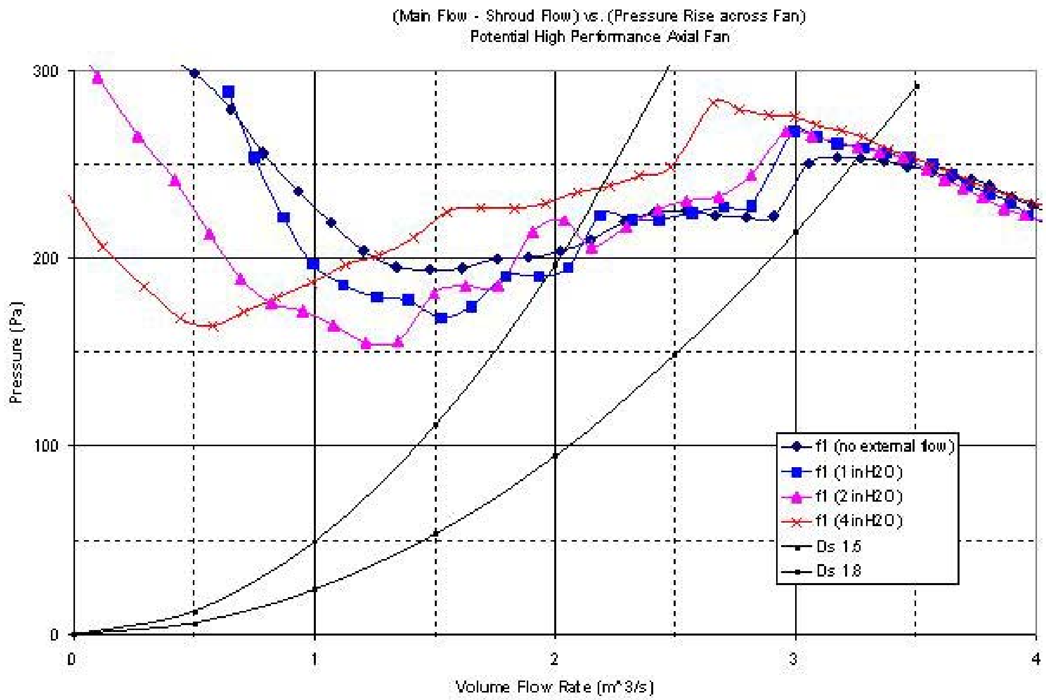

These results show that the amount of shroud air flow can significantly change the stall point of the fan, but had no effect on the performance of the fan in the axial region. To compare with earlier Michigan State University claims, we were able to demonstrate significant fan performance benefits in *low* flow conditions, but saw no performance benefits in *high* air flow conditions.

System efficiency was also a significant concern for these tests, so the following plot compares the total efficiency of the system (input power of the fan plus the auxiliary fan powering the aeroshroud) for different shroud pressurization levels. First, under the assumption that the airflow required for the shroud could be provided with a delivery system operating at 100% efficiency:

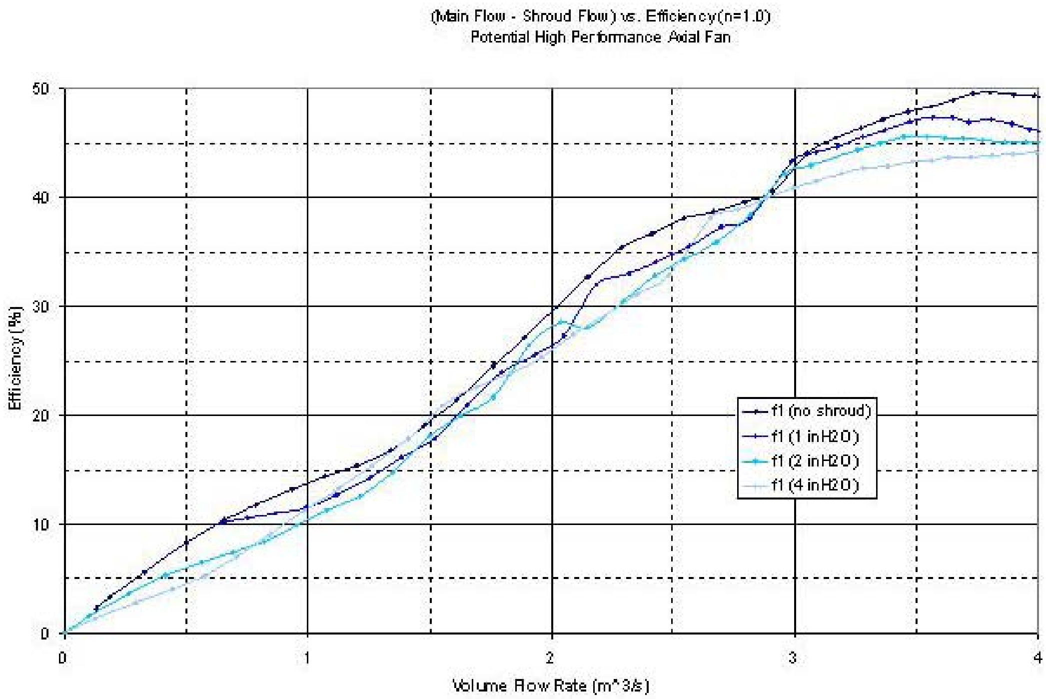

And second, at a more realistic 70% efficient fan/motor system:

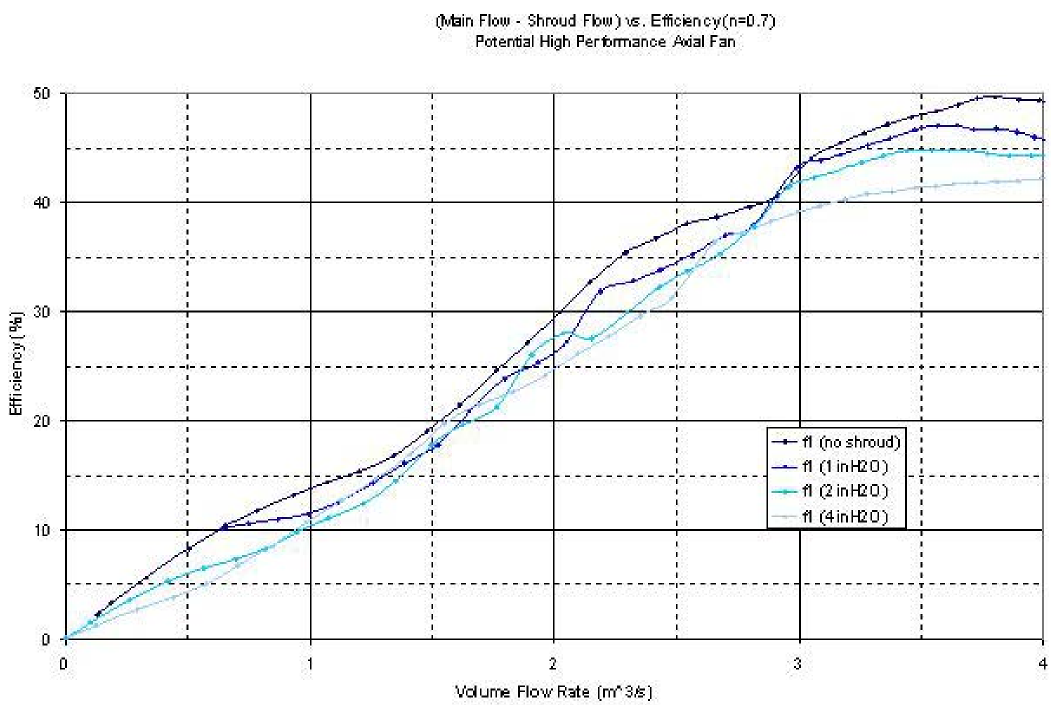

A more detailed look at the area of flow interest, assuming a 70% efficient fan shows this:

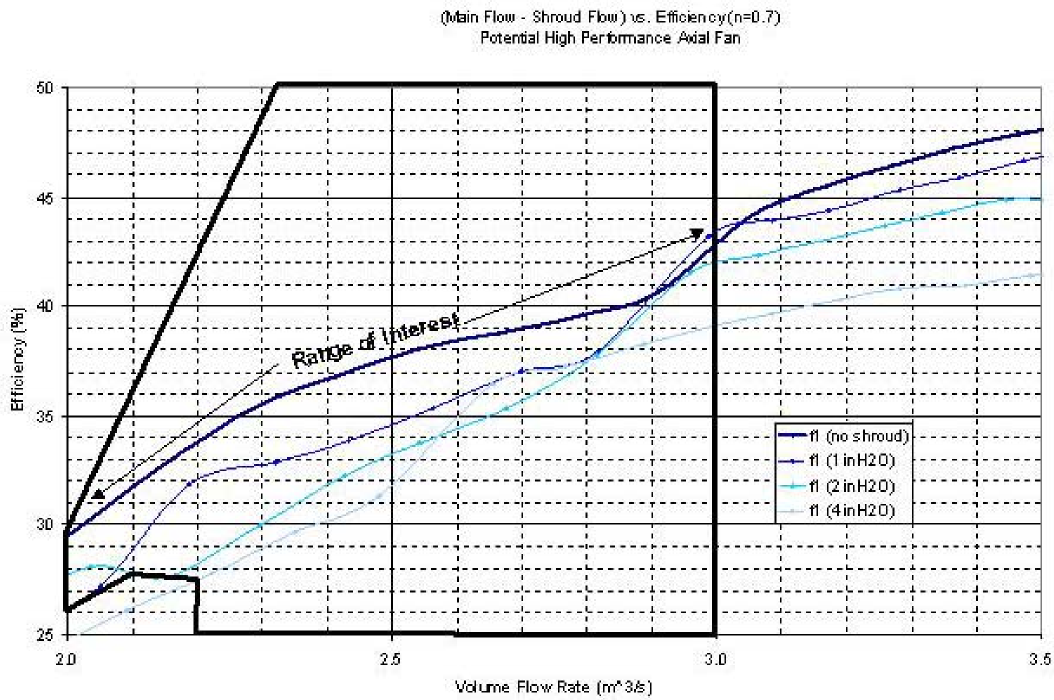

At this point, we had demonstrated that the aeroshroud could dramatically change the fan stall point and provide higher flows at operating points where the fan would traditionally be in stall, but we could not affect fan performance in higher flow lower restriction region of fan performance, and the aeroshroud was providing no efficiency benefits. Instead of proceeding to a field test of the system, the lab testing was continued with two different fans to study the fan/shroud interaction to determine if there was a better fan to use with the aeroshroud concept.

Aeroshroud performance with different fans

To insure that the performance of the aeroshroud was not a fluke due to the chosen prototype fan, two sheet metal fans were provided for evaluation:

Fan 2 was a low chord angle design

Fan 3 was a high chord angle design, to explore the potential range of conventional fans that might be available for use with the aeroshroud.
The results for fan 2 were similar to the initial fan:

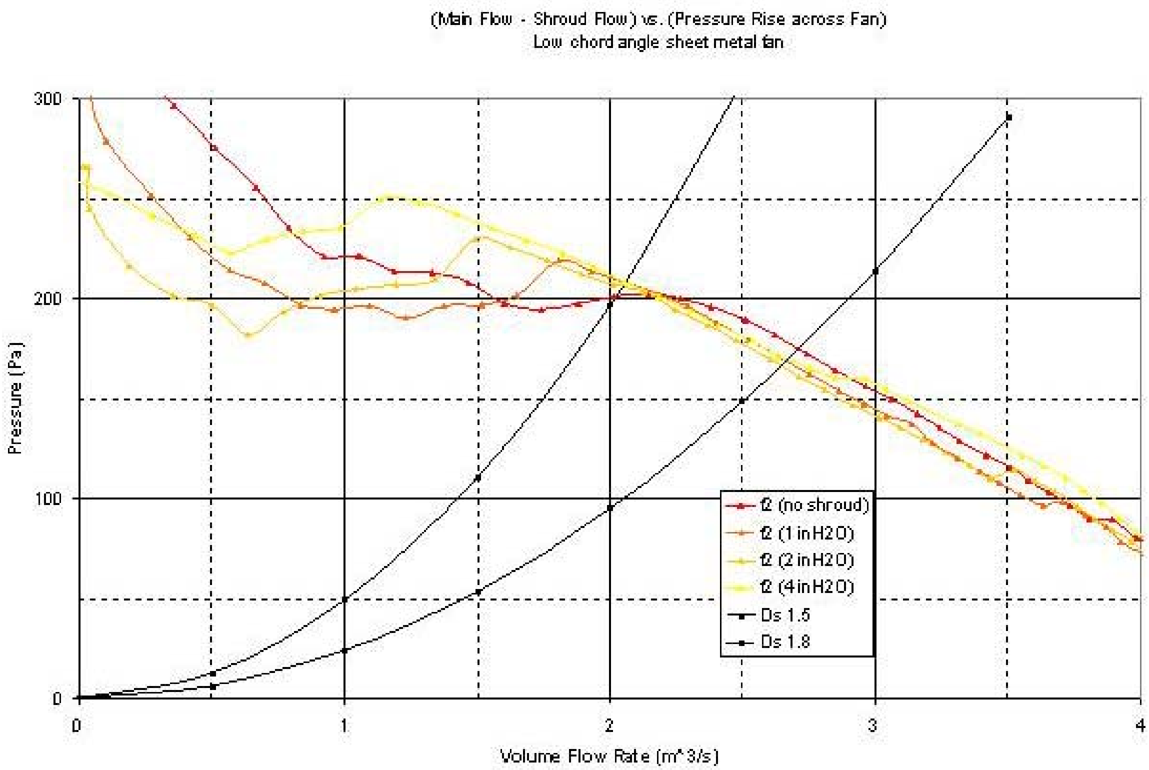

As well as the results for fan 3:

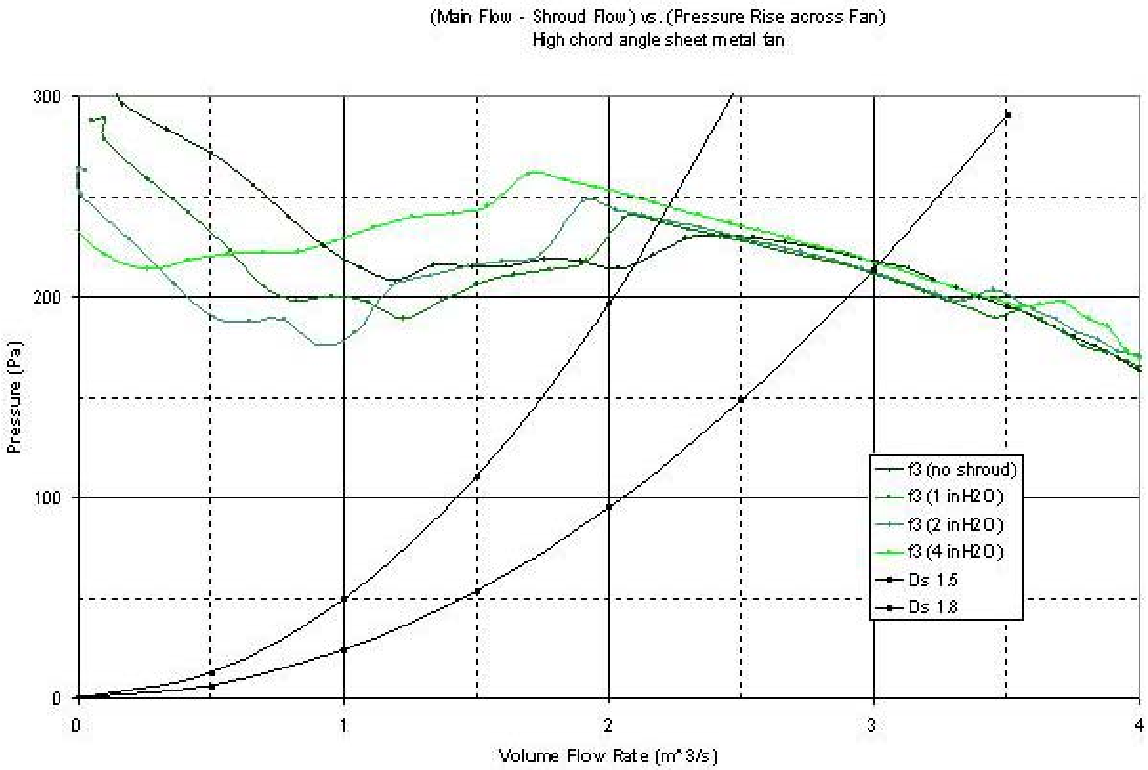

Michigan State University does not have noise measurement capabilities at their facility, so the aeroshroud system was delivered to Caterpillar for noise evaluation. The aeroshroud was mounted on a cooling system mockup as shown below for evaluation:

With the following specific noise test results measured with fan 3, at 950 fan rpm.

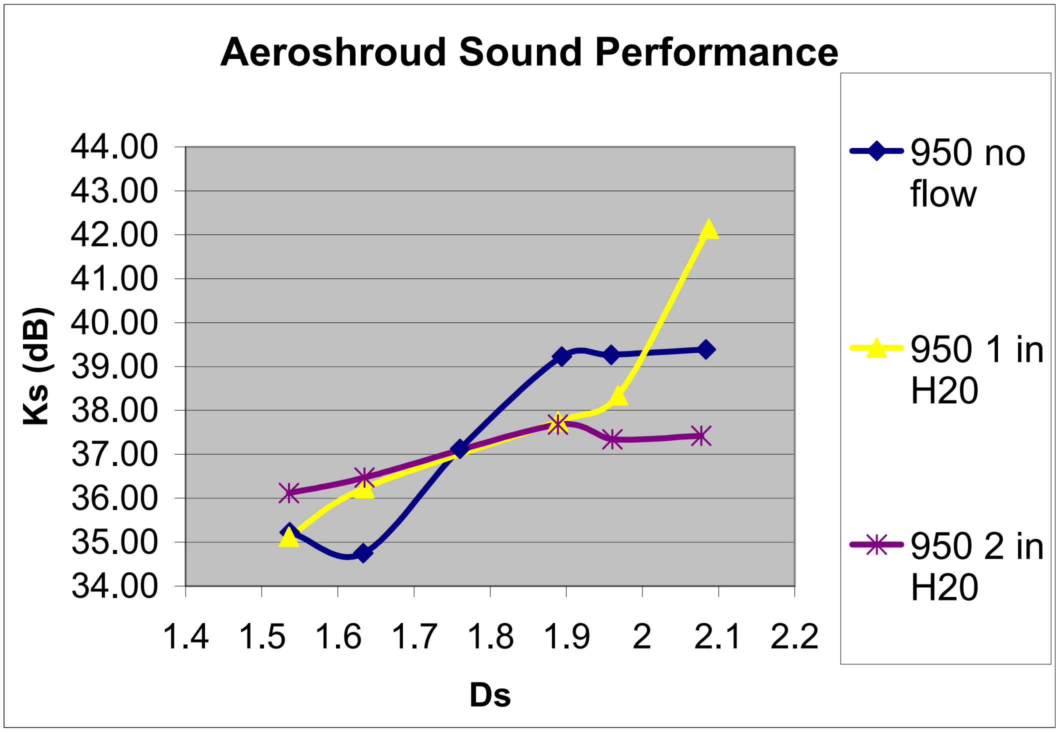

Specific noise is a relationship between the theoretical noise level of the fan based on its pressure and flow, compared with the actual noise level measured. The lower the specific noise, the quieter the fan. The blower system for the aeroshroud was located outside of the hemi anechoic test chamber to minimize its effect on fan noise. The aeroshroud has a similar effect on noise that it has on fan performance. In the fan stall region, the aeroshroud can provide significant specific noise level reductions, in addition to the flow gains, while in the axial flow region, the aeroshroud may actually increase fan noise levels over a similar shroud design without air injection.

The conclusions from this work are that *regardless of fan tested* the aeroshroud had a significant effect on the performance in the stall region, but virtually no effect on the fan performance in the axial flow region. This narrow region of performance improvement, combined with the lack of effect on system efficiency in the axial flow range make the system unattractive for further development.

Task 3 – Improve the axial fan system modeling process accuracy to accommodate the numbers of cooling systems to be redesigned to meet lower emissions requirements

Background

Computational Fluid Dynamics (CFD) has historically been used for the study of relative performance differences between design concepts. As the development of CFD codes has improved, CFD has become a much more valuable design tool in the development of axial fan based cooling systems. The cooling system designer is still faced with the problem of correlating models with measured performance, both in the area of fan performance, and flow distribution across the heat exchanger. Tier 2 and Tier 3 emissions legal installations make the analysis problem more difficult, because many of these systems use multiple heat exchangers, with parallel heat exchangers in a plane, and even multiple planes of heat exchangers. The CFD analysis must now not only predict the system air flow, but it must also accurately predict the flow through each individual heat exchanger. The problem of flow prediction through the individual cores is complicated by the fact that there can be a significant difference in the pressure losses of a radiator and an aftercooler core, which are mounted side by side in the same plane. The inability to properly predict the flow through each heat exchanger can lead to unacceptable performance for the core with the underpredicted flow, and an expensive redesign of the cooling system. The best source for validation of CFD models is experimental measurements on design prototypes, but the build of these prototype machines may not occur for up to two years after the CFD analysis was completed. To provide the analysts with a methodology that could improve the accuracy and repeatability of CFD analyses, a special test mockup was built for evaluation at Michigan State University. MSU has demonstrated the ability to measure localized velocities in the field of a rotating fan[4]. The data from these tests was used in conjunction with extensive CFD modeling at Caterpillar to determine the important variables to control during the construction, gridding, and solving of the fan performance model.

Mockup configuration

A 482.6 mm diameter sheet metal axial fan was tested at Caterpillar for FIFO (Free Inlet Free Outlet) performance, as well as installed in a specially designed mockup, prior to shipment to MSU for performance and detailed air velocity measurements in their fan performance test facility. The mockup was designed as shown below:

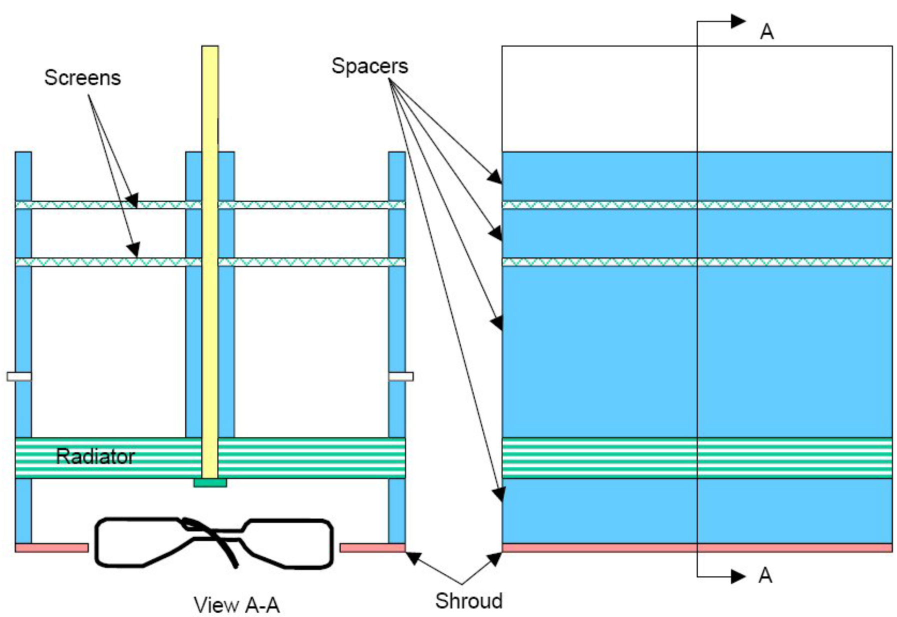

The system mockup was split into two side-by-side sections. A radiator core was placed in the mockup upstream of the fan to simulate the kind of airflow conditions the fan might experience in a machine installation. In addition to the heat exchanger core, slots were provided in the mockup to allow the inlet restriction to be changed through the use of perforated screens. These screens could be installed to provide a low restriction (no screens) full across core, or a high restriction (multiple screens) full across core, or asymmetric (high restriction on one side and low restriction on the other side) to evaluate the fan performance in multiple system types. Correlation between Caterpillar and MSU system flow measurements were made before acquiring any detailed flow field data, and correlation between CFD and measured data was accomplished with a combination of flow and pressure comparisons, along with flow field comparisons, as appropriate. The CFD modeling software used for all analysis work was Fluent^{tm} Multiple Reference Frame (MRF).

FIFO modeling

Initial testing and CFD correlation was done on a FIFO configuration, that consisted of only the fan and shroud. The shroud was installed in a flat wall of the test facility, so the air was in a "Free Inlet/Free Outlet" configuration, as evaluated in a typical supplier fan performance test. Following testing, and CFD correlation to the FIFO configuration, work would be done to both predict and measure the fan performance with the radiator and various screen configurations in place.

Impact of the size of MRF on accuracy-

Initial results provided poor pressure rise, airflow, and input torque correlation to measured data. A given flow rate resulted in pressure rise values that were 50% - 85% below measured, depending on the point on the fan performance curve at which the simulation was run. A simplified one-blade model was constructed that did not include any of the MSU facility features such as exit plenum walls. Results were similar to those from the complete MSU-facility model. However, by increasing the axial length and diameter of the moving reference frame boundaries by 50%, the simulated results of the one-blade model correlated within 5% of Caterpillar's measured data for simulations at both low and high pressure rise.MRF dimensions were extended in the model of the MSU test facility, though not to the same degree as in the simple one-blade model. The MSU-facility model included additional framing that held the shroud and made up the top of the outlet plenum. Increasing the radial dimension by 50% would cause the MRF boundary to interfere with the framing, resulting in non-axisymmetric stationary boundaries being included within the rotating fluid volume. To avoid the complications in mesh generation and problem solution arising from this situation, the radial dimension was increased only 8.6%, which left it just inside the frame boundary. The axial length was increased 20%. This brought the model results within 12% of the measured value, at low pressure rise.

Because of the improved accuracy, the MRF axial length was again increased by 16.7% while keeping the radial dimension constant. At low pressure rise, this brought the simulation results to within 7.5% of measured. However, at high pressure rise, simulation results were 64% below measured values. At low pressure rise, most of the fan flow is directed in the axial direction. Therefore, increasing the axial length of the MRF improved results for this condition. However, at high pressure rise, much of the fan flow is directed radially outward. The extended radial dimension of the MRF in the one-blade model could accurately model this radial flow. However, the smaller diameter MRF used in the ACFRD facility model could not. As a result, the MRF diameter was increased in the MSU-facility model, causing the outer diameter to intersect the plenum frame.

By increasing the radial and axial dimensions of the MRF in the MSU-facility model by 50% from the original values, the complexity of the geometry and mesh generation increased significantly because of the number of intersecting faces. Because the final MRF had a diameter of 736.5 mm and intersected the plenum framing, the framing would then be perceived as rotating relative to the moving reference frame fluid volume. Axisymmetric boundaries should not be affected by this condition, but non-axisymmetric boundaries would have "false velocities" generated at the corners where the rotational flow is disturbed. The following image shows the surface velocities at the corners of the intersection between the moving reference frame and the stationary plenum structure to be higher than the velocities on the nearby surfaces.

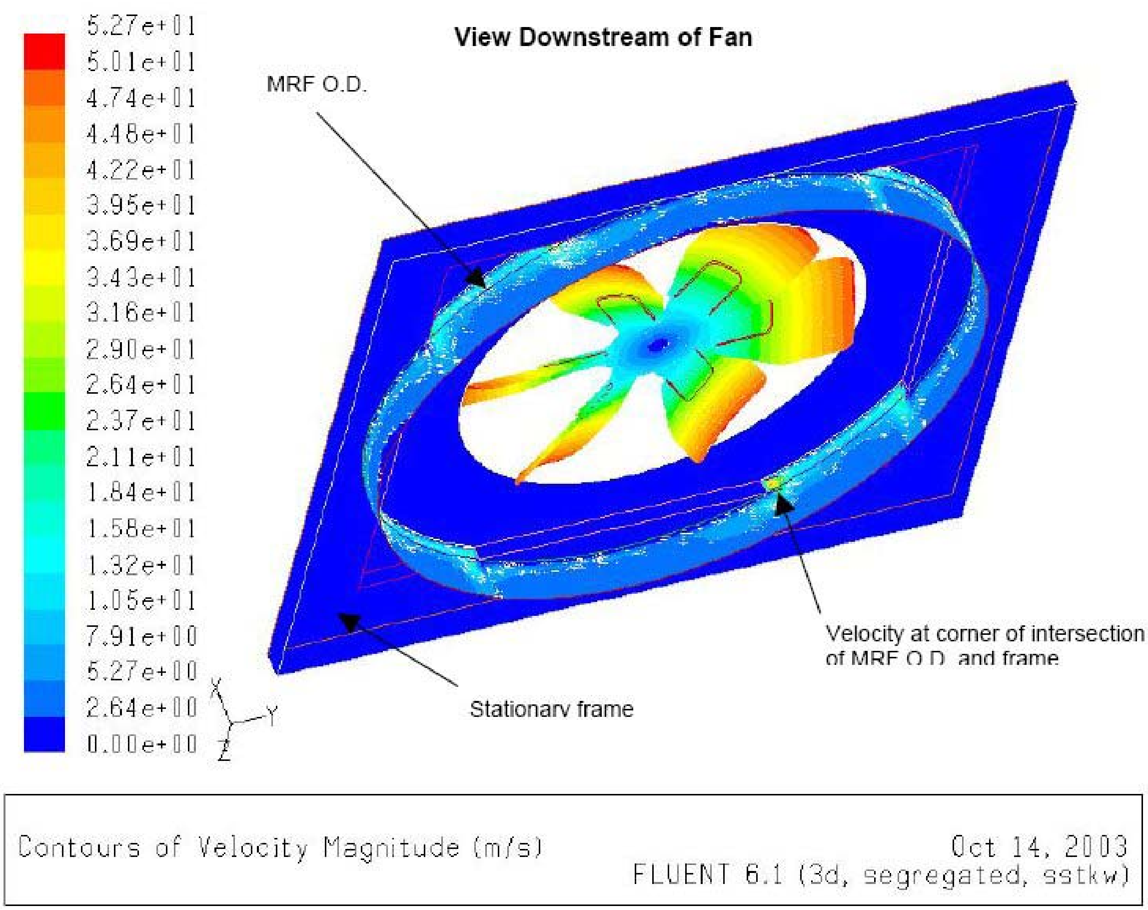

The velocity magnitudes within the fluid, at a plane 8.65 mm downstream of the bottom face of the shroud, are shown below. The velocities within the fluid are higher near the corners but are sufficiently isolated so as to not have a large effect on the flow field downstream of the fan.

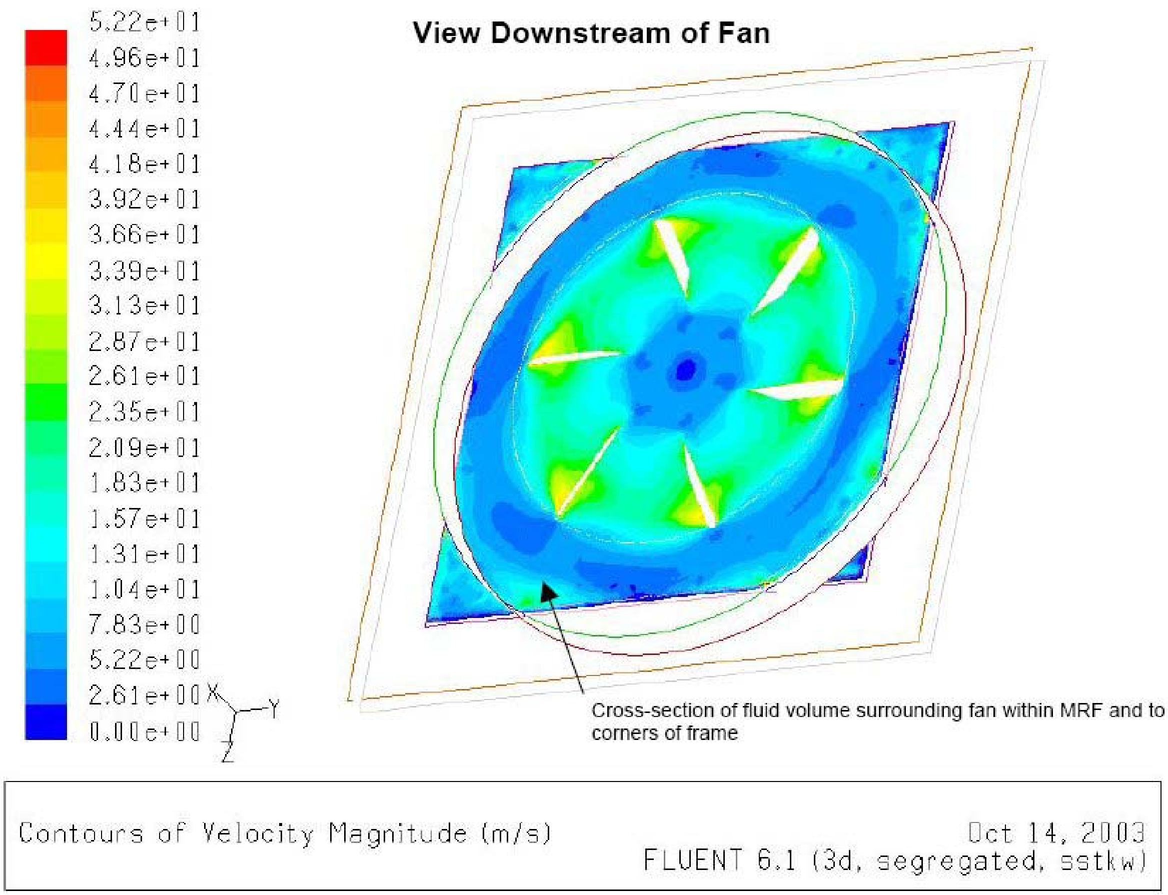

A 50% increase in original MRF axial length required the cylinder's end faces to extend 75 mm both upstream and downstream from the shroud. This caused the MRF upstream face to intersect with the heat exchanger core, once the model was in the "installed" condition. This was a situation that was thought best to be avoided since the effects on both the porous-media flow and MRF flow are unknown. It was desired to have the same basic model for both FIFO and installed from a modeling-commonality standpoint, especially for something as critical as the MRF size. Therefore, it was decided to extend the MRF face only 60 mm upstream but to incorporate the full 75 mm downstream. The downstream face intersected the driveshaft; but this was considered to be of minor consequence since it was a "dead cell" zone (no fluid flow), it was of small diameter that lay along the axial centerline of the rotating fan, and it would not be expected to interfere with the downstream airflow.

The iterations in MRF size can be summarized by the following graphic:

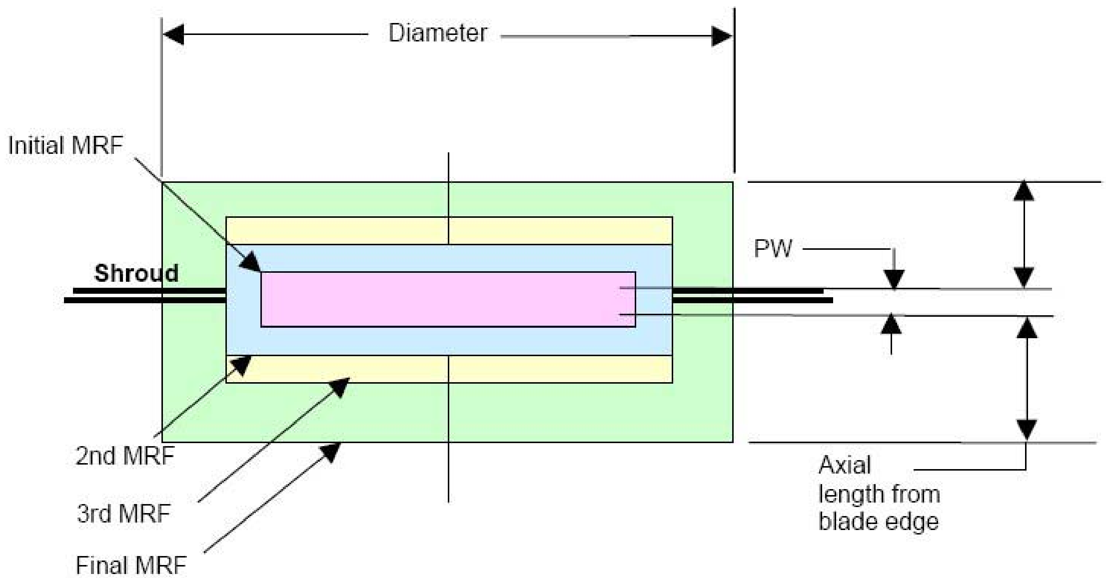

The following plots show the error between average measured airflow and CFD results as the multiple reference frame's boundaries were changed. Results are for both a low pressure rise condition (204 Pa) and a high pressure rise condition (700 Pa)-

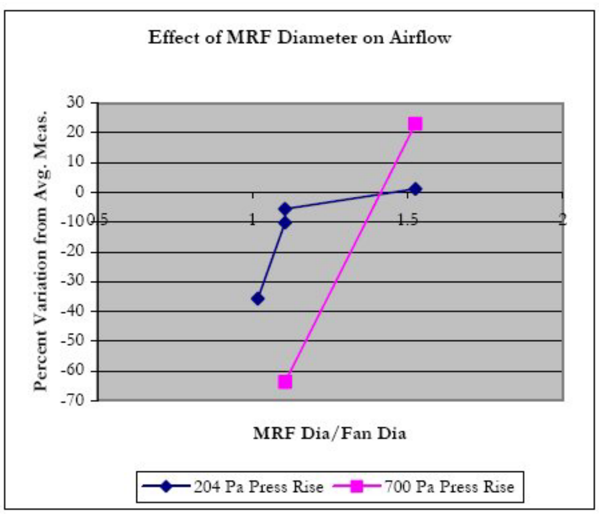

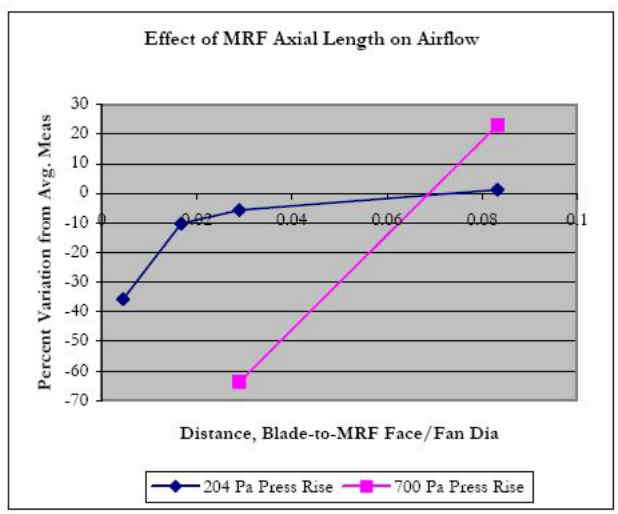

As a result of the previous findings, for a given fan diameter with projected width (PW), the following multiple reference frame dimensions should be viewed as an initial guideline when modeling axial fans:

MRF Diameter as a Percentage of Fan Diameter	Axial Length from Leading/Trailing Edge of Fan to MRF Face as a Percentage of Fan Diameter
150%	10%

Impact of Solver Controls on Model Accuracy

Another issue dealt with the solver controls. Initially the k-ε turbulence formulation was used. However, CFD analysts at MSU recommended using k-ω. Therefore, the SST version of the k-ω turbulence model was ultimately used for all FIFO correlation. There was also significant investigation into the proper discretization schemes. Different CFD analysts recommended different approaches, some of which led to unstable residuals and non-converged solutions. The fan was simulated to run at 2,000 rpm. This necessitated a two-step approach in reaching the desired fan speed, 200 rpm and 2000 rpm. Also, second-order upwind differencing led to unstable residuals if it was invoked at the same time as the speed increase. As a result, the solution progressed through 200 rpm with default, first-order discretization, to 2000 rpm with firstorder, to 2000 rpm with second-order. Under-relaxation factors were also taken into consideration. The default values provided steadily decreasing residuals under first-order discretization. However, some "oscillations" would occur in the residuals once the switch was made to second-order. Therefore, the under-relaxation factors for pressure, momentum, turbulence kinetic energy, and specific dissipation rate were all slightly reduced in accordance with Fluent's documented recommendations.

The previous steps are outlined in the table below:

Speed	No. Iterations	Discretization					Under-relaxation Factors						
		Pressure	Pressure-Velocity Coupling	Momentum	Turbulence Kinetic Energy	Specific Dissipation Rate	Pressure	Density	Body Forces	Momentum	Turbulence Kinetic Energy	Specific Dissipation Rate	Turbulence Viscosity
200	50	Std	SIMPLE	1st	1st	1st	0.3	1	1	0.7	0.7	0.7	1
2000	100-150	Std	SIMPLE	1st	1st	1st	0.3	1	1	0.7	0.7	0.7	1
2000	2000	PRESTO!	SIMPLE	2nd	2nd	2nd	0.2	1	1	0.5	0.5	0.5	1

Though the table lists 2000 iterations after the discretization and under-relaxation changes, the behavior of the residuals and/or other parameters of interest (such as inlet flow rate) could result in more or fewer iterations.

Model Results

The following images show the axial fan in place in the ACFRD facility model. Air enters through the upper surfaces (+X); is forced through the fan; and exits the narrow, curved sections at the bottom of the exit plenum. Boundary conditions are specified as zero-gauge at the inlet surfaces, the prescribed pressure rise value is defined at the outlet surfaces, and the model calculates the flow rate necessary to generate the defined pressure rise.

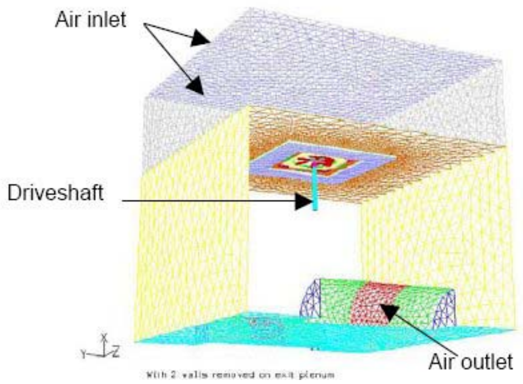

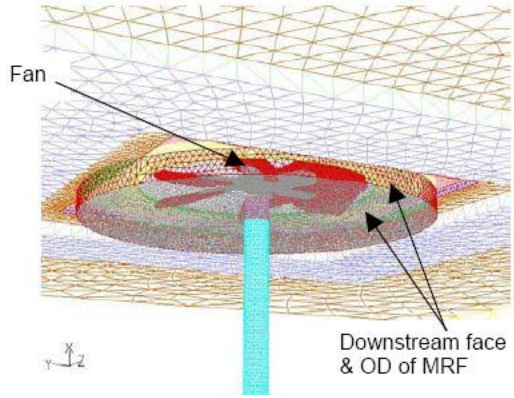

The image below shows the velocity vectors in a plane along the centerline of the fan and driveshaft. These results are for 143 Pa pressure rise. The outline of the fan blade and spider, the shroud, and the frame supporting the shroud are visible. The image also shows the extent of the moving reference frame volume surrounding the fan.

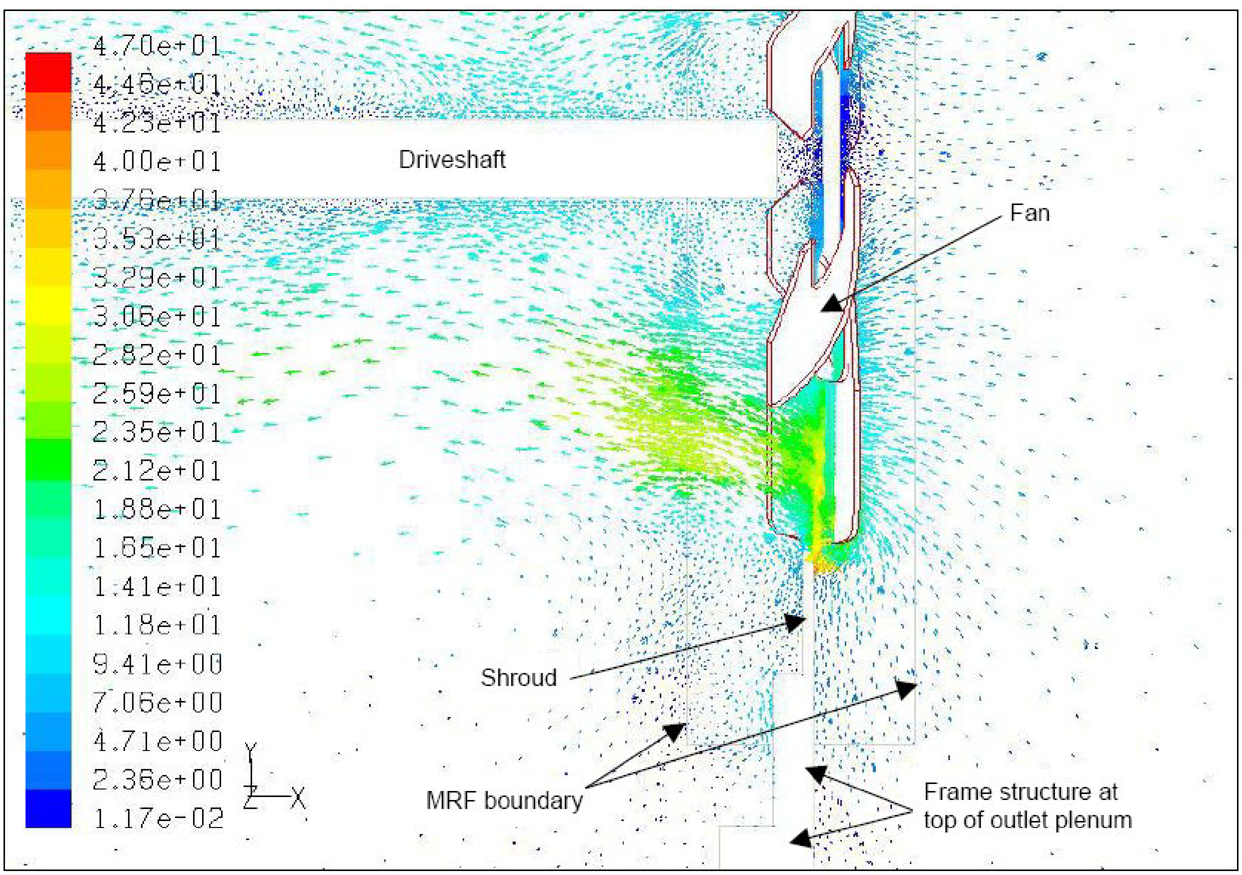

The following image shows similar velocity vectors for a pressure rise of 700 Pa. At the higher pressure, airflow is primarily directed radially outward from the fan rather than axially along the driveshaft. This is the main reason why the MRF diameter had to be increased to better simulate the high pressure rise cases.

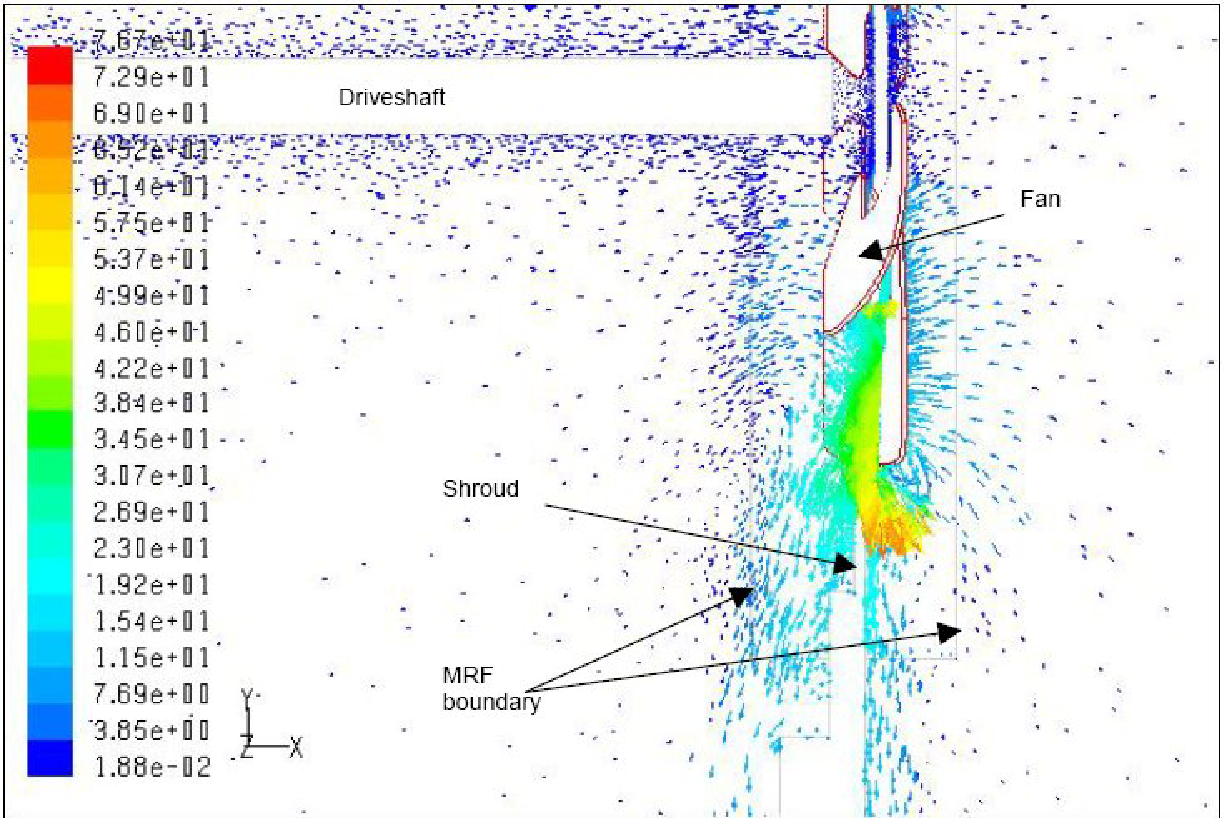

Correlation to Test Data

No detailed velocity measurements were taken on the fan in the FIFO condition. Therefore, the parameters used for correlation purposes were airflow, pressure rise, and input torque. The original tests were run at Caterpillar's Sound and Cooling Research Lab, and were repeated at MSU prior to detailed velocity measurement testing. Tolerance limits based on AMCA recommendations[5] were established as ±3 to 5% of the measured values to meet the criteria that performance estimates must be within 5% of measured data. MSU and Caterpillar test data, recorded under identical test conditions, fell within this tolerance band. The CFD model was then exercised over a range of pressure rise values, and the calculated flow rates and input torques were compared against Caterpillar's and MSU's measured data. The following plot shows the measured data and the CFD simulation results for pressure rise as a function of airflow. The CFD model experiences some problems around the stall point in the fan performance curve when air flow is transitioning from primarily axial to primarily radial.

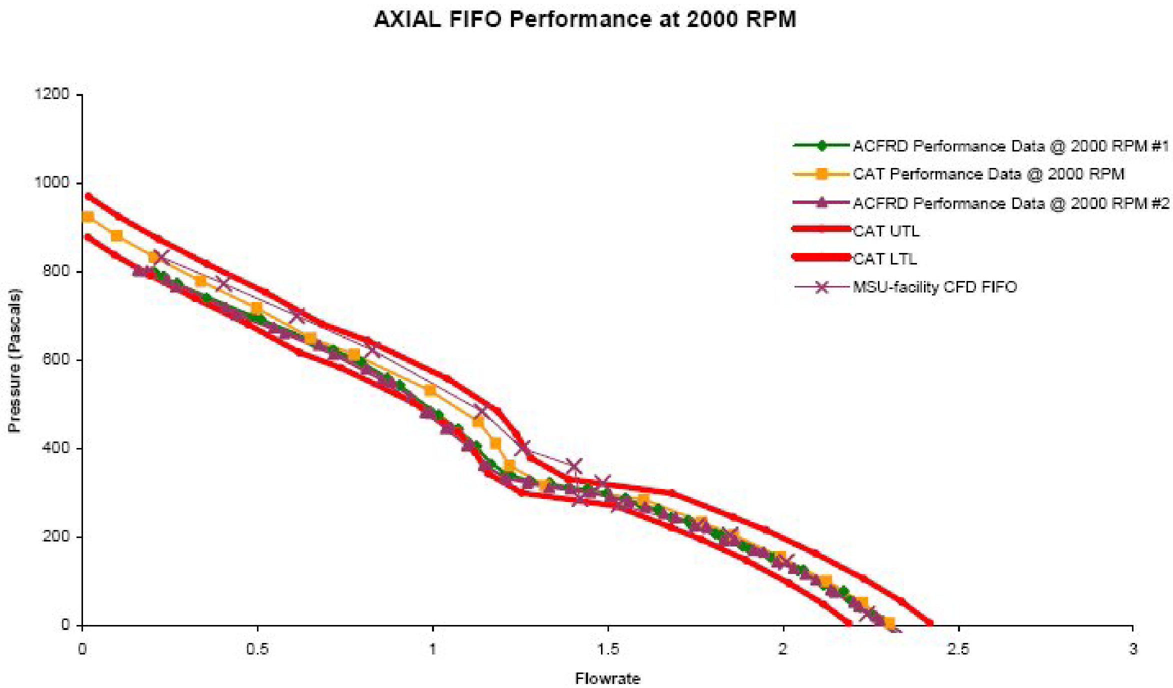

Below is a plot that compares the measured data and the CFD simulation results for input torque to the fan blade and spider as a function of air flow rate. Correlation, particularly at the lower airflows, is not as good as the pressure rise correlation and does not fall within the ±5% tolerance band.

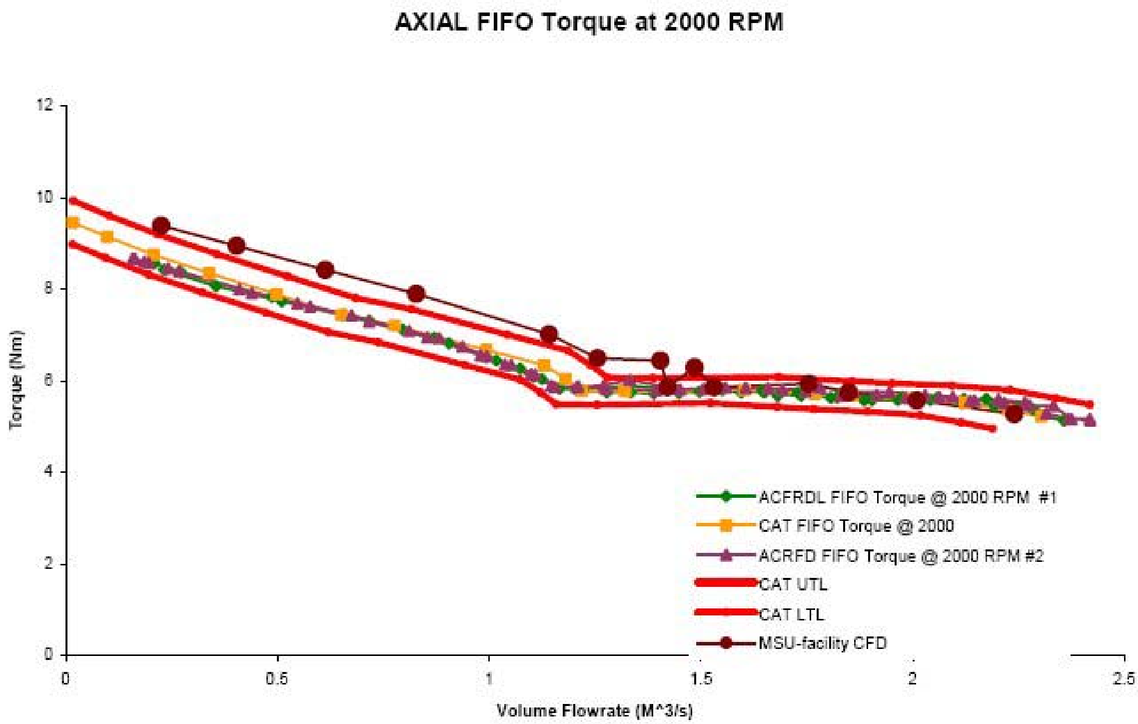

The effect that this difference in torque has on efficiency prediction is shown below:

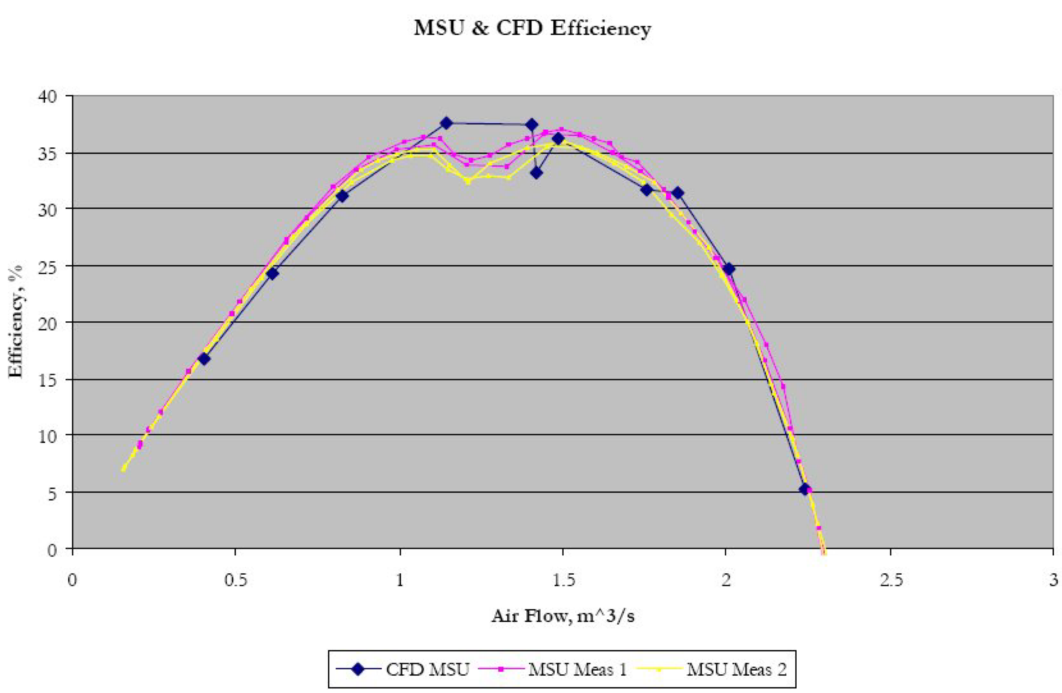

The point of fan stall creates difficulties for the CFD model as flow patterns are very confused between the axial and radial regimes. However, away from stall, efficiencies between the model and the MSU data compares very favorably. Exact shaft speed was not available for the Caterpillar-measured data, so it is not included for comparison.

Of particular interest was how well the CFD model predicted airflow for a given pressure rise. A system restriction curve was generated for a specific diameter of 1.7. The goal was to be able to predict, within ±3%, the airflow necessary to achieve the pressure rise obtained where the system restriction curve crossed the FIFO fan performance curve. This is shown below.

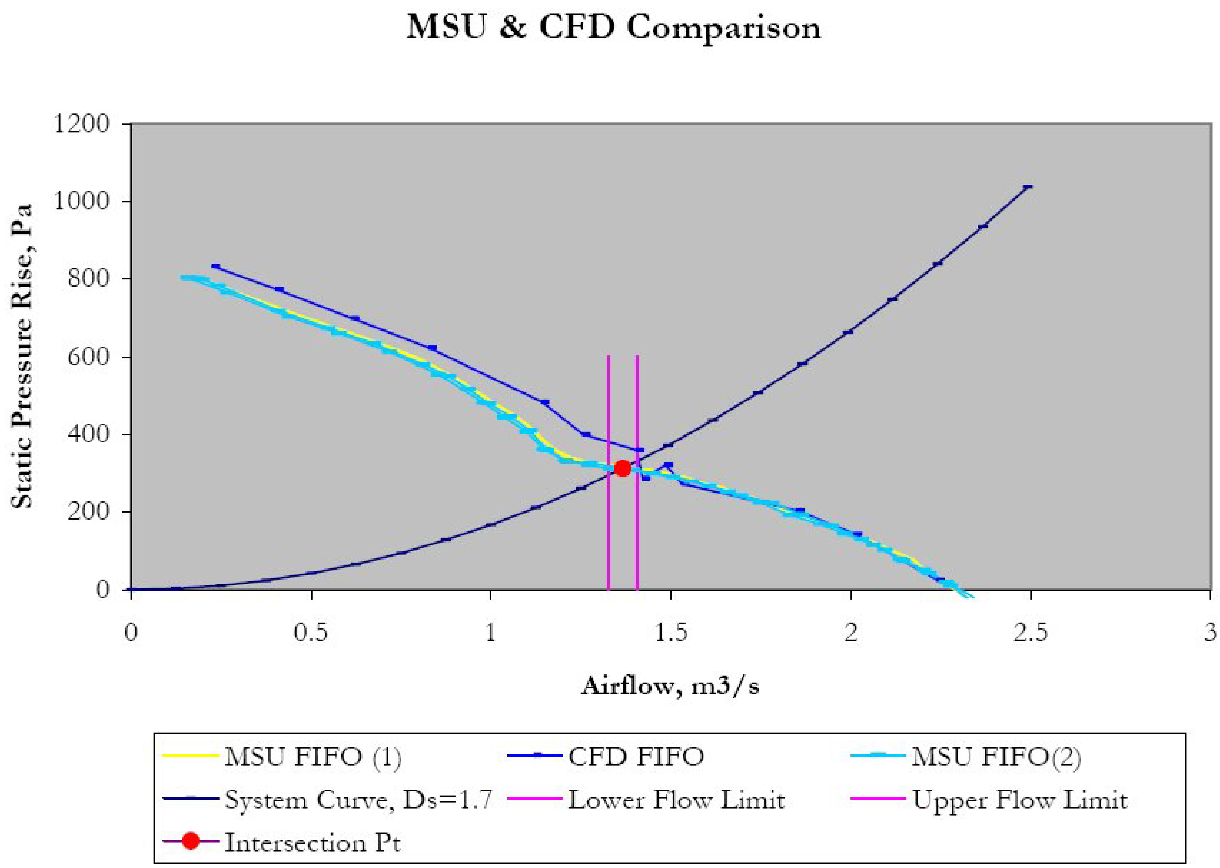

The vertical lines designate the upper and lower tolerance limits on the airflow. A Ds of 1.7 forces the pressure rise high enough for this fan that the flow predictions from the CFD have entered the range where they begin to deviate from the measured data. As noted earlier, a simple, one-blade model of the fan, operating within a plenum that consisted of only a shroud, showed good correlation to test data even at the higher pressure rise conditions. That model predicted flow within 1.3% of measured at a pressure rise of 700 Pa. It appears that the framing around the downstream side of the shroud in MSU test facility, combined with the radial flow that occurs during high pressure rise, disrupts the flow patterns sufficiently that the CFD model displays poorer absolute value correlation, although the trends still match very well.

System modeling

Most of the installed CFD model remained unchanged from the FIFO model. The main difference with the installed model concerned proper modeling of the upstream restrictions in the mockup since the mockup was not part of the FIFO model. The mockup was divided into two sections along the axis of the fan driveshaft. The mockup contained a commercial radiator core like this:

The core type was specifically chosen to have tubes parallel to the fan centerline to minimize unnecessary disruption of the airflow at the fan inlet, since the core was simulated using a porous media, and the details of the core were not modeled. "Installed conditions" consisted of the heat exchanger alone in the mockup (low symmetrical load), the heat exchanger plus two screens in series on both sides of the mockup (high symmetrical load), and the heat exchanger plus two screens in series on one side of the mockup and the heat exchanger alone on the other side (asymmetrical load). The symmetrical conditions simulated full-plane cores in front of the fan. The asymmetrical condition simulated partial cores placed side-by-side, resulting in uneven loading on the fan.

The porous jump surface was defined as the downstream surface of the heat exchanger and was arbitrarily assigned a thickness of 1 mm. The fluid volume surrounded by the heat exchanger surfaces was defined as a "porous zone" where the viscous and inertial resistances in the direction crosswise to the flow direction were given values of 1000. The resistance in the direction of flow was zero. The effect was that the heat exchanger fluid volume acted as a flow straightener, similar to the way cooling fins behave.

Prior to sending the test setup to MSU, an extensive set of lab experiments was completed at the Caterpillar Machine Research lab. Airflow and pressure drop data was obtained on the two screens alone in one side of the mockup. The data was used to establish a pressure-velocity curve, thereby simulating another heat exchanger core. One porous jump surface defined the characteristics of the two perforated screens combined. Using one porous jump for the screens and another for the heat exchanger would help establish whether porous jump characteristics, calculated for separate restrictions in the flow path, could simply be added together, or whether the system had to be modeled as a whole. If the system had to be modeled as a whole, then testing would be required on the system setup in order to establish a P-V curve, and associated porous jump values, thereby severely limiting the usefulness of this modeling approach.

MSU Correlation

The installed model was exercised over a range of airflow and pressure rise conditions in an attempt to match the fan performance curves obtained by MSU. Model correlation was not intended to extend to detailed velocity measurements near the blade tip/shroud region. Modeling accuracy needs can be met if CFD can accurately predict macro-level airflow and pressure rise. The following curve shows the correlation between the data obtained at MSU and several points predicted by the CFD model for the Low Symmetry condition. AMCA®-recommended (Air Movement & Control Association) tolerance bands are shown for reference (approximately 3%-5% error band in predicted value). The plot is based on static pressure, which is simply the total pressure minus the velocity head (½*ρ*V2, where V equals flowrate divided by the fan's swept area, πD2/4).

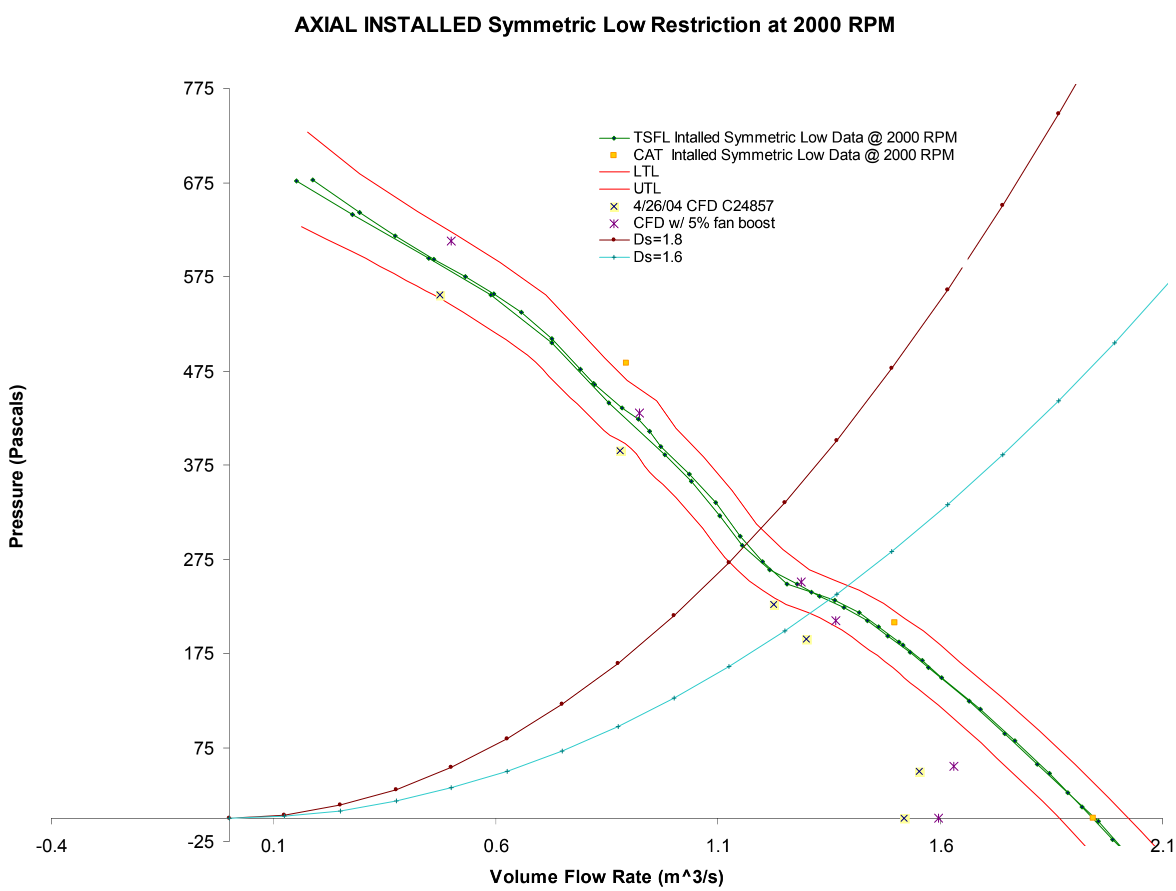

The green line represents two sets of data taken in the MSU test facility. The two system restriction curves represent Ds values of 1.6 and 1.8. One set of CFD results (the 4/26/04 data) shows the airflow-pressure rise prediction based on the original model. The second is based on a

5% boost added to the fan speed to help account for incomplete modeling of the flow in the blade tip/shroud region and additional system loss details that were not included in the model. Though the baseline results matched measured data within commercially accepted accuracy ranges of $\pm$10%, our performance goal was to predict performance within the AMCA® tolerance bands. The "5% boost" prediction points reflect the CFD results when fan speed was increased 5% to 2100 rpm. Fan flow increased by a factor of 1.05 and pressure rise increased by a factor of 1.052. This adjustment put the CFD predictions within the tolerance bands in the Ds region of interest. At lower system restrictions, as pressure rise decreased and airflow increased, the CFD underprediction became more severe. Additional work would be required in order to improve prediction accuracy in this range, but is not justified, since few machines have cooling system restrictions this low.

Localized air velocity was measured at MSU using laser Doppler velocimetry. These measurements provided a visual representation of the flow velocity vectors near the driveshaft and in the fan blade tip/shroud region. Velocity magnitude contour plots and vectors/pathlines are shown below, comparing the MSU measured results, left, against those obtained from the CFD model, right.

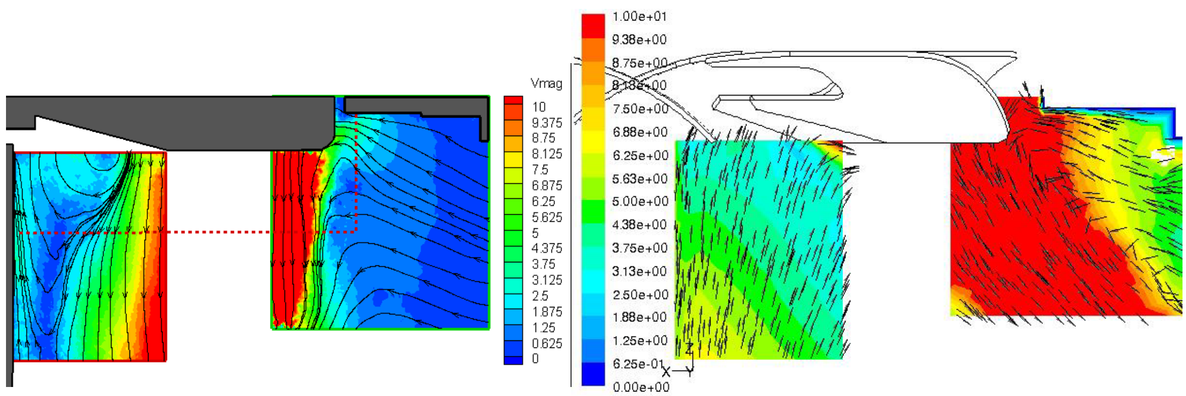

The results shown above show that Fluent's® MRF formulation for rotating fluids does not currently possess the capability to accurately predict these localized flow patterns in sufficient detail to allow the software to be used to predict the performance of the fan blade tip/shroud area.. As a result, the MRF formulation should not be used for shroud design or fan projection studies, where an accurate representation of flow in the tip/shroud region would be critical. Curves similar to those above for Low Symmetry were also generated for both the High Symmetry and Asymmetrical loading conditions. These are shown below.

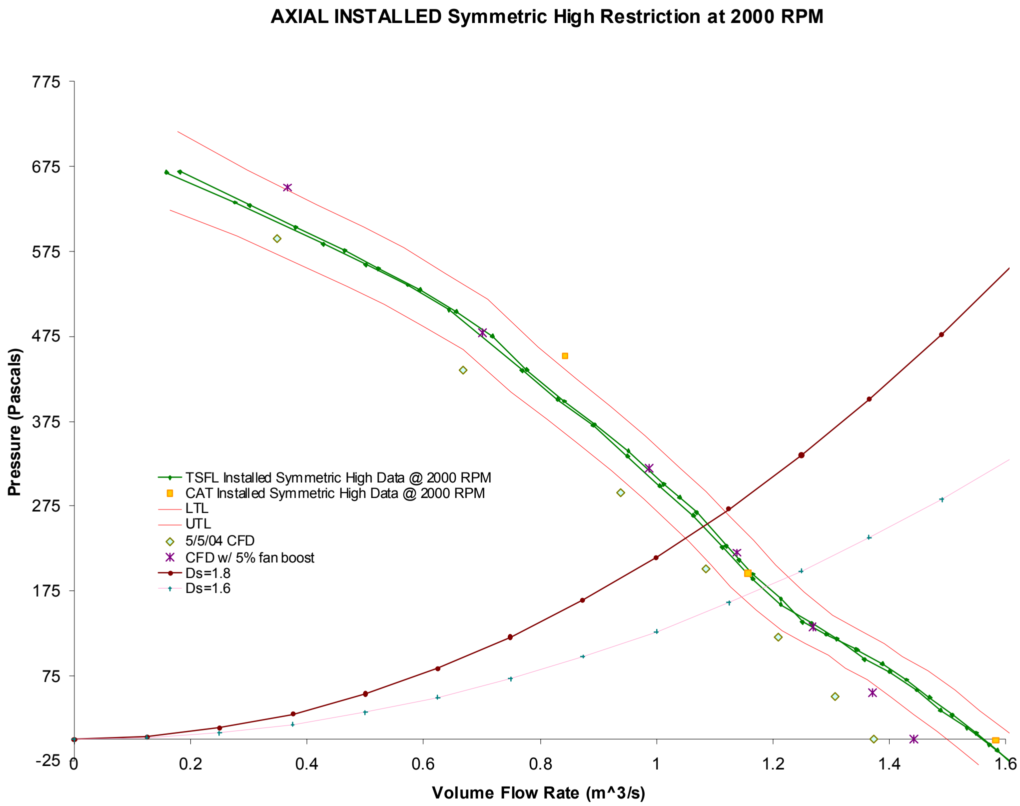

AXIAL INSTALLED Symmetric High Restriction at 2000 RPM
Pressure (Pascals)
Volume Flow Rate (m^3/s)
775
675
575
475
375
275
175
75
-25
0
0.2
0.4
0.6
0.8
1
1.2
1.4
1.6
TSFL Installed Symmetric High Data @ 2000 RPM
CAT Installed Symmetric High Data @ 2000 RPM
LTL
UTL
5/5/04 CFD
CFD w/ 5% fan boost
Ds=1.8
Ds=1.6

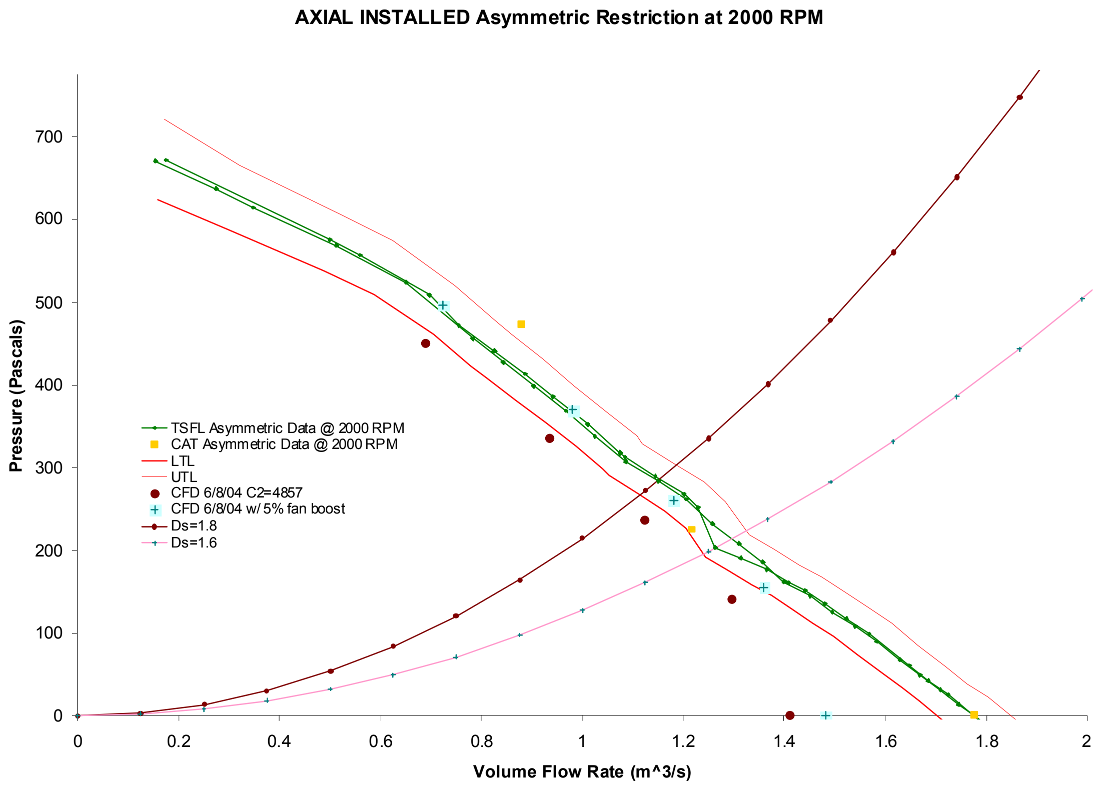

Fan degradation is a measure of the reduction in FIFO fan performance when the fan is operated in an "installed" condition where upstream and/or downstream flow restrictions are present. Plotting the FIFO curve with the installed curves demonstrated the fan performance degradation in the modeled installed condition. The following figure shows the four curves overplotted.

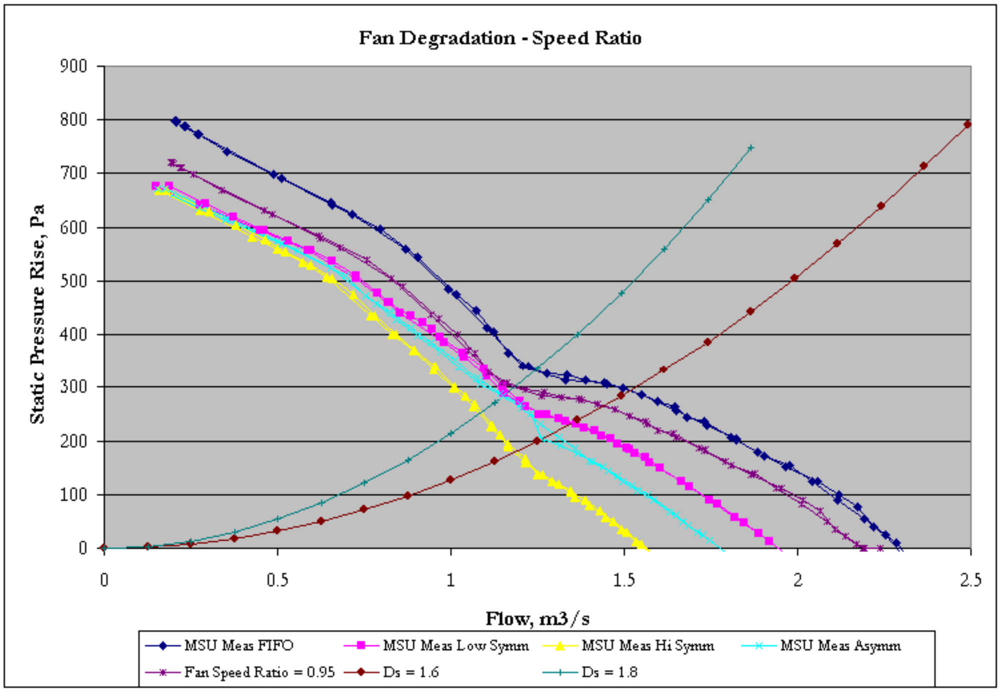

FIFO test results showed a distinct "knee" in the curve in the stall region. This "knee" became less evident as the upstream flow restriction was increased. An example of fan curve scaling is the FIFO performance curve scaled to 1900 rpm, or a fan speed ratio of 0.95 (0.95*2000 rpm). Fan degradation was determined by scaling the FIFO curve so as to intersect each of the installed curves at the specific diameter values of interest (Ds = 1.6 and Ds = 1.8). Because the fan performance curve became flatter as restriction increased, it was somewhat problematic that at a single fan degradation value could be defined. Instead, two fan degradation values were determined, one at each Ds value, for each of the fan performance curves. The values obtained are show below:

Degradation of FIFO Fan Performance Curve (Fan Speed Ratio)
Specific Diameters of 1.6 and 1.8
High & Low Symmetrical Fan Loading, Aysmmetrical Fan Loading

D_s =	1.6	1.8
Low Symmetrical Loading	11% (0.89)	6.5% (0.935)
High Symmetrical Loading	22% (0.78)	13% (0.87)
Asymmetrical Loading	15% (0.85)	7.5% (0.925)

The mockup was also calibrated for flow splits between the two sides when one side had two screens plus the heat exchanger (high restriction) and the other had only the heat exchanger (low restriction). Flow splits were evaluated for CFD simulations that involved asymmetrical loading. There was less than a 5% error in the predicted percentage of total flow going through each side of the mockup when compared to the lab calibration as shown in the figure below. The baseline model was deemed to be sufficiently accurate to allow the determination of which factors were critical to the modeling process to maintain the desired level of accuracy.

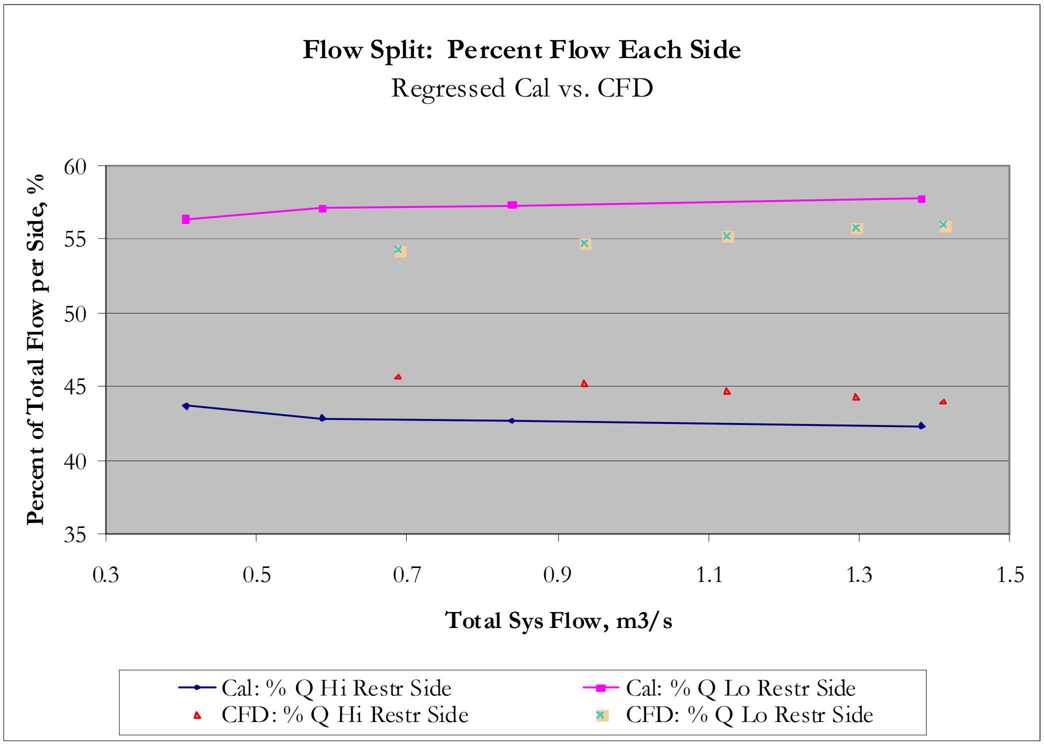

Now that we have a model that can predict acceptable results, we can use a Design of Experiments (DofE) to determine the effects of modeling variables on analysis results.

Factor Definition for DofE

Factors that were considered to be part of the modeling process included:

- **Fan surface mesh type (triangular, quadrilateral, combination)**
- **Fan surface/edge mesh density and uniformity**
- **Domain volume mesh type (tetrahedral, tetrahedral plus prisms, hexahedral, or mix)**
- **Domain volume mesh density and mesh refinements**
- **Number of cells within the MRF**
- **Size of the MRF**
- **Flow regime modeled (radial, transitional, and/or axial)**
- Turbulence models used
- Fluid type (compressible/incompressible)
- **Definition of boundary conditions for surfaces**
- Initial condition values

- Solver controls
- Criteria for determining solution convergence
- Data for modeled heat exchangers
- How the heat exchanger data was input to the model

The significant modeling factors were evaluated and ranked in terms of their importance in meeting modeling needs for:

- Flow accuracy
- Pressure accuracy
- Consistency between analysts
- Flow split accuracy
- The ability to correctly predict trends (relative changes)
- The modeling process to be consistent and repeatable
- Ease of changing fan designs within the model
- Ease of changing the sizes of side-by-side heat exchangers within the model
- Reducing analysts' time spent on creating the model
- Reducing the time needed to run a model

Solution accuracy (overall flowrate, pressure rise, and flow splits) was clearly the most important consideration. Rankings, both in terms of the analysts' needs and the factors' importance in meeting those needs, were used to define which factors should be evaluated in the design of experiments. These are shown in bold above. The remaining factors were considered less important for a variety of reasons. Only triangular element surface meshes were considered because of the ease of employing automatic meshing software for complex geometries,. Fluent® documentation recommended the k-ω turbulence model for swirling flows, but most CDC analysts used the k-ε formulation. Analysts expected the differences in the final solution to be minor. Air was always treated as an incompressible fluid, negating the need for a reference pressure value and location. Initial condition settings varied between analysts. Although these settings are primarily intended to set the model on the path towards solution convergence, the ultimate solution for these kinds of fan models should not depend on the initial condition settings. Problems with convergence or obviously erroneous results may indicate that initial conditions should be reviewed by the analyst. Solver controls are settings for under-relaxation values and discretization schemes, and there were some differences between analysts in this area. However, though they may affect the rate of convergence, these settings were thought to have minimal impact on solution accuracy. Criteria for determining convergence was discussed but was not considered as a factor that would affect the accuracy of the model. Heat exchanger pressure drop data was obtained from supplier data. This data was considered valid for heat exchangers used in underhood CFD models, and, therefore, no other sources were considered. The supplier data matched lab calibration data for the heat exchanger used in the MSU tests.. Though it would be desirable to consider all of the factors in the modeling process, the design of experiments matrix would have quickly become overwhelming. Other model parameters that could be part of any future investigation are fan diameter, fan projection, tip clearance, shroud type, optimum MRF size, solver software, and sliding mesh viability.

Design of Experiments

The modeling factors in bold above were considered to be potentially the most significant contributors to an effective modeling process. They were divided into six control-factor categories and two noise-factor categories. Control factors were: Mesh Density, Hybrid Mesh, Downstream Mesh Refinement, Domain Size, Flow Regime, and Boundary Type. Noise factors were: MRFvolume size and Mesh Quality. Control factors are those factors that the analyst must take care to control within specified limits. Noise factors are those factors that are expensive or time consuming to control and which the analyst would prefer not to have to control, if possible. Mesh density dealt with the minimum node spacing of the surface mesh on the fan. The spacing was defined as a percentage of tip clearance. It was also related to the amount of refinement (number of cells) within the MRF-volume surrounding the fan. The degree of refinement was described as the ratio of maximum-to-minimum cell size within the MRF. Hybrid mesh related to the presence or absence of layers of prism cells to capture boundary layer effects on the fan. Downstream mesh refinement dealt with the maximum-to-minimum cell size ratio in the exit plenum downstream of the fan. A smaller ratio resulted in more cells which could improve the solution accuracy but with longer solution time. Domain size related to the size of the fluid domain downstream of the fan. For the MSU-facility model, the fluid volume downstream of the fan was enclosed within the exit plenum. However, the downstream fluid domain size could grow to include the atmosphere surrounding the exit plenum. The domain-size factor considered this option. Though flow regime was considered as a factor, in fact, models would have to be capable of producing accurate results throughout the axial-to-radial flow regimes, particularly in the specific diameter (Ds) range of 1.6 to 1.8. However, to help limit the number of simulations, flow regime was used as a control factor so that not every run would have to be simulated at both the radial and the axial flow regimes. Boundary type concerned whether the inlet boundary was defined as a velocity-inlet (calculating pressure) or as a pressure-inlet (calculating flow). The outlet was always defined as a pressure-outlet boundary.

The MRF-size noise factor addressed the question of whether a small MRF, tightly constrained around the fan, was more accurate. MRF sizing also involved geometry and meshing issues due to the fact that, if the MRF size grew too large in diameter, it would eventually intersect with nonaxisymmetric features of the model. This could potentially create solution problems in addition to significantly complicating the surface definition and meshing process. The large MRF modeled as a noise factor included only axisymmetric features of the shroud. Also, it was limited axially to avoid interference with the upstream heat exchanger. Intersecting surfaces and the resulting complications in meshing make it desirable to not have to control MRF size. The mesh quality noise factor referred to the degree of skewness of the fan surface cells and the fluid cells within the MRF volume. It was also related to the uniformity of the fan surface mesh.
Two levels were established for each of the control and noise factors. The factors and the level definitions are shown in chart below. Actual node spacing values used in the design of experiments simulations were different from those originally proposed due to either an inability to meet skewness targets (Level 1) or memory limitations on model size (Level 2).

	Control Factors	Level 1	Level 2	Type
	Mesh Density	Surf mesh = 5*tip clearance Base max/min cell size ratio (MRF Vol)	Surf mesh = 0.1*tip clearance 0.1*Base max/min cell size ratio (MRF Vol)	Control
	Hybrid Mesh (prisms on fan surf)	No Prisms	2 layers of prisms (1mm/layer)	Control
	Mesh Refinement Non Rotating Zone Region downstream of MRF Volume	Base max/min cell size ratio (entire outlet volume)	Volume adaption 0.1* Base max/min cell size ratio (entire outlet volume)	Control
	Domain Size. Outlet plenum on Exhaust	No outlet plenum	With outlet plenum	Control
	Flow Regime	Axial	Radial	Control
	Boundary Type	Volume In/Pressure Out	Pressure In/Pressure Out	Control
	Noise factors			
N2	MRF Radius/PW	R + 0.5 * Tip Clearance LE/TE +.05*Tip Clearance	R + 5*Tip Clearance LE/TE +.Min (0.7*Space, 0.1*Fan Dia)	Noise
N1	Quality	0.5*(Surf-Fan Skew) 0.9*(Vol-MRF Region Skew) Uniform Cell Size	0.8*(Surf-Fan Skew) 0.96 Mrf Region Skew 0.98* Whole Domain Skew Non Uniform Cell Size	Noise
	Actual Mesh Density Used	Node Spacing ~ 6mm (1.2% of Fan Dia, 1.3*Tip Clearance)	Node Spacing ~ 1mm (0.21% of Fan Dia, 0.22*Tip Clearance	

After the factors and levels were defined, a L12 Taguchi matrix was created. The design of experiments simulations were run according to this plan. The matrix is shown in table below. The “inner array” shows twelve runs. Each factor used an equal number of each level across the twelve runs but in varying order. There are four noise conditions – two MRF-size levels and two quality levels for each MRF size. Each of the twelve runs contained four iterations, one for each of the noisefactor combinations. This resulted in 48 total simulations

Taguchi
L12

Outer Array

	Inner Array						Outer Array - Noise Factors			
							MRF Size - 1		MRF Size -2	
Run #	Density	Hybrid	NonMRF	DomainSize	FlowRegime	BCType	Quality-1	Quality-2	Quality-1	Quality-2
1	1	1	1	1	1	1				
2	1	1	1	1	1	2				
3	1	1	2	2	2	1				
4	1	2	1	2	2	1				
5	1	2	[illegible]	[illegible]	2	2				
6	1	2	2	2	1	2				
7	2	1	2	2	1	1				
8	2	1	2	1	2	2				
9	2	1	1	2	2	2				
10	2	2	2	1	1	1				
11	2	2	1	2	1	2				
12	2	2	1	1	2	1				

Inner Array

y = Fan Speed Ratio

Two operating conditions were simulated that bracketed the Ds range of interest. The two simulation points were 1.409 m3/s at 160 Pa static pressure rise and 1.008 m3/s at 350 Pa pressure rise. These target points are shown in figure below.

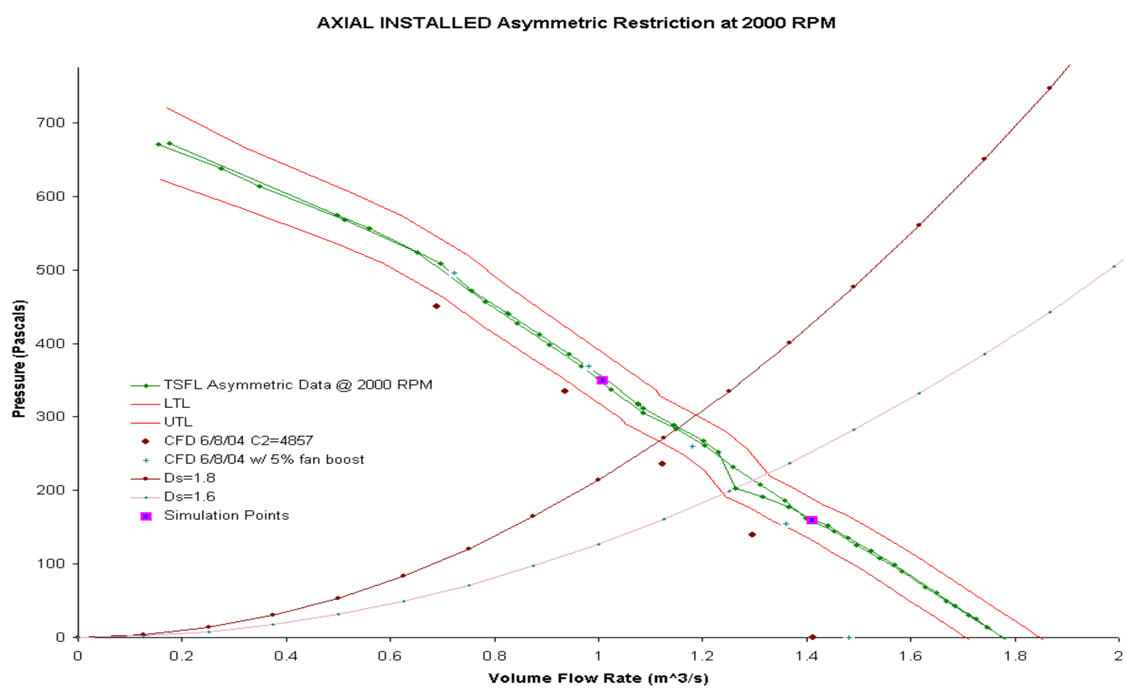

Of the 48 CFD simulations, 11 models had convergence problems, so the turbulence model for those 11 runs were switched from k-ω to k-ε. Residuals convergence improved, but this resulted in 11 additional runs, for a total of 59 CFD simulations. A percent difference from measured was calculated for each prediction, either static pressure rise or volume airflow, depending on the boundary condition imposed. Prediction errors ranged from 0.6% to over 100% where predicted values were negative. Since either pressure rise or flowrate was being predicted fan speed ratio was chosen as the measure of simulation accuracy. The measured data was taken at a fan speed of 2000 rpm. Fan speed ratio is the factor by which 2000 rpm was multiplied in order to obtain the predicted flow and pressure. A fan speed ratio of 1.00 for any given data point indicated that the predicted point perfectly matched the measured data for the test fan at the test speed. A CFD prediction resulting in a fan speed ratio of 0.9 indicated that the predicted flow and pressure represented a 10% reduction from the tested fan speed. Fan speed ratios varied from a low of 0.708 to a high of 1.017 as shown in the table below. Fan speed ratio could not be calculated for those CFD runs that resulted in either negative flow or negative pressure predictions. For those conditions where a follow-up run was made using the k-ε turbulence model, the result of the follow-up run is reported. Use of the k-ε model did not provide consistently better or worse predictions than the k-ω model. Residuals convergence, however, was much improved from the k-ω model.

							ResponseFan Speed Ratio			
							Nominal-the-best			
							Outer Array			
	Inner Array - Control						MRF Size -1		MRF Size -2	
Run#	MRFDen	Hybrid	NonMRFDen	DomSIze	FlowReg	BCType	Quality-1	Quality-2	Quality-1	Quality-2
1	1	1	1	1	1	1	*	*	0.903	0.907
2	1	1	1	1	1	2	0.712	0.715	0.88	0.907
3	1	1	2	2	2	1	0.74	0.731	0.972	0.979
4	1	2	1	2	2	1	0.719	0.726	0.984	0.972
5	1	2	2	1	2	2	*	*	0.995	0.984
6	1	2	2	2	1	2	0.708	0.709	0.902	0.906
7	2	1	2	2	1	1	*	*	0.91	0.934
8	2	1	2	1	2	2	*	*	1.006	0.995
9	2	1	1	2	2	2	*	*	1.017	0.971
10	2	2	2	1	1	1	*	*	0.946	0.923
11	2	2	1	2	1	2	0.714	0.716	0.936	0.972
12	2	2	1	1	2	1	0.73	0.727	1.008	0.979

The simulations that resulted in negative airflow or pressure rise predictions (designated by an asterisk) were from models that used MRF Size Level 1 (small MRF). Also, all of the fan speed ratios for models that used MRF Size Level 1 were substantially lower than the results from models that used MRF Size Level 2 (large MRF, highlighted in yellow). MRF size obviously played a critical role in model prediction accuracy. Though it was desirable to have MRF size treated as a noise factor (a factor than can be left uncontrolled), the data indicated that the MRF size must be controlled, and that the larger MRF responded better than the small one.

Therefore, results from the models that used the small MRF were neglected in the statistical analysis.

The responses for MRF Size Level 2 showed that neither level of the Quality noise factor provided a consistent or significant advantage. The practical significance is that the tighter mesh quality control values used in Level 1 are not required in order to ensure reasonably accurate results and that the analyst need not spend time manually correcting cells to achieve volume cell skewness levels below 0.9. Of course, highly skewed cells in critical regions of the flow domain, such as in the tip/shroud interface, should still be avoided. Neither a uniform surface mesh on the fan (quicker setup) nor a non-uniform surface mesh (fewer cells) provided any clear advantage.

Flow split accuracy is shown in the figure below. Flow through each side of the mockup was determined for each condition simulated in the design of experiments. Predicted flow splits were compared to those measured in the Research Cooling Lab during calibration of the mockup using the same heat exchanger core and screens as were used in the MSU tests.

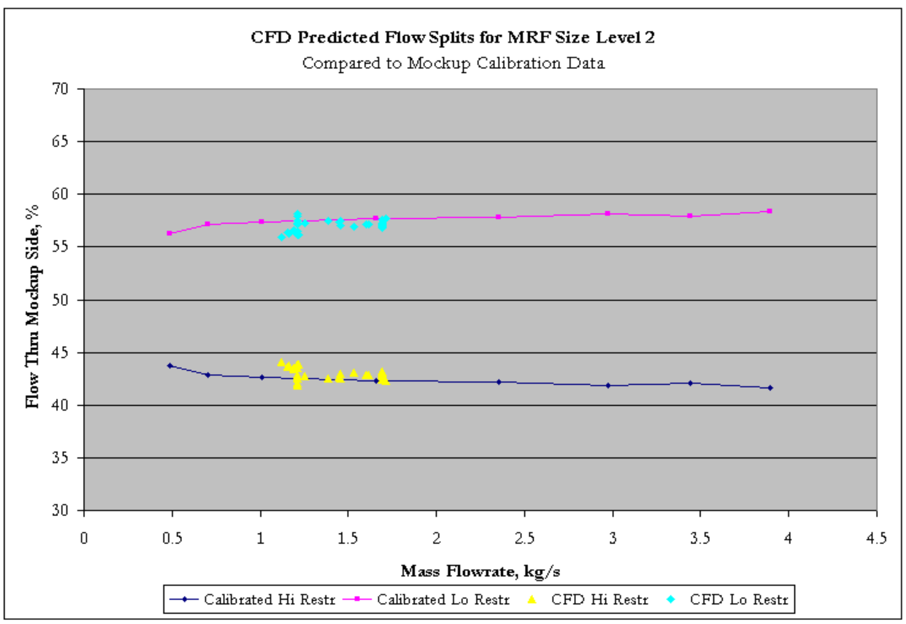

The flow splits observed in the CFD models compared very favorably with those measured in the lab. Over the range of simulated flowrates, the CFD flow split variation was less than 4% different from the measured value. The flow split values used for comparison were only from those simulations that used MRF Size Level 2.

A brief investigation was conducted to determine if other solution factors besides MRF size played a role in the prediction of negative values. The factors of interest were ones that had been dismissed in the early consideration of significant factors under the assumption that their effect on the ultimate model solution would be minimal. This assumption was tested on one of the simulation conditions that resulted in a negative pressure rise prediction. The following solution controls were implemented, individually, on the model representing the first condition of Run 1 (Run 1-1, or Run 1 using Level 1 for both of the Noise factors, MRF Size and Mesh Quality):

- Initial condition values
- Node-based or cell-based gradient
- Coupled solver
- Pressure-velocity coupling
- Pressure discretization

The settings for initial conditions, solver controls, and discretization, were as used in the original CFD model and the design of experiments models.

Initial conditions were left at their default values of zero for the three directional velocities and one for both the turbulence kinetic energy and the specific dissipation rate. Alternatively, the turbulence kinetic energy and specific dissipation rate were defined at something other than one, while maintaining the X-, Y-, and Z-velocities at the default value of zero. Neither setting produced a solution that was more than 2.5% different from the original result.

The node-based gradient solver option was used with both the k-ω and k-ε turbulence models. Changes from the original CFD result varied from 18%-21%. However, the result was a more negative pressure rise value.

The node-based gradient option was also used with the coupled, implicit solver, rather than the segregated, implicit solver. The solution diverged and could not be run to completion.

Using SIMPLEC pressure-velocity coupling produced a predicted pressure rise that was 8% more negative when compared to the SIMPLE setting.

The Standard pressure discretization resulted in a pressure rise prediction that was unchanged from that produced by using the PRESTO! option.

The conclusions based on these few simulations were as follows:

- Default initial condition values were sufficient
- The cell-based gradient option provided a more stable solution than the node-based option
- The segregated implicit solver was more stable than the coupled solver
- SIMPLEC did not offer any advantage over SIMPLE pressure-velocity coupling
- Neither PRESTO! nor “Standard” pressure discretization provided an advantage over the other

Statistical Treatment

A statistical analysis of the fan speed ratios was used to determine which of the control factors was critical to achieving good model response. The mean, standard deviation, and signal-to-noise ratio (S/N) were calculated for each run. The S/N value was calculated from the equation:

S/N = 10 * log(Ybar2/s2) where: Ybar = the average of the speed ratios, S = standard deviation of the speed ratios

The figure below shows the calculated values of mean, standard deviation and S/N ratio for each of the twelve runs. Only the data from models using MRF Size Level 2 were included.

								Response - Fan Speed Ratio					
								Nominal-the-best					
								Outer Array Noise Factors					
	Inner Array - Control Factors							MRF Size -2					
Run#	MRFDen	Hybrid	NonMRFDen	DomSIze	FlowReg	BCType		Quality-1	Quality-2		Mean	Std Dev	S/N
1	1	1	1	1	1	1		0.903	0.907		0.905	0.00283	50.1
2	1	1	1	1	1	2		0.88	0.907		0.894	0.01909	33.4
3	1	1	2	2	2	1		0.972	0.979		0.976	0.00495	45.9
4	1	2	1	2	2	1		0.984	0.972		0.978	0.00849	41.2
5	1	2	2	1	2	2		0.995	0.984		0.990	0.00778	42.1
6	1	2	2	2	1	2		0.902	0.906		0.904	0.00283	50.1
7	2	1	2	2	1	1		0.91	0.934		0.922	0.01697	34.7
8	2	1	2	1	2	2		1.006	0.995		1.001	0.00778	42.2
9	2	1	1	2	2	2		1.017	0.971		0.994	0.03253	29.7
10	2	2	2	1	1	1		0.946	0.923		0.935	0.01626	35.2
11	2	2	1	2	1	2		0.936	0.972		0.954	0.02546	31.5
12	2	2	1	1	2	1		1.008	0.979		0.994	0.02051	33.7

Each control factor was evaluated for its ability to reduce response variability (high S/N ratio). The remaining factors were then evaluated for their ability to drive the mean closer to the target value of 1.00. The procedure is diagrammed in the chart below:

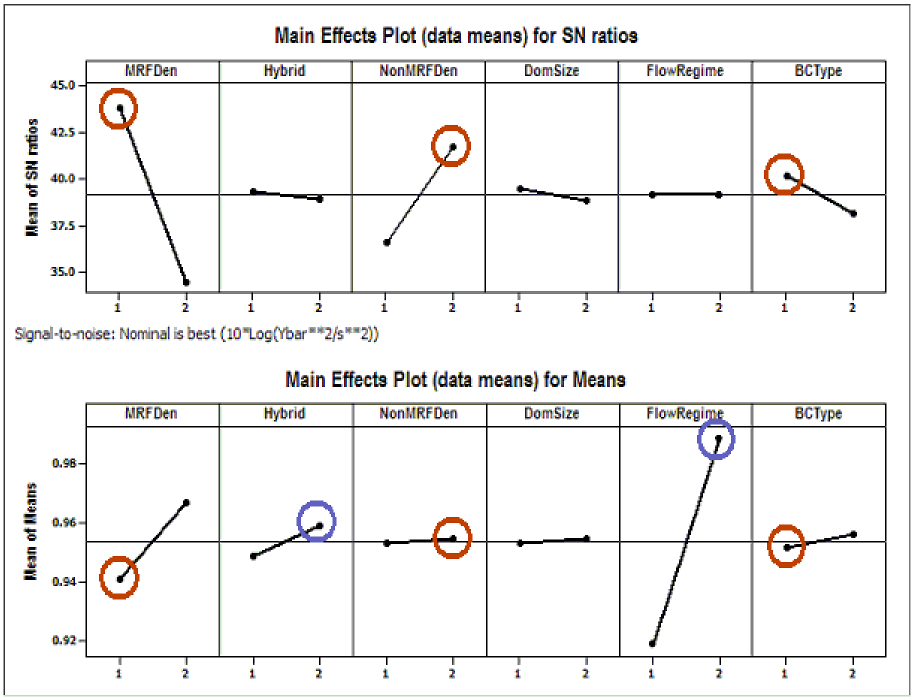

The S/N values for the six runs where the MRF Density level was 1 (Runs 1-6) were averaged, resulting in a value of 43.8. Then the S/N values for the six runs where the MRF Density was at level 2 (Runs 7-12) were averaged to obtain a value of 34.5. These two points were plotted on the "Mean of S/N ratios" chart. The same procedure was followed for each of the control factors. The mean values were then averaged in a similar manner and plotted on the "Mean of Means" chart. The factors that had the greatest effect on increasing the S/N ratio were determined and the factor level was set (red circles). The remaining factors were then evaluated to determine which ones had the greatest effect on driving the mean of the fan speed ratio towards 1.00 (blue circles). By evaluating each control factor in turn, it is seen that:

- MRF Density showed a strong correlation to improved S/N ratio when set to Level 1
- Hybrid mesh at Level 2 was slightly beneficial at moving the mean towards 1.00
- NonMRF Density at Level 2 showed a relatively strong effect on improving S/N ratio but practically no effect on improving the mean
- Domain Size had essentially no effect on either S/N ratio or mean
- Flow Regime at Level 2 showed a strong correlation to improving the mean. However, this is somewhat misleading since any model must be able to accurately predict a solution in either flow regime. This simply means that the model did a better job at predicting the actual flow at Flow Regime Level 2.
- BC Type did not have much effect on either S/N ratio or mean, and the two move in opposite directions. Level 1 provided a little more benefit to S/N ratio than Level 2 did to the mean.

Confirmation Data

The recommended levels for each of the control factors resulting from the above statistical analysis are shown in following table:

MRF Density	Hybrid	Non MRF Density	Domain Size	Flow Regime	BC Type
1	2	2	½	2	1

A new CFD model was created based on these settings. Since neither Domain Size level provided a distinct advantage, Level 1 was used since it allowed a simpler geometry and fewer cells resulting in a somewhat smaller model. In effect, the confirmation model was the same as that used for Run 5 except that the BC Type was changed to Level 1. The model was run at both Mesh Quality noise factor levels but only at MRF Size level 2. The runs were intended to confirm that the control factor settings would result in fan speed ratio predictions with a high signal-to-noise ratio and a value near 1.00. The resulting fan speed ratios, mean, and S/N ratio are shown below. In accordance with the modeling practice used for the baseline model, results are also shown using the 5% fan boost.

Run Without 5% Fan Boost	Fan Speed Ratio
Run 5-3 with BC Type 1	0.987
Run 5-4 with TC Type 1	0.988
S/N Ratio: 62.9	
Mean: 0.9875	

Run Using 5% Fan Boost	Fan Speed Ratio
Run 5-3 with BC Type 1	1.036
Run 5-4 with TC Type 1	1.037
S/N Ratio: 63.3	
Mean: 1.0365	

For comparison, fan speed ratios were calculated for the baseline model predictions for asymmetrical loading, with and without the 5% fan boost. Results for data surrounding specific diameter values in the range of 1.6 to 1.8 are shown in the table below. Also shown in that table are the factor level settings for the baseline model, according to the design of experiments definitions, as well as the resulting S/N ratios and response means. The preferred level settings were not used for the baseline model, and the MRF volume extended into nonaxisymmetric geometry. Though response was good, it was not as good as it could have been. This, in effect, validated the process: a baseline model was created that gave adequate results, with some modification (5% fan boost); the design of experiments and subsequent statistical analysis pointed to the critical modeling factors; a validation run confirmed that by using the proper values for the critical factors, accuracy was improved. The results shown in the preceding and following tables indicate that the 5% fan boost adjustment should not be needed if the proposed modeling guidelines are followed.

Fan Speed Ratio		
Baseline CFD Model, without 5% Fan Boost		
Flow, m^3/s	Press, Pa	Speed Ratio
1.3	140.1	0.927
1.12	236.1	0.942
0.935	335.1	0.959
0.689	450.1	0.959

Fan Speed Ratio		
Baseline CFD Model, with 5% Fan Boost		
Flow, m^3/s	Press, Pa	Speed Ratio
1.36	154.4	0.973
1.18	260.3	0.989
0.982	369.4	1.007
0.723	496.2	1.007

Original baseline model with large MRF

MRF Density	Hybrid	Non MRF Den	Domain Size	Flow Regime	BC Type
1/2	1	1	1	1/2	2

Fan speed ratio in D_s region of interest: 0.927 - 0.959

w/o Fan Boost	w/ Fan Boost
S/N = 35.8	S/N = 35.7
Mean = 0.947	Mean = 0.994

Task 4 - Demonstrate the performance and design versatility of a high performance fan

Background

Reduced engine emissions levels have typically brought with them increased demands on the performance of the cooling system components. This has often brought about an increased demand on the fan to provide more airflow at constant speed, through a more restrictive heat exchanger package. Mixed flow fans have been used by some truck manufacturers[6] as a way to provide more airflow, and help reduce the effect of the blockage of the outlet airflow path by an engine mounted directly behind the fan. Caterpillar had completed the development of a *Swept Blade Mixed Flow* (SBMF) fan as shown in the photo below-

This design concept incorporates a large tapered hub to induce the mixed flow, forward sweep blades, and a rotating shroud in a single casting. FIFO testing showed that at constant restriction and constant flow, the SBMF could operate at 20% lower fan speed than a typical axial fan, with 15% less input power, and 8 dB quieter. The purpose of this task was to design and build an SBMF fan to install in an off-road machine to demonstrate this performance in chassis, on a path that would lead to eventual volume production of the fan.

Machine related test results

The machine used for the SBMF fan evaluation was a Caterpillar backhoe loader. The cooling system configuration for this machine consisted of:

Component	Description
ATAAC	2 Tube Row , 5.5 fpi, 191.1 x 640 x 144
Radiator	5 Tube Row , 9 fpi, 619.5 x 633 x 104.76
Hydraulic Cooler	26 Plates, 9fpi, 77mm Core x 660 x 380.4
A/C Condenser	28 Tubes, 9fpi, 378.5 x 662.5 x 76.2
Fans	20"Kysor 20" LD9 BorgWarner SBMF Fan

Typical of many smaller off-road machines, there is little excess room in the engine compartment of this machine as shown below:

The fan is in the white oval. The radiator and heat exchangers are to the left, while the engine is mounted very close to the fan on the right.

This Pro-E drawing shows the radiator installation in more detail:

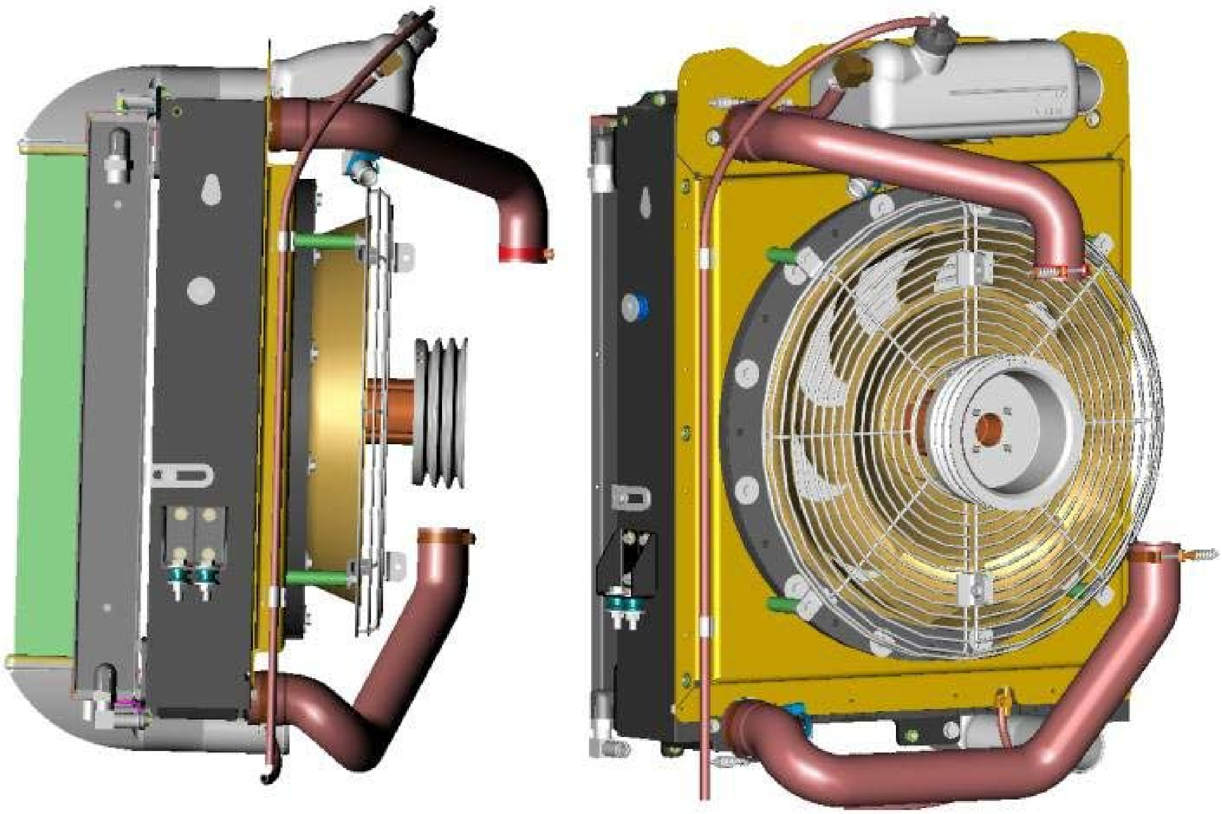

The photos below show the front and rear views of the prototype SBMF fan made as a rapid prototype aluminum casting:

The airflow of the SBMF fan was compared with two state of the art nylon fans in the machine installation. The Kysor fan is the production fan for this machine, and the baseline for our testing, while the LD9 is another 'state of the art' axial fan produced by Borg Warner. The table below summarizes the installation conditions for the various fan airflow performance tests.

Configuration				
	Shroud Type	Wire Fan Guard	Additional Grill	Airflow at 2400 fan rpm
SBMF_1	U Seal	yes	no	95.9 m3/min
SBMF_2	U Seal	yes	yes	87.9 m3/min
SBMF_3	U Seal	no	no	102.8 m3/min
SBMF_4	L Seal	yes	no	98.5 m3/min
SBMF_5	L Seal	yes	yes	86.2 m3/min
Kysor	**Knife Edge**	**yes**	**no**	**142.4 m3/min**
LD9	Knife Edge	yes	no	124.6 m3/min

In addition to the airflow measurements, sound as a function of airflow was also measured in the machine, as shown in the curves below:

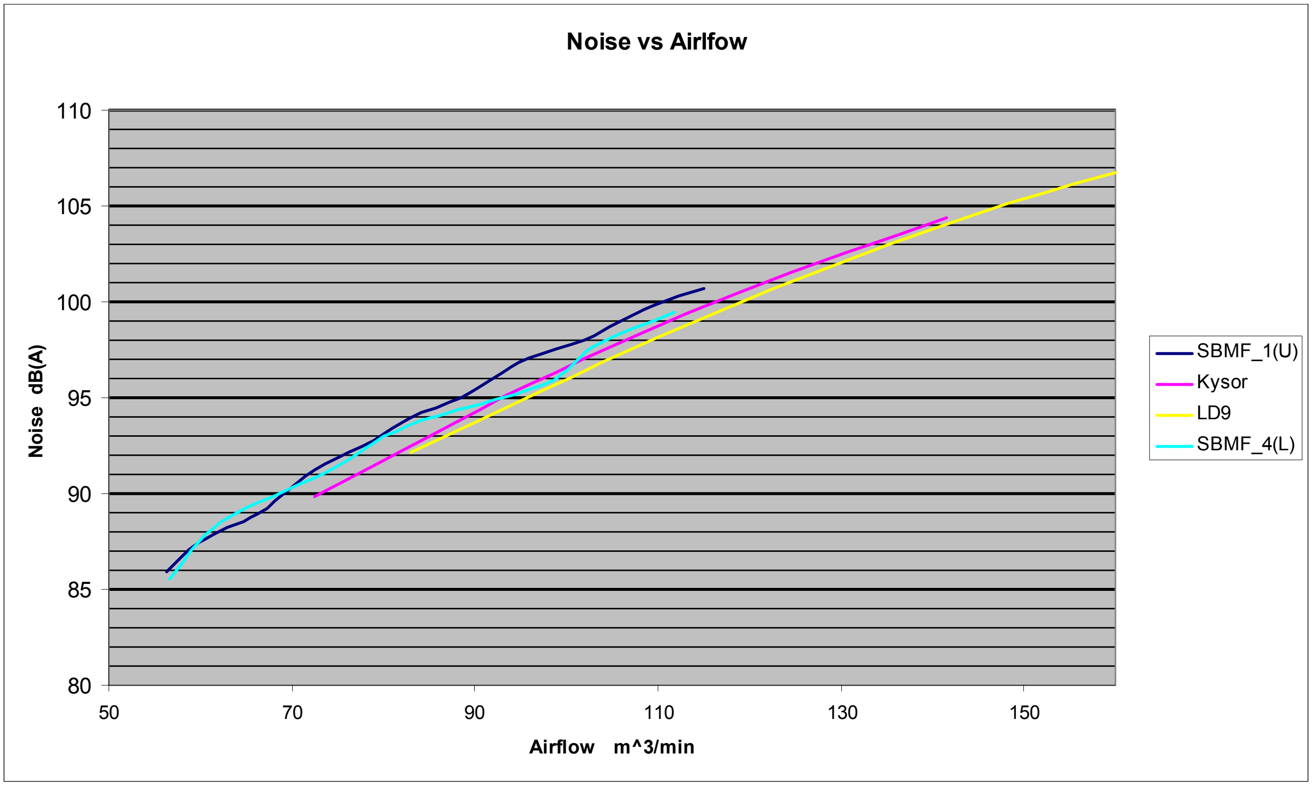

The results of these performance comparisons in the machine were clearly not expected, so the planned cooling system performance comparisons were suspended in favor of a series of controlled lab tests to determine the root cause of the loss of performance between previous lab FIFO fan performance data, and the in-chassis performance of the SBMF fan.

Lab test results

The baseline Kysor axial fan and the SBMF fan were both brought to a lab test facility for performance and noise comparisons to determine the root cause of the poor performance of the SBMF fan in the machine.

One problem we noted early in the lab testing phase was a difference in the location where the fan diameter was measured. The diameter of the production fan is 508 mm as measured across the maximum diameter of the blades as shown below:

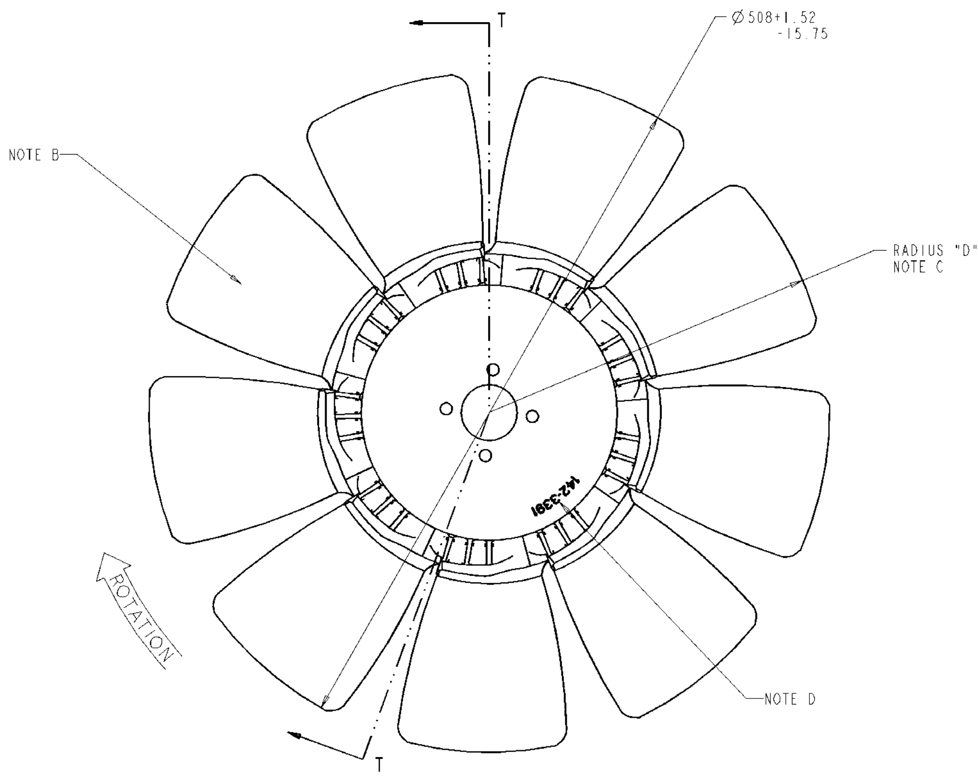

The SBMF design for this evaluation was sized as shown in the drawing below:

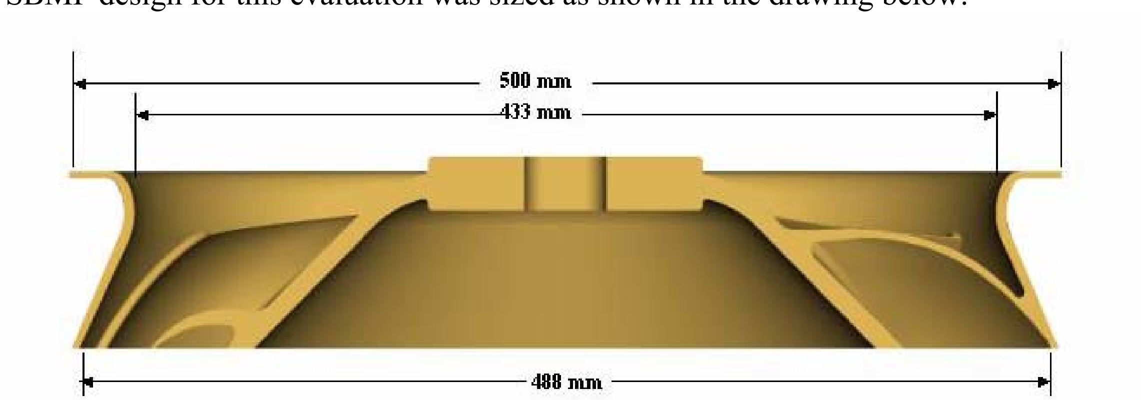

The shroud limited the diameter of the inlet ring to 500 mm, based on the space needed for the inlet seal. This limited the fan exit diameter to 488 mm. This fan exit diameter (not the 433 mm inlet diameter) is the reference diameter that was used to define the fan and scale the performance. The drawing below shows how a seal is attached to the shroud around the od of the SBMF fan inlet bell. To provide space for the seal without increasing the width of the fan shroud required compromising the fan diameter.

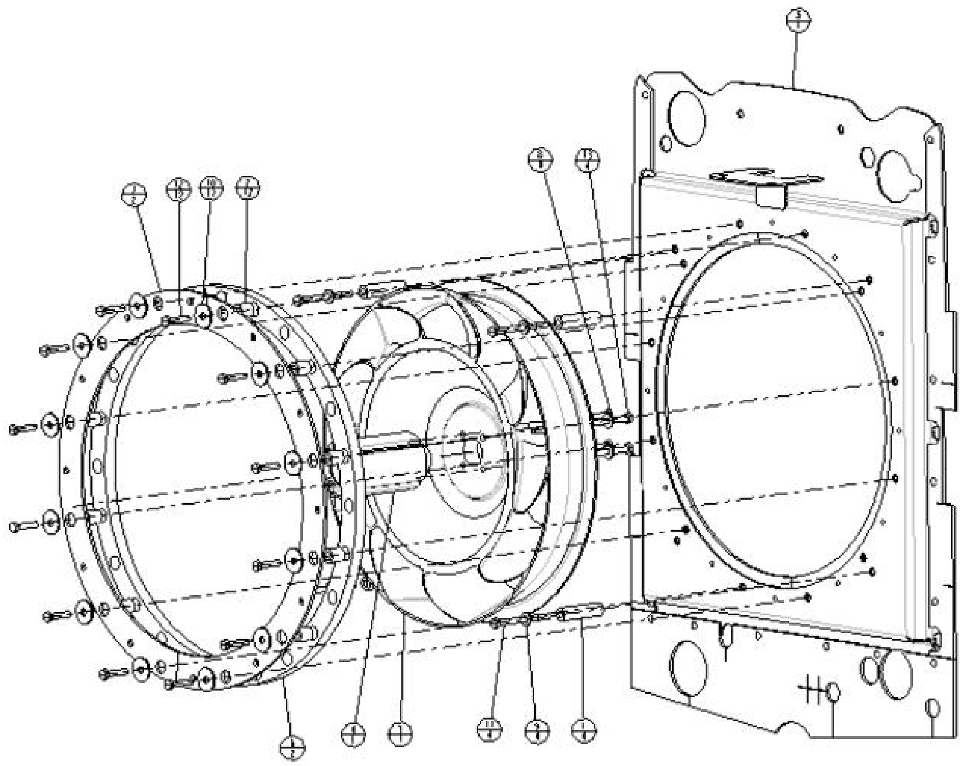

To insure that the fan performance as measured in the machine was truly typical of the performance to expect from the SBMF fan, back to back FIFO fan performance testing comparing the Kysor and SBMF fan were completed, and the results were plotted against prior measured SBMF fan data that was used to justify this development work, with the following results-

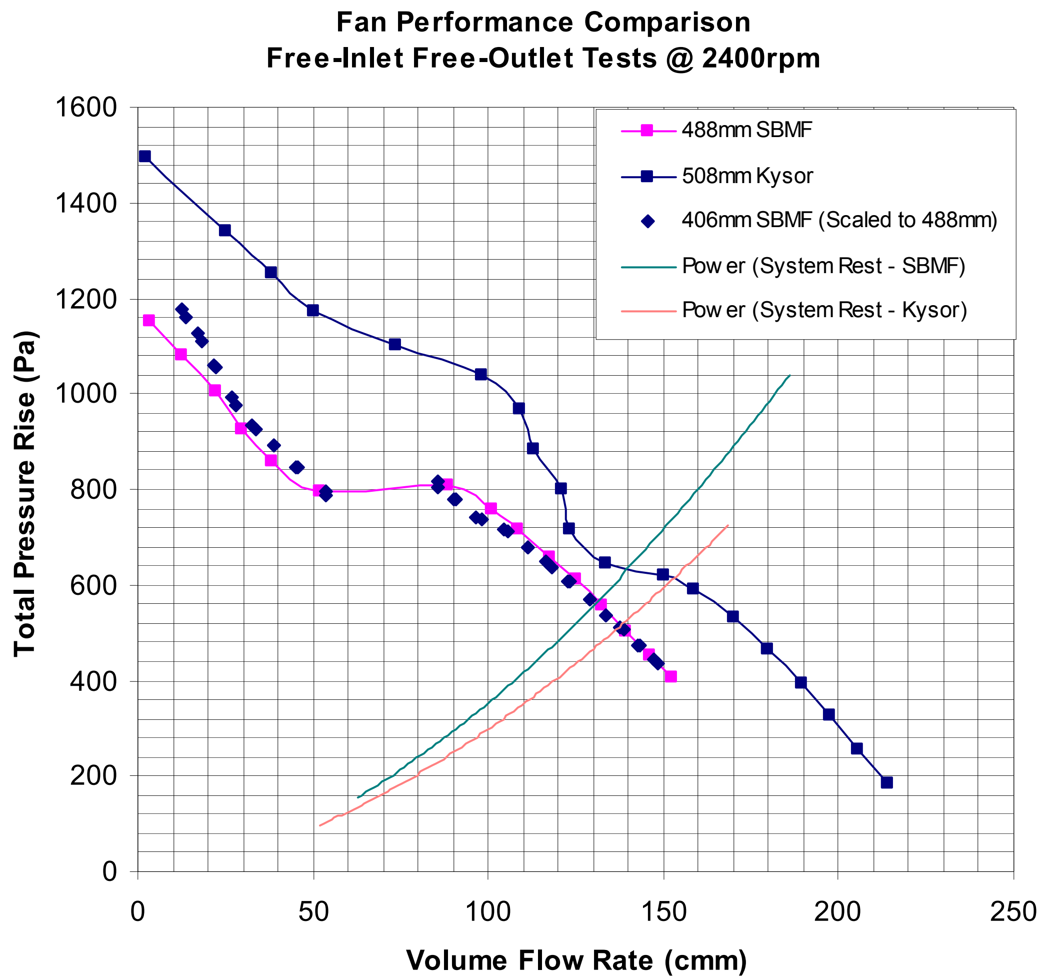

The airflow of the Kysor fan was 162 m3/min, while the airflow of the SBMF test fan was 145 m3/min if both fan curves were overplotted over the measured system restriction of the Kysor fan. Scaling the SBMF fan from 488 mm od to 500 mm od, would have increased the airflow to 153 m3/min. Based on FIFO data, the Kysor fan has an 11.7% flow advantage over the SBMF fan as built and running at the same speed, or a 5.9% flow advantage over an SBMF fan built to 500 mm outlet diameter.

The FIFO performance both verified that the protoype fan showed the same performance as earlier prototypes, but did not explain the poor performance shown on the machine. To identify the effect of installation on fan performance, a mockup of the installation was built as shown below:

The mockup dimensions duplicated the inside dimensions of the machine hood, and was equipped with a moveable wall downstream of the fan to duplicate the obstruction of the engine. The proximity of the fan to the front of the engine is shown in the drawing below:

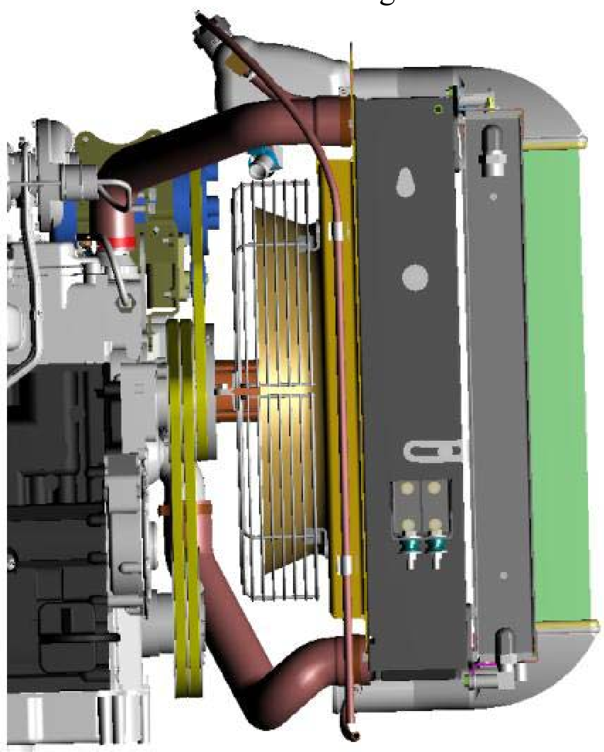

Fan airflow as a function of the distance from the back side of the fan to the downstream obstruction (representing the front of the engine) showed that the downstream obstruction had a much larger effect on the airflow of the SBMF fan than on the Kysor fan as shown below:

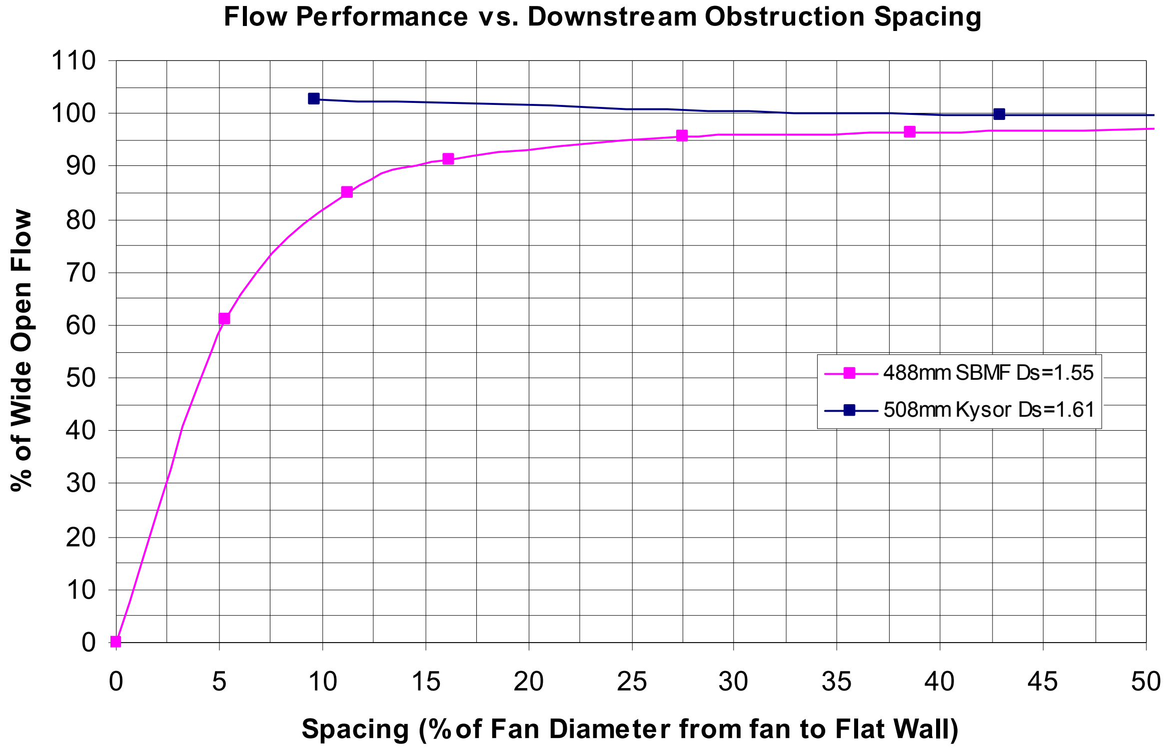

The sensitivity of the fan performance to downstream obstructions means this fan concept will not be an acceptable alternative for engine mounted cooling fans, and further development of the concept has been cancelled.

Fan efficiency

While the SBMF design was adversely affected by downstream obstructions, if the fan can be used in a system with a relatively unobstructed outlet, the potential efficiency improvements are significant as shown in the chart below:

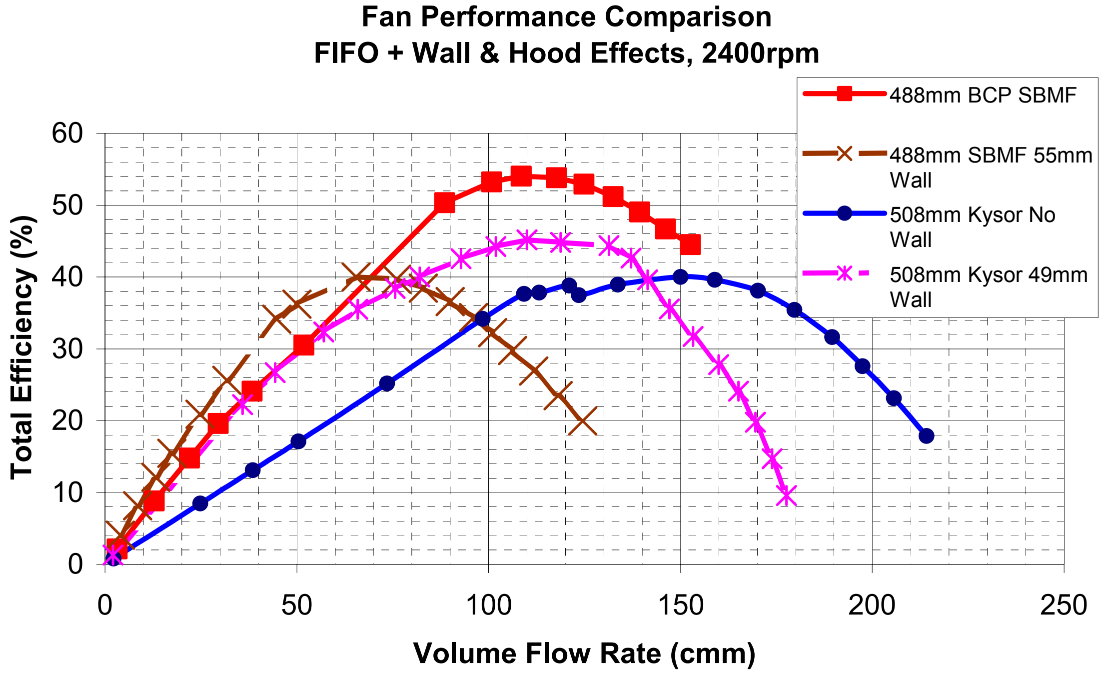

The peak total efficiency of the SBMF fan without downstream obstructions is approximately 54% over a relatively broad range, while the peak efficiency of the Kysor fan in the same installation is roughly 39%. The input power, under the same operating conditions, for the SBMF fan should be 72% of the power required for the Kysor fan.

Task 5 - Develop a high efficiency variable speed fan drive to replace existing slipping clutch style fan drives.

Predicting fuel savings of a variable speed fan drive

The value of demand fan drives, either in the form of variable speed or declutching fan drives, for reducing the fuel consumption of trucks and other on-road machines is well recognized. The cooling system of the truck is designed to maintain acceptable operating temperatures at very high load factors, at relatively low travel speeds, and high ambient temperatures. The net result is that the average truck has significantly more cooling system performance than needed during most operations. The value of variable speed fan drives in reducing the fuel consumption of off-road machines is less well understood, so the first challenge for this task was to provide a means for demonstrating the fuel savings potential of different variable speed fan drives. By combining machine performance, fan drive performance, and ambient temperature data, we can provide an accurate estimate of the potential fuel savings that a continuously variable speed fan drive can provide for a specific machine application.

A critical piece of input data is the relationship of fan speed vs. ambient temperature. The required cooling system fan speed is a function of the machine operation (load factor), the cooling system performance, and the ambient air temperature. Some form of modeling must be done to determine the relationship of fan speed vs. ambient temperature for the operating cycle being evaluated. In the curves below, the fan speed vs. ambient temperature was estimated for a machine that did not require air to air aftercooling (ATAAC), versus a similar machine requiring ATAAC to meet emissions requirements, with the ATAAC sized to require full fan speed to meet inlet manifold temperature requirements at 25°C ambient, vs. a system with a higher performance ATAAC designed to meet inlet manifold temperature requirements at full fan speed at 37°C ambient.

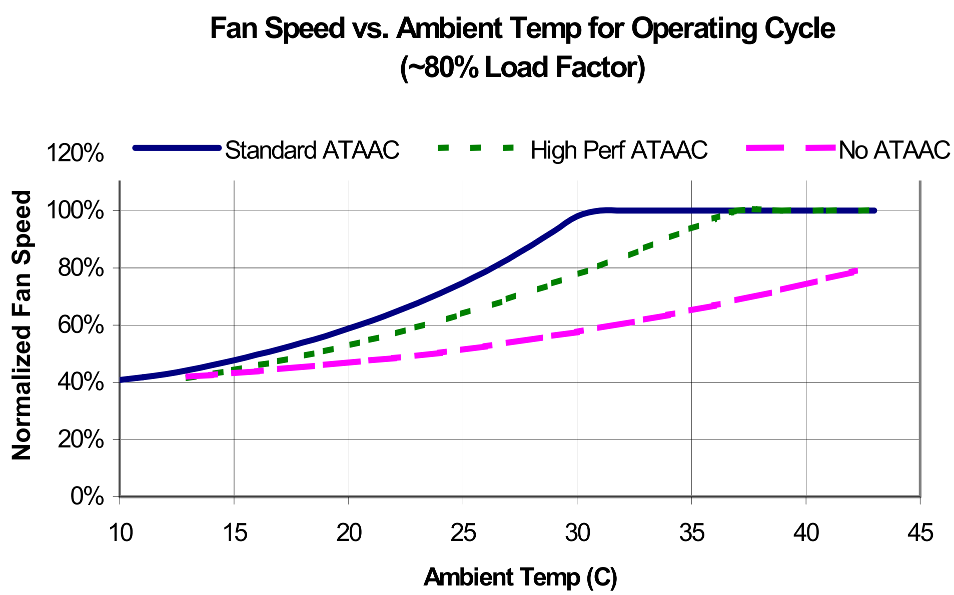

Figure 1. Fan Speed vs. Ambient Temperature

The next step is to determine the fan system (combination of fan and fan drive) input power as a function of fan speed. The figure below compares the input power of a conventional belt driven fan with the power LOSSES of a continuously variable speed fan drive utilizing a single ratio slipping clutch, versus a similar fan drive design with dual ratio clutches to minimize power losses. The fan input power for the clutch equipped fans would be the sum of the fan input power and the slip power (the power loss in the clutch). The chart compares the slip power of the two fan clutch concepts to contrast the losses between the two designs. The losses are very similar at high drive ratios (corresponding to high ambient temperatures), but the dual ratio concept significantly reduces drive losses at lower drive ratios (corresponding to lower ambient temperatures).

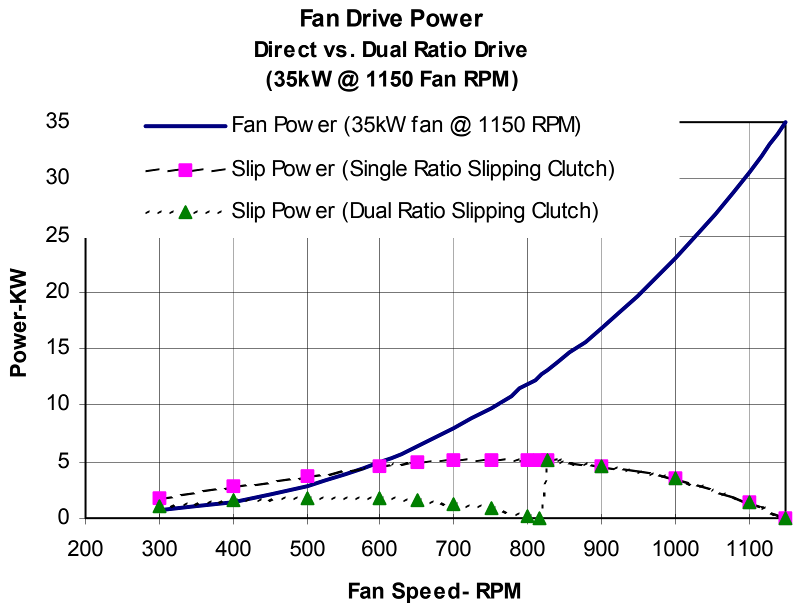

Ambient air temperature data, is available from from the EnergyPlus database on the U.S. Department of Energy's web site (http://www.eere.energy.gov/buildings/energyplus/). This location provides weather data from an ASHRAE/DOE data base used to calculate building energy savings. Temperature data is average *per hour* for each month of the year. This lets us look at first shift only, all three shifts, or only summer operation if we choose. ASHRAE has selected the data to provide *typical* temperatures for that hour, month, and location, so quoted temperatures are slightly different from Weather Bureau data, and may be 2 – 3°C different from what the Weather Bureau will quote for average or high temperature for the month. The partial screen shot below shows what data is available for worldwide locations:

Statistics for USA_IL_Peoria_TMY2
Location -- PEORIA IL USA
{N 40° 40'} {W 89° 40'} {GMT -6.0 Hours}
Elevation -- 199m above sea level
Standard Pressure at Elevation -- 98957Pa
Data Source -- TMY2-14842

WMO Station 725320

- Using Design Conditions from "Climate Design Data 2005 ASHRAE Handbook"
- If the design condition source is ASHRAE, the design conditions are carefully generated
- from a period of record (typically 30 years) to be representative of that location and
- be suitable for use in heating/cooling load calculations. If the source is not ASHRAE,
- please consult the referenced source for the reasoning behind the data.

Design Stat		Coldest month		HDB 99.6%		HDB 99%	Hm-DP 99.6%		Hm-HR 99.6%		Hm-
Units	{}	{°C}	{°C}	{°C}	{}	{°C}	{°C}	{}	{°C}	{m/s}	{°C}
Heating	1	-20.8	-17.7	-26.2	0.4	-19.9	-22.8	0.5	-17.2	12.7	-8.7

Design Stat		Hottest month		HMn-DB Range		CDB .4%	CMCWB .4%		CDB 1%	CMCWB 1% 2% 2%	
Units	{}	{°C}	{°C}	{°C}	{°C}	{°C}	{°C}	{°C}	{°C}	{°C}	{°C}
Cooling	7	10.7	33.5	24.8	31.9	24	30.4	23.1	26.2	31.5	25.3

Design Stat		X WS 1%	X WS 2.5%		X WS 5%	X Max WB		X Max DBX Min DB Sdev Max DB
Units	{m/s}	{m/s}	{m/s}	{°C}	{°C}	{°C}	{°C}	{°C}
Extremes	10.7	9.1	8.3	29.3	35.6	-24.5	1.7	3.9

- Monthly Statistics for Dry Bulb temperatures °C

	Jan	Feb	Mar	Apr	May	Jun	Jul	Aug	Sep	Oct	Nov
Maximum	10.6	13.9	26.1	30.0	31.7	33.3	36.1	32.8	31.1	27.8	23.3
Day:Hour	29:12	8:12	11:16	29:14	9:15	25:16	1:15	4:16	5:14	14:15	14:14
Minimum	-25.6	-15.6	-12.2	-3.9	1.7	8.9	10.6	9.4	6.7	-2.2	-10.0
Day:Hour	7:06	20:06	5:06	5:06	22:04	3:04	21:05	8:04	25:05	29:06	7:06
Daily Avg	-5.3	-2.3	2.8	11.0	15.4	22.0	23.7	22.4	18.5	12.2	4.8

- Maximum Dry Bulb temperature of 36.1°C on Jul 1
- Minimum Dry Bulb temperature of -25.6°C on Jan 7

- Average Hourly Statistics for Dry Bulb temperatures °C

	Jan	Feb	Mar	Apr	May	Jun	Jul	Aug	Sep	Oct	Nov
0:01- 1:00	-6.9	-4.0	0.7	8.0	11.6	18.4	19.9	19.0	14.9	9.2	3.1
1:01- 2:00	-7.1	-4.3	0.3	7.5	10.8	17.7	19.4	18.7	14.8	9.0	2.7
2:01- 3:00	-7.3	-4.7	0.0	7.1	10.3	17.5	19.2	18.3	14.5	8.7	2.2
3:01- 4:00	-7.5	-4.9	0.0	6.8	10.0	17.1	18.7	18.1	13.9	8.4	1.8
4:01- 5:00	-7.6	-5.1	-0.2	6.6	9.8	17.0	18.2	17.7	13.7	8.2	1.6
5:01- 6:00	-7.8	-5.3	-0.4	6.5	10.7	18.0	19.3	17.8	13.6	8.0	1.4
6:01- 7:00	-7.5	-4.8	-0.2	7.8	12.5	19.4	21.2	19.3	14.7	9.3	1.5
7:01- 8:00	-7.2	-4.3	0.7	9.5	14.3	20.8	23.1	21.2	16.8	10.7	2.5
8:01- 9:00	-6.9	-3.7	2.0	10.8	15.9	22.3	24.7	22.9	19.0	12.0	3.9
9:01-10:00		-5.8	-2.3	3.3	12.3	17.1	23.8	26.2	24.4	20.9	13.4
10:01-11:00		-4.7	-0.8	4.7	13.5	18.1	24.5	27.3	25.2	22.4	14.9
11:01-12:00		-3.5	0.6	5.6	14.3	19.2	25.2	28.3	26.0	23.1	16.3
12:01-13:00		-3.1	0.9	6.3	15.1	19.7	25.8	28.7	26.7	23.9	16.6
13:01-14:00		-2.7	1.2	6.8	15.6	20.2	26.6	28.9	27.1	24.3	17.0
14:01-15:00		-2.2	1.6	6.8	15.8	20.4	26.9	28.6	27.5	24.2	17.4
15:01-16:00		-2.7	0.8	6.6	15.4	20.5	26.9	28.5	27.1	23.8	16.3
16:01-17:00		-3.2	0.0	5.6	14.8	20.1	26.7	27.7	26.6	23.1	15.2
17:01-18:00		-3.7	-0.8	4.5	13.8	19.3	26.0	26.8	25.2	21.0	14.2
18:01-19:00		-4.1	-1.4	3.4	12.6	17.9	24.5	25.5	23.7	19.0	13.3
19:01-20:00		-4.5	-2.0	2.8	11.7	16.2	22.8	23.8	22.4	17.6	12.3
20:01-21:00		-4.9	-2.7	2.4	11.0	15.0	21.5	22.4	21.5	16.9	11.4
21:01-22:00		-5.2	-2.9	1.9	10.2	14.1	20.4	21.5	20.7	16.2	10.8
22:01-23:00		-5.5	-3.2	1.4	9.6	13.4	19.7	20.9	20.0	15.7	10.2
23:01-24:00		-5.8	-3.4	1.0	8.6	12.5	19.2	20.3	19.5	15.1	9.5
Max Hour		15	15	14	15	16	16	14	15	14	15
Min Hour		6	6	6	6	5	5	5	5	6	6

The fuel consumption for the belt driven fan is $fuel = fanpower * time(hours) * bsfc$ regardless of load factor or ambient temperature. The fuel consumed by the continuously variable speed drive is determined by calculating the fuel used in each hour/month combination (288 cells of data for 24 hour/day operation) for the year. For each hour/month combination we know the average temperature from the Energy+ data in the chart above. The ambient temperature determines the fan speed from the previous fan speed vs. ambient temperature curve. The fan input power is the sum of the required fan power plus the slip power (or drive losses). The total fuel consumed in a day is the sum of the fuel consumed in the individual 24 hourly segments (assuming the machine is used 24 hours/day). The individual hourly data was converted into monthly data by assuming the number of working days in a month (up to 30 days/month for high production machines) and assuming the machine was in use 80% of the time it was available.

Example fan drive fuel savings calculations

The machine to be evaluated is an off-road machine used in mining. The fan requires 35kW at 1150 rpm, and will be evaluated using the fan speed vs. ambient temperature relationships shown prevoiusly, for a work cycle that represents an 80% load factor (the machine burns 80% of the fuel that would be consumed if the machine were operating at rated speed and power). The fan drives to be considered are: direct drive, single ratio slipping clutch and dual ratio slipping clutch with the loss characteristics as shown previously, and the machine is assumed to be operating in the Midwest in ambient temperature conditions as shown previously. The machine is available for use 24 hours per day, 30 days per month, and is actually in use 80% of the time it is available. The fuel consumed to operate the cooling system under these operating conditions is:

Aftercooling	Ideal (no losses)	Dual ratio clutch	Single ratio clutch
Jacket Water	5427 liters/yr	9434 liters/yr	14214 liters/yr
Large ATAAC	7198 liters/yr	11243 liters/yr	16663 liters/yr
Small ATAAC	9813 liters/yr	14555 liters/yr	19770 liters/yr

To put these numbers in perspective, a 35kW fan would consume 61,824 liters/yr of fuel, out of a total machine fuel consumption of approximately 650,000 liters/yr. The “Ideal” fuel consumption is the power required by the fan itself, and assumes a drive that is 100% efficient. If the machine consumes 650,000 liters/yr of fuel, and the fixed ratio fan consumes roughly 62,000 liters of fuel/yr then the fuel consumption of the machine without the fan would be 588,000 liters/yr. Total machine fuel consumption would then become:

Aftercooling	Ideal (no losses)	Dual ratio clutch	Single ratio clutch
Jacket Water	593,427 liters/yr	597,434 liters/yr	602,214 liters/yr
Large ATAAC	595,198 liters/yr	599,243 liters/yr	604,663 liters/yr
Small ATAAC	597,813 liters/yr	602,555 liters/yr	607,770 liters/yr

Installing the single ratio fan clutch on a machine with a small ATAAC could reduce total fuel consumption from 650,000 liters/yr to 607,770 liters/yr, a savings of 6.5% in fuel consumption. The dual ratio clutch design considered would save 7.3%, and an ideal variable speed fan drive would save 8% of the total fuel consumed by the machine. The example machine represents a high percentage of engine output power being used by the cooling fan, but is not out of line with potential tier 3 losses on machines that are significantly constrained relative to frontal area, and must provide more cooling performance by increasing fan speeds. If our same example machine is used for eight hours/day, 20 days/month from the months of March through October, the fuel consumed by a fixed ratio fan would be 9,114 liters, vs. 4631 liters for a single ratio clutch. This is a 3.3% fuel savings, based on fuel consumption of the machine (not including the fuel consumption of the fan) of 130,667 liters during this same time frame.

Dual Ratio Mechanical Clutching Fan Drive

A fan drive uses power from the machine’s engine to spin the cooling fan. The cooling fan pulls air through the radiator, and other heat exchangers to cool the engine and other systems on the machine. The simplest type of fan drive consists of a pulley supported by bearings on a shaft mounted to the front of the engine. A set of v-belts connects the crankshaft pulley to the fan drive pulley, and the fan attaches to the fan drive pulley. This type of fan drive is called direct drive, and the fan speed is directly proportional to engine speed. With a direct drive fan, if the engine speed is high, the fan spins at a high speed regardless of the cooling system needs. However, the power used by a fan is proportional to the fan speed cubed, so running the fan at lower speeds when the cooling needs are low saves a significant amount of power. Since large earthmoving equipment can use 40kW or more to run the cooling fan at rated speed, significant savings in fuel can be realized by running the fan at only the speed necessary to cool the engine radiator and other cooling cores.

The dual clutch, variable speed (DCVS) fan drive was developed to become a higher efficiency alternative to the modulating single clutch fan drive currently available for large off-road machines. Other fan drive concepts have the potential for even better efficiency, like a variation of the hydrostatic, variable speed transmission as used in the the Bradley Fighting Vehicle, belt-type continuously variable transmissions (CVTs), toroidal infinitely variable transmissions (IVTs), magnetic clutches, and magnetorheological fluid fan clutches (MRF). Even variable pitch, constant speed fans would be a fuel savings over a constant drive ratio, constant geometry fan.

A significant constraint on the fan drive design is the allowable volume that the drive can occupy. This drawing shows the standard fan drive, whose only function is to support the weight of the fan:

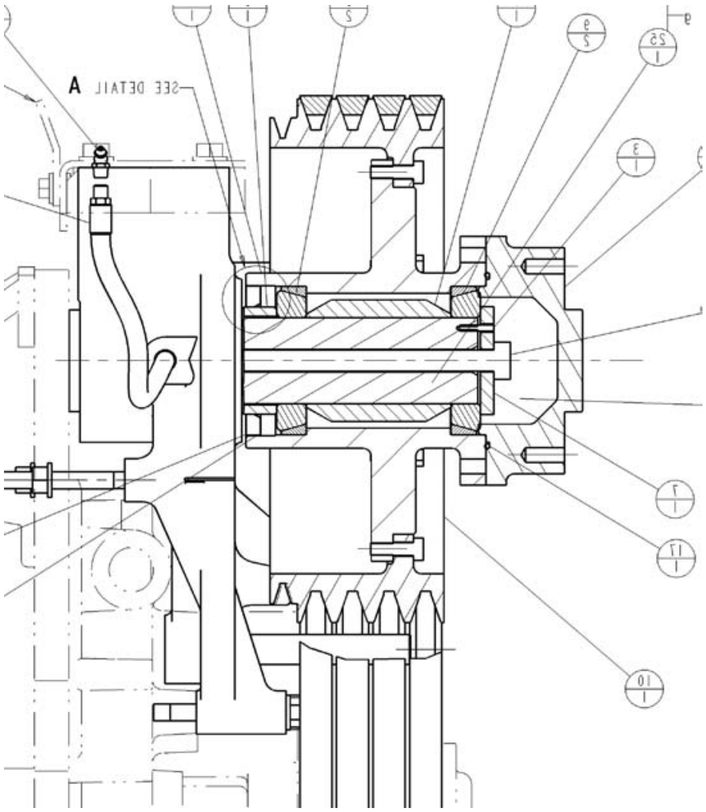

Any variable speed drive must be capable of directly replacing the existing fixed ratio fan drive. In addition, the fan belts may be used to drive other devices, like the air conditioning condenser or alternator, so a variable speed drive that changes the speed of the driving pulley would not be acceptable. The dual ratio clutch design shown below WAS able to provide a dual range variable speed drive, while mounting within the envelope of the constant speed fan drive:

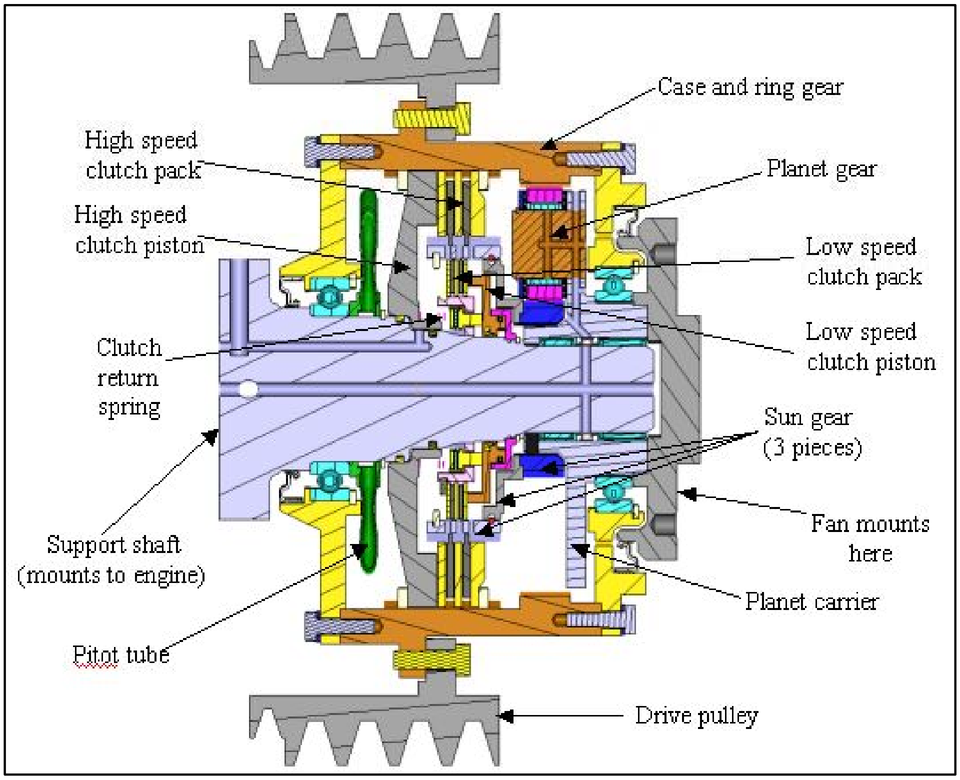

Concept overview

The DCVS fan drive design achieved variable speed through the control of two independent clutches and a planetary gear set. Power from the engine entered the drive through v-belts running on a drive pulley attached to the fan drive case. The fan drive input speed was directly proportional to engine speed as determined by the pulley ratio between the engine and fan drive. Hydraulically controlled clutches were modulated to change the power flow through the fan drive, thereby changing output speed (fan speed) even with a fixed input speed. The fan drive case was the ring gear for the planetary gear set, and the fan was attached the planet carrier. The figure above shows the cross sectional view of the fan drive.

Modulating the high-speed clutch, the clutch located between the ring gear and sun gear, controlled fan speed between 71% and 100% of pulley speed. Locking this clutch made all parts of the planetary set rotate at the same speed as the input pulley, thereby turning the unit into a direct drive system. The figure below shows the planetary gear set during operation of the high-speed clutch. The torque of the fan attempted to rotate the sun gear the opposite direction from the ring gear, so as pressure in the high speed clutch was reduced, the rotation of the sun gear slowed until it was nearly zero, relative to ground. This slowing of the sun gear caused a decrease in the planet carrier speed, which reduced the fan speed. With the sun gear speed at zero, the fan speed was about 71% of pulley speed. During the operation of the high-speed clutch as described above, the low-speed clutch was disengaged.

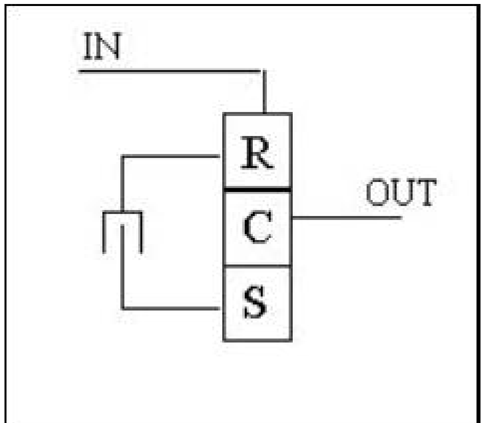

High-speed clutch

Modulating the low-speed clutch, the clutch between the support shaft and the sun gear, controlled the fan speed at and below about 71% of pulley speed. With the low-speed clutch fully applied, the fan speed would be about 71% of pulley speed. The figure bolow shows the planetary gear set during operation of the low-speed clutch. As with the high-speed clutch operation, the torque of the fan attempted to rotate the sun gear the opposite direction from the ring gear. Therefore, as pressure was released from the low-speed clutch, the sun gear began rotating in the direction opposite of the ring gear. This change in sun gear speed caused the planet carrier to slow, which reduced the fan speed. Fully releasing the low-speed clutch would cause the fan to rotate at a minimum speed determined by the clutch drag inside the fan drive. During the operation of the low-speed clutch as described above, the high-speed clutch was disengaged.

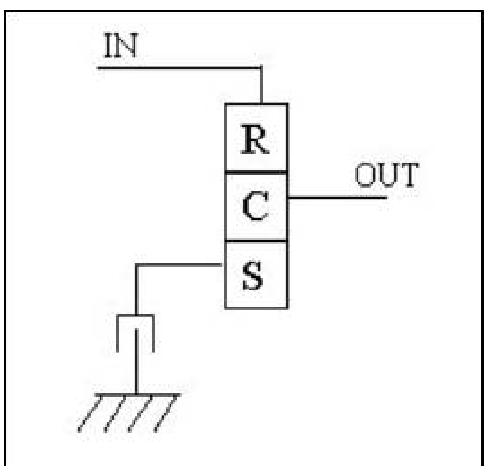

Low-speed clutch

Switching from the high-speed clutch to the low-speed clutch or vice-versa was done with the sun gear nearly stopped. Except for the transitioning between the two clutches, whenever one of the clutches was used, the other clutch was fully released.

The specifications of the DCVS fan drive are shown in table below. The modulating single clutch fan drive used on the D10R required a control pressure of about 275 kPa because the piston area of the clutch was large. To package the planetary gear components and extra clutch into the same envelope, the DCVS design had smaller clutch pistons that required higher control pressures to fully apply the clutch. Control pressures would need to be close to 2100 kPa, which was in line with transmission control pressures. The length of the DCVS fan drive was kept the same as the fixed ratio fan drive.

Weight (approx.)	52 kg
Length	248 mm (engine mounting surface to fan mounting surface
No. of control circuits	2
Power capacity (designed)	35 kW @ 1150 rpm
Max. fan weight	68 kg
Oil type	Transmission and Drive Train oil
Control oil requirement	2100 kPa @ < 4 lpm
Lube oil requirement	275 kPa @ < 11 lpm

Efficiency analysis

The total power consumed by a modulating clutch fan drive is the sum of the power used by the fan and the power lost in clutch slip, neglecting unintended losses such as gear friction and drag from the oil. However, neither fan power nor slip power is linear with respect to fan speed. The fan power is proportional to the fan speed cubed. The slip power is zero if the clutch is locked, increases as the fan is slowed because the slip increases, and then decreases as the fan is slowed further because the torque required to run the fan decreases faster than the increase in slip.
The figure below shows a comparison of slip power and total power for the DCVS and the modulating single clutch fan drive. This graph shows the fan drive power for a fan that requires 35kW to drive at 1150 rpm, driven by an engine operating at 1780 engine rpm. The clutch slip power for both units is zero at 1150 rpm because the drives are fully locked and no clutch slip is occurring. From about 1150 rpm down to about 820 rpm, the slip power is identical for the two drives, but at 820 rpm, the control of the DCVS fan drive switches from the high speed clutch to the low speed clutch. This switch significantly reduces the clutch slip power. At 800 rpm, for example, just over 5 kW of power is lost to clutch slip in the modulating single clutch fan drive, but only 0.25 kW of power is lost to slip in the DCVS fan drive. The effect of this difference between the fan drives can also be seen in the total power used by the fan drives as indicated by the fan drive input power curves.

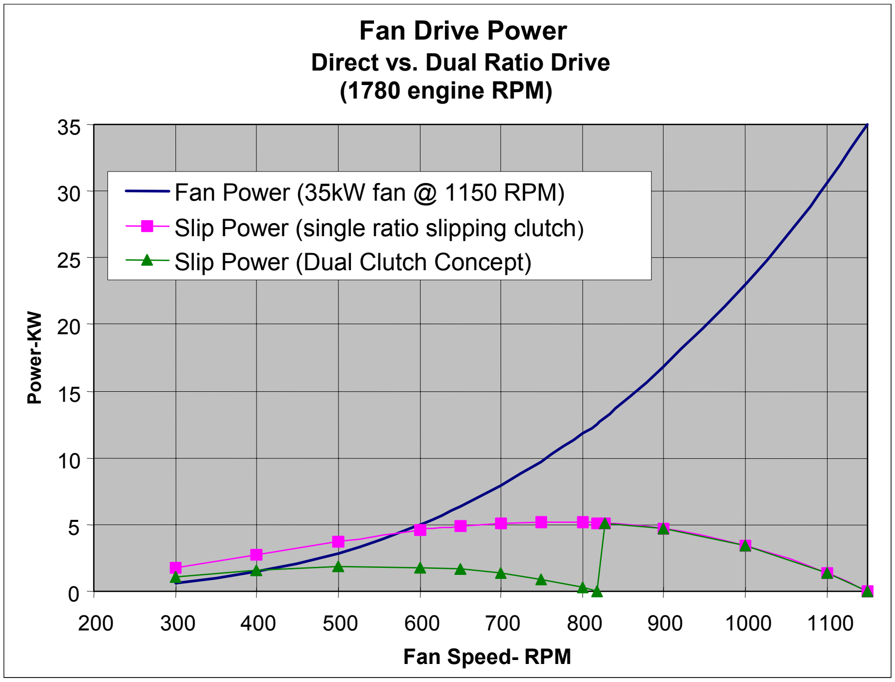

Note that both fan drives provide a tremendous efficiency advantage over a direct drive fan. With engine speed at 1780 rpm, a direct drive fan would consume 35 kW regardless of the engine's cooling needs. The graph clearly shows the efficiency gains from the DCVS fan drive in the speed ranges controlled by low speed clutch. The speed at which the low speed clutch locks (in this case 820 rpm) is determined by the planetary gear ratio. This ratio, or e-value, is the ratio of the number of teeth on the ring gear to the number of teeth on the sun gear, and was 2.45 for the concept design. The e-value could be changed to optimize the speed at which the low-speed clutch engages, but space limitations would only allow small changes.

Fuel savings benefits

Estimates of the fuel savings possible through the use of a DCVS and modulating single clutch fan drive were made to quantify the benefit of the variable speed fan drives over a direct drive fan. Fuel savings result from the fan speed being reduced when maximum cooling is not necessary. The use of electronic control systems makes matching fan speed to the cooling requirements of the machine a relatively straightforward process. Using the fuel savings estimation method described at the start of this task we estimated the fuel savings value of the DCVS for a specific application using the following estimation of fan speed vs. ambient temperature:

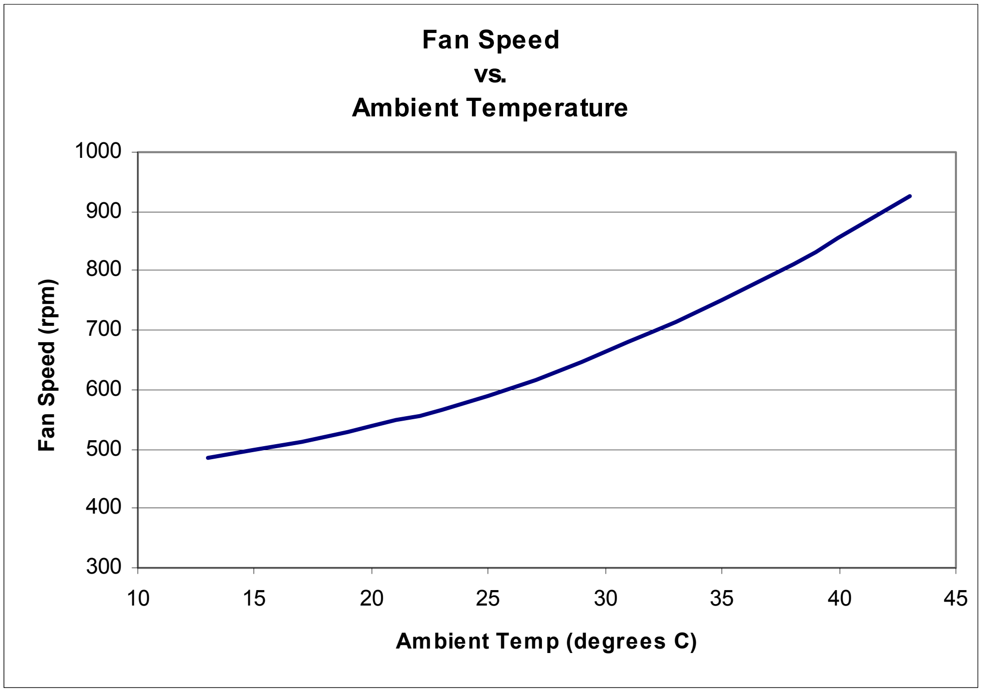

The ambient temperature for both the Peoria, Il, and Phoenix, Az, areas was taken from the DOE Energy+ web site, and a spreadsheet was used to calculate the fuel savings for both the single and dual ratio fan drives:

June											
Time	Hour	Temp C	Fan Spd	Fan Power kW	Fan Torque Nm	DCVS Slip Power kW	DCVS Fan Input Power kW	DCVS savings vs. Direct Drive kW	DCVS Fuel Savings vs. Dirct Drive L	DCVS 24 hr cum. fuel savings L	DCVS 8 hr cum fuel savings L
0:01- 1:00	1	18.4	522	2.9	53.1	2.08	5.0	26.0	6.19	6.19	
1:01- 2:00	2	17.7	517	2.8	51.9	2.06	4.9	26.1	6.21	12.40	
2:01- 3:00	3	17.5	515	2.8	51.6	2.06	4.8	26.2	6.22	18.62	
3:01- 4:00	4	17.1	512	2.7	51.0	2.05	4.8	26.2	6.23	24.85	
4:01- 5:00	5	17.0	511	2.7	50.9	2.05	4.8	26.2	6.24	31.09	
5:01- 6:00	6	18.0	519	2.8	52.4	2.07	4.9	26.1	6.20	37.29	
6:01- 7:00	7	19.4	531	3.0	54.9	2.10	5.1	25.9	6.15	43.44	
7:01- 8:00	8	20.8	544	3.3	57.6	2.12	5.4	25.6	6.09	49.52	
8:01- 9:00	9	22.3	560	3.6	61.0	2.15	5.7	25.3	6.01	55.53	6.01
9:01-10:0(	10	23.8	577	3.9	64.8	2.16	6.1	24.9	5.93	61.46	11.94
10:01-11:0	11	24.5	585	4.1	66.7	2.17	6.3	24.7	5.88	67.34	17.82
11:01-12:0	12	25.2	594	4.3	68.7	2.17	6.4	24.6	5.84	73.18	23.66
12:01-13:0	13	25.8	602	4.4	70.5	2.17	6.6	24.4	5.80	78.98	29.46
13:01-14:0	14	26.6	613	4.7	73.1	2.17	6.9	24.1	5.74	84.72	35.20
14:01-15:0	15	26.9	617	4.8	74.0	2.17	6.9	24.1	5.72	90.44	40.92
15:01-16:0	16	26.9	617	4.8	74.0	2.17	6.9	24.1	5.72	96.16	46.64
16:01-17:0	17	26.7	614	4.7	73.4	2.17	6.9	24.1	5.73	101.89	
17:01-18:0	18	26.0	605	4.5	71.1	2.17	6.7	24.3	5.78	107.68	
18:01-19:0	19	24.5	585	4.1	66.7	2.17	6.3	24.7	5.88	113.56	
19:01-20:0	20	22.8	565	3.7	62.2	2.15	5.8	25.2	5.98	119.54	
20:01-21:0	21	21.5	551	3.4	59.1	2.14	5.5	25.5	6.05	125.60	
21:01-22:0	22	20.4	540	3.2	56.8	2.12	5.3	25.7	6.10	131.70	
22:01-23:0	23	19.7	534	3.1	55.4	2.10	5.2	25.8	6.13	137.83	
23:01-24:0	24	19.2	529	3.0	54.5	2.09	5.1	25.9	6.16	143.99	

Example of fuel savings calculations

The fuel savings compared to direct drive were calculated for each hour in the day and summed. The highlighted columns show cumulative totals for a 24-hour/day operation, and for an 8-hour/day operation. Adjustments for the number of days worked in a month and the amount of running time in a day were made when the monthly totals were summed.

The following table compares the estimated fuel savings potential of both the single ratio and dual ratio fan clutches for a mild climate (Peoria) and a hot climate (Phoenix). Fuel savings estimates on other machines, and for an 8 hour day produced similar results…The use of a single ratio variable speed slipping clutch fan drive would reduce machine fuel consumption by between 5% and 6% compared to a fixed ratio fan drive, and the DCVS drive would reduce fuel consumption by another approximately 1%.

Operating Scenario	Modulating single clutch Fuel Savings % of total used	DCVS Fuel Savings % of total used
Machine in Peoria, IL 21Hrs/day, 360 days/year	5.9%	6.7%
Machine in Phoenix, AZ 21Hrs/day, 360 days/year	5.2%	6.2%

Design review results

The design of the DCVS was completed to the point of validating bearing and clutch life, as well as validating the performance and fuel savings potential of the device, as well as preliminary cost estimates. The design did not pass the gate review, and further development was terminated because:

Demonstrated fuel savings did not meet the requirements established for this task
Incremental fuel savings above a single ratio clutch were small, while the complexity of the DCVS was significantly greater than a commercially available single ratio clutch
The design and operation of the DCVS depended upon the availability of 2100kPa oil pressure for clutch operation. This would limit applicability of the DCVS to a limited range of mobile machines. To be applicable to all mobile machines, as well as stationary engine applications, the clutch must function over its entire operating range with a control pressure of approximately 400kPa.

Task 6 – Develop a cooling system air filtration device to allow the use of automotive style high performance heat exchangers currently in off road machines

Baseline Measurement of Susceptibility to Inorganic Debris Clogging

Cooling air system susceptibility to debris clogging (both organic and inorganic debris types) is a significant problem in certain machine applications and serves as a limiting factor in design of airside cooling packages with increased heat transfer performance. Without a clogging constraint, denser heat exchangers could be used to increase heat transfer capability by up to 30% with equivalent volume flow within the same frontal area. The overall task goal was to develop a means, mechanical or otherwise, to eliminate debris clogging in a typical high performance heat exchanger used in on-highway truck applications. This portion of the task is to compare the plugging tendencies of different core types, and evaluate the relationship of air velocity to core plugging. The air velocity to plugging relationship could be important, because the use of demand fans for fuel conservation and noise reduction will result in the cooling fan spending more time operating at lower speeds, so the cooling system air velocity will be correspondingly reduced.

The core types evaluated included-

'Conventional off road core' that serves as a baseline. This core is a 9 fin per inch core, with flat fins and canted and staggered tubes was used as the baseline since it was recommended as a very good compromise design for organic fouling in prior testing[7]. Photos of this core type are shown below. The dimensions in the left photo are in inches:

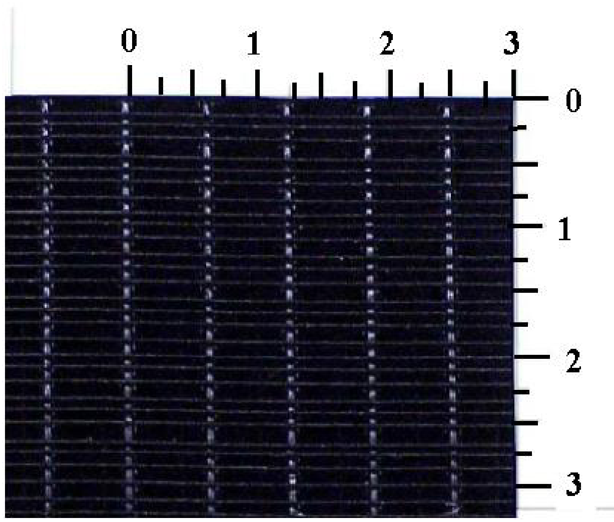

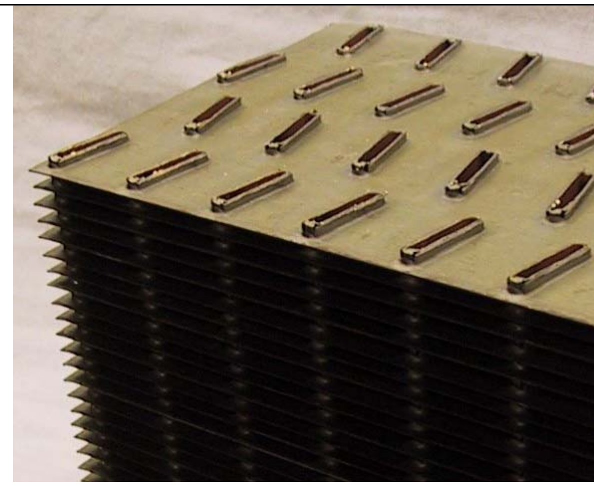

'High density ATAAC' This core is used in a specialized application in conjunction with filtration that limits the incoming debris to generally less than 10 microns. The cooling air side filtration is provided because this aluminum core has 18 louvered fins per inch versus a typical fin density of 9 fins per inch without louvers. This core has debris fouling problems in some applications. Photos of this core type are shown below. The dimensions in the photo are in inches:

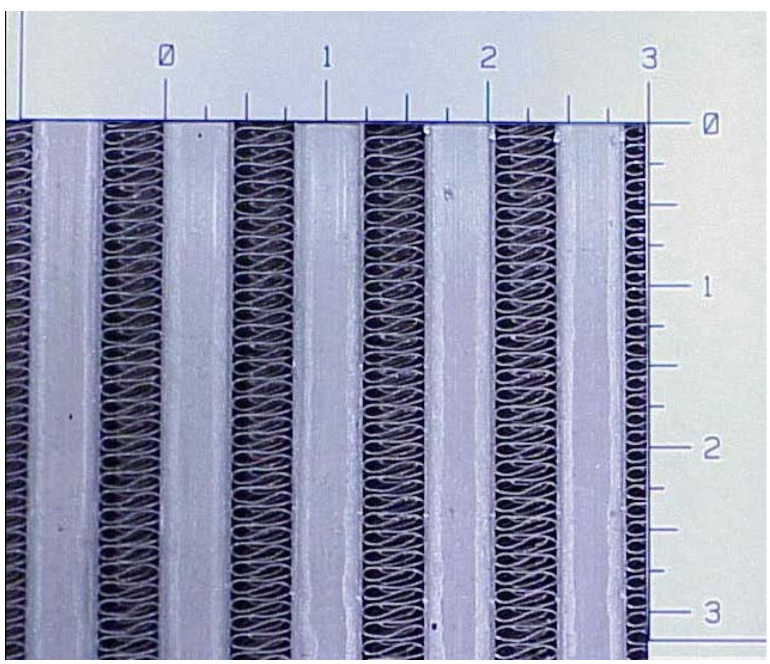

'Typical on-road truck' is constructed of copper and uses 16 louvered fins per inch on the air side. Photos of this core type are shown below. The dimensions in the photo are in inches:

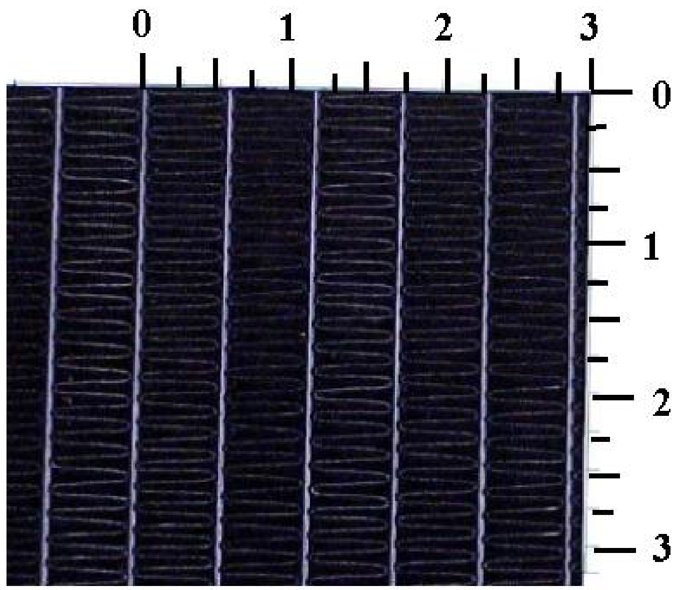

'High performance on-highway truck' uses the same fin design as 'typical on-highway truck', but uses a narrower tube spacing to provide more heat transfer within the same frontal area. Photos of this core type are shown below. The dimensions in the photo are in inches:

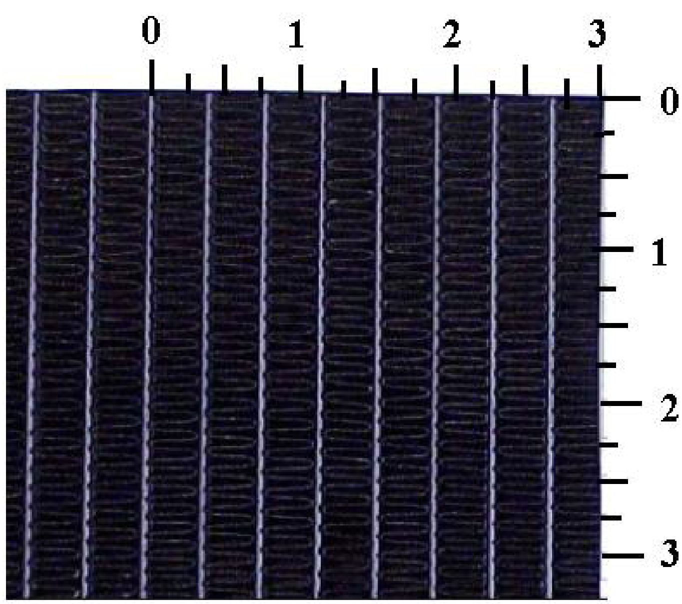

The overall test plan called for evaluating the debris fouling to be measured by measuring the change of pressure drop across the cores while dusty air was circulated through them. Before starting the test, the clean core pressure drop of each core was measured as shown in the curves below:

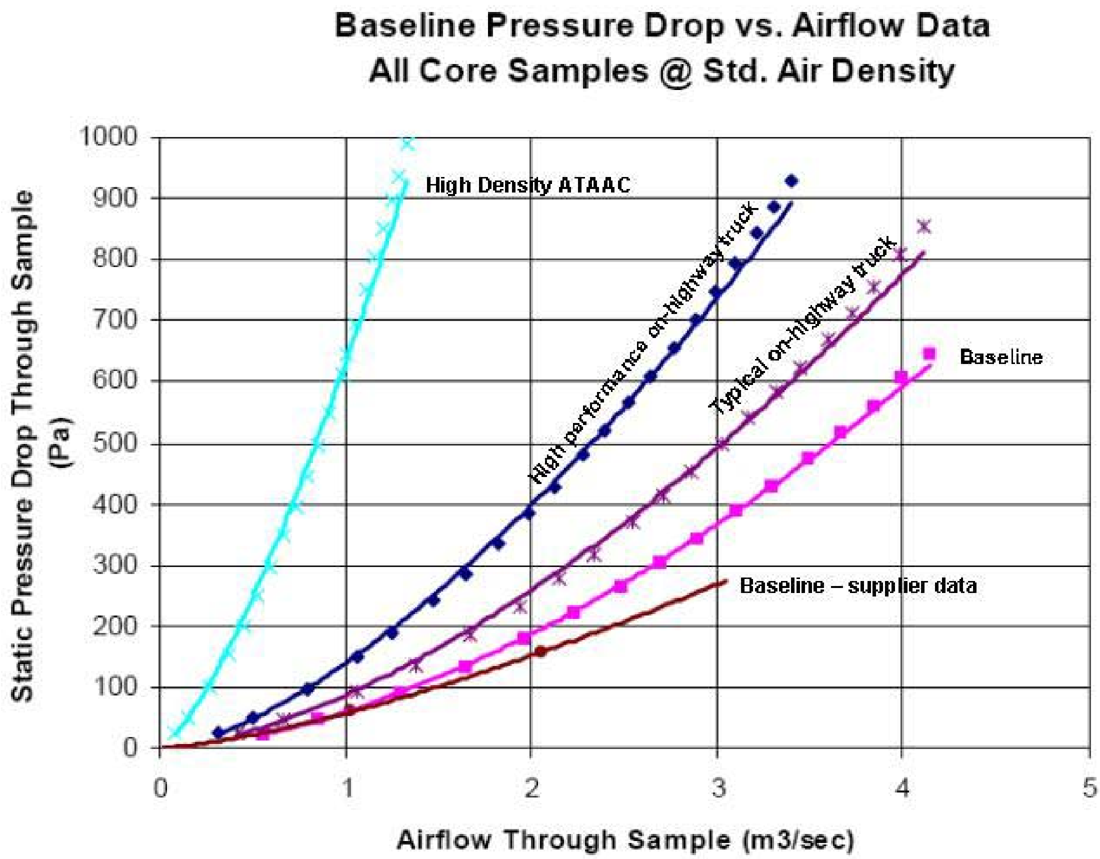

The measured results were as expected.

The second test series was established in the plan to serve as a relative comparison between cores geometries while holding clean approach velocity and debris injection rate constant. The procedure and debris used for this evaluation are explained in full in the **EXPERIMENTAL** section of this report. For this round of testing, the fan speed in the test facility was maintained at 1150 rpm, for a 'nominal' air flow rate, and debris was injected at a rate of 10 g/min. This resulted in the following comparison of pressure drop vs. time-

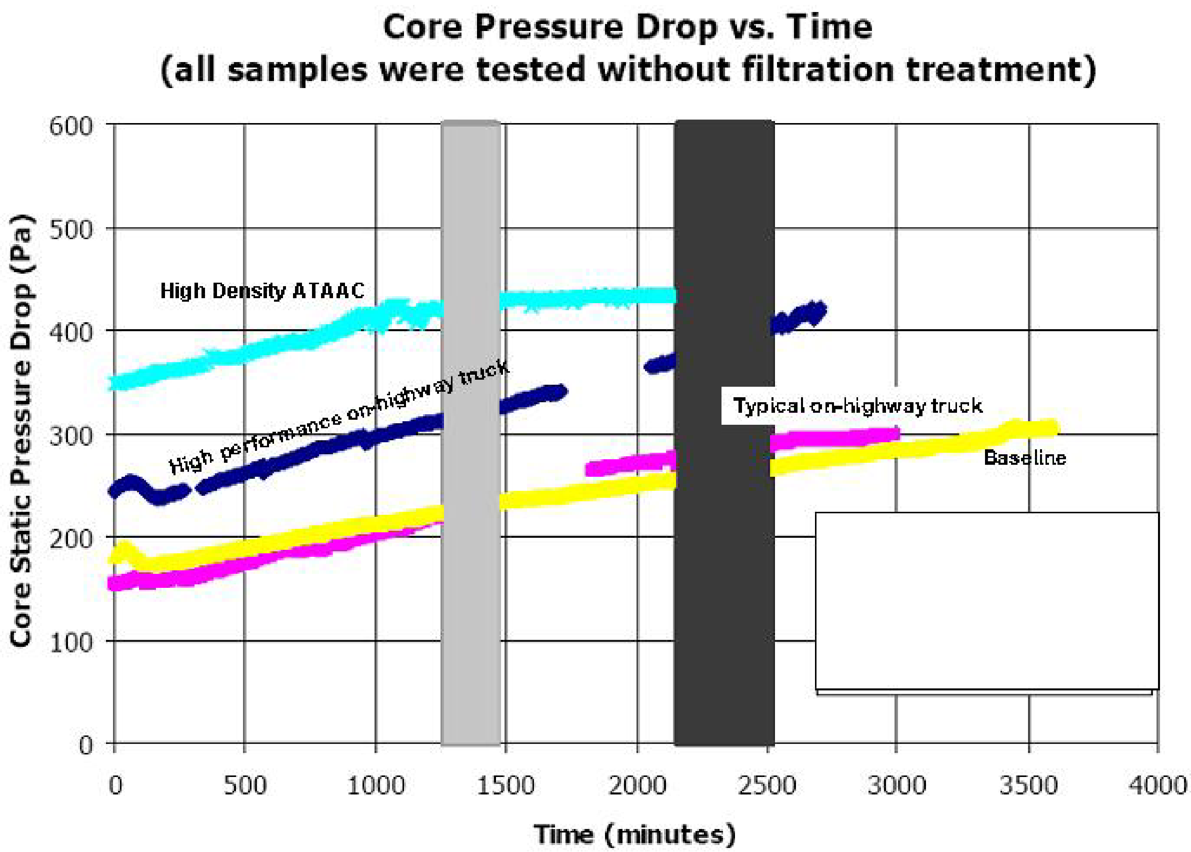

An initial investigation of the pressure drop vs. time data would indicate that the 'typical on-highway truck' core was very near the 'baseline' core in its sensitivity to dust fouling. This table looks at the *filtration* efficiency of each core by comparing total weight of the core plus dust at the end of testing, vs the initial weight of the core plus the amount of dust injected into the test facility. This data was, again, taken at 1150 rpm fan speed, with an injection rate of 10g/min:

Core	**Duration**	**Dust accumulated**	Dust added	Percent retained
Baseline	59 hours	6.801 kg	35.4 kg	19.21
Typical truck	61	6.159	36.6	16.83
High perf truck	44.4	6.342	26.6	23.81
High dens ATAAC	36	5.359	21.6	24.81

The following photos show the plugging effects vs. time of the baseline and high performance truck cores. All of the photographs were taken in the same area of the core (in the lower left quadrant, and the photos are of the inlet side of the core):

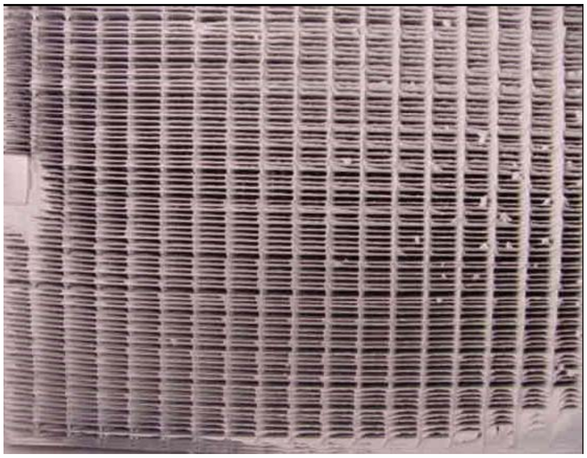	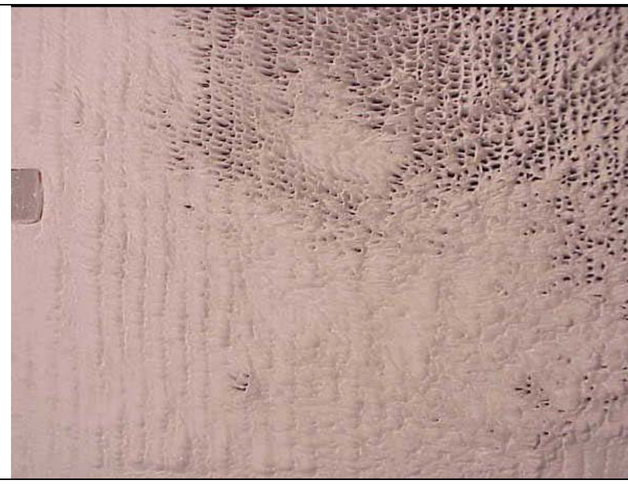
Baseline core at 21 hours	High performance truck core at 24.5 hours
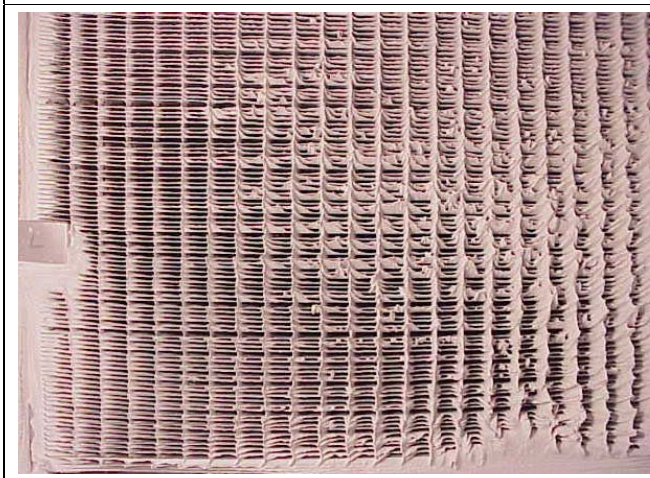	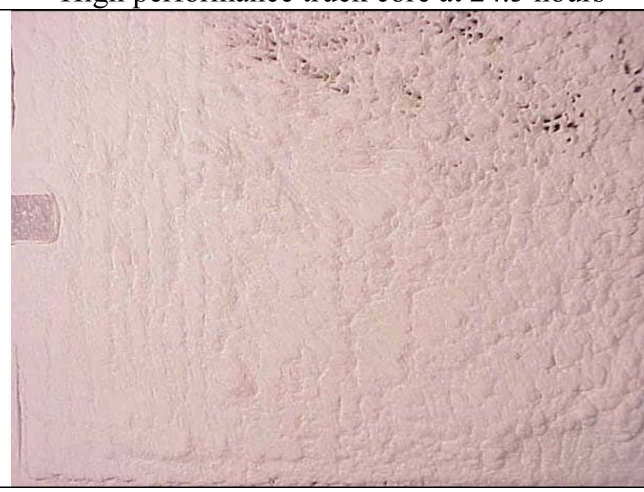
Baseline at 36 hours	High performance truck core at 39 hours

Clearly there is a significant difference in the visual core plugging that our data does not capture.

Field experience has shown that the typical truck core design is much more sensitive to dust accumulation than the baseline core, so a further series of tests was done at different fan speeds to evaluate the difference of face velocity on debris fouling. These tests were run at 575 rpm (slow), 1150 rpm (medium) and 1725 rpm (fast), with the following results:

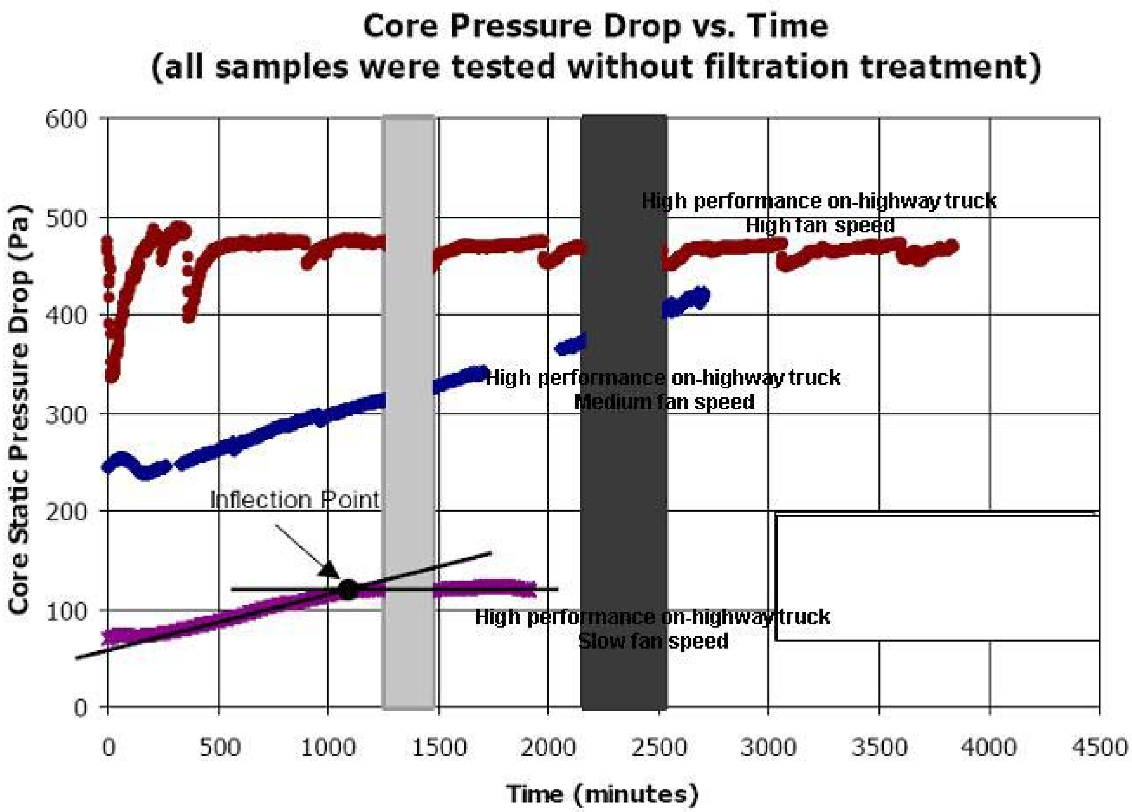

A comparison of the *filtration efficiency* of the same core at different airflow rates produced the following results:

Fan Speed	**Duration**	**Dust accumulated**	Dust added	Percent retained
575 rpm	32ours	1.774 kg	19.2 kg	9.24
1150	44.4	6.342	26.6	23.81
1725	64	2.370	38.4	6.17

Clearly, there is an effect of debris accumulation, where the debris tends to accumulate until some maximum level is reached, then it is ‘plugged’. Based on the fact that the debris accumulation is worse at lower flow rates, and the core tends to plug faster, all debris filtration development was done at the slow fan speed.

A photo comparison shows the significant difference of dust plugging as a function of velocity with the high performance truck core:

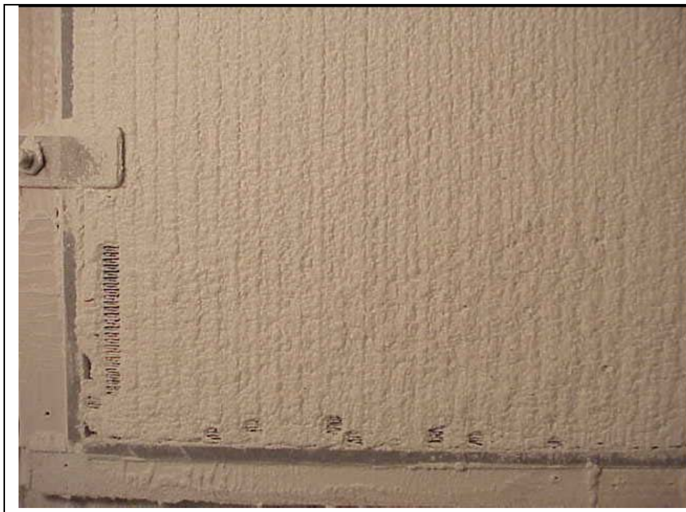	
High performance truck core at 575 rpm at 23 hours	High performance truck core at 575 rpm at 32 hours
	
High perf truck core at 1150 rpm at 24.5 hours	High perf truck core at 1150 rpm at 39 hours

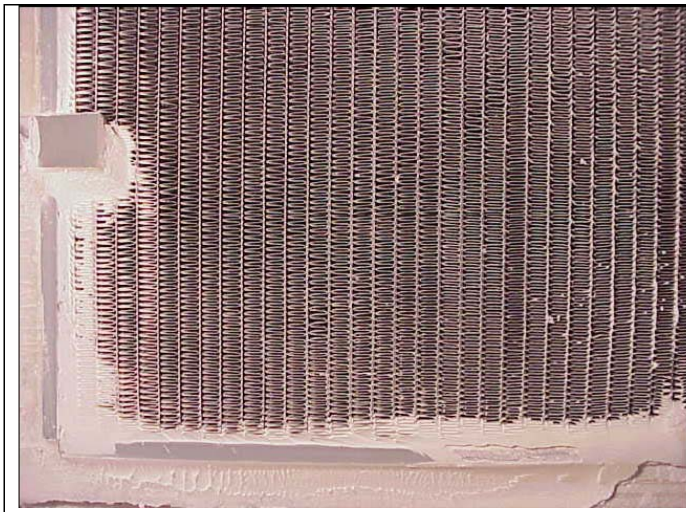

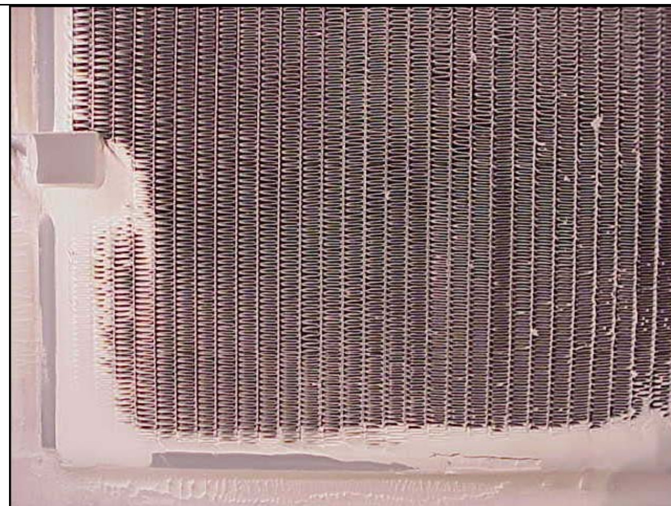

High perf truck core at 1725 rpm at 24 hours	High perf truck core at 1725 rpm at 42 hours

These comparisons again demonstrate the sensitivity of plugging to debris velocity, which both drove us to running further tests at low fan speed, and bring up a concern to increases in plugging problems with the use of temperature controlled variable speed fan drives which will allow the fan to run at significantly lower fan speeds for much of the time than the system would see with a constant ratio fan drive.

Radiator Filtration Developments

Increased fin spacing, and coarse screens are typical methods of providing a cooling system that is less sensitive to debris fouling[7]. The screens may either be static (an opening in a panel, with either perforated metal or woven screen material installed), or moving, as shown on the combine in the picture below:

The filtration capability is limited by the pore size in the screen. This kind of filtration can be effective for organic debris, and may be part of a radiator filtration *system* for off-road machines, but some other technology is needed for the sub 50 micron inorganic debris that can also be a significant fouling medium for off-road machines. The very fine nature of the debris means that filtration comparable to engine combustion air quality is needed to allow dense, high performance, heat exchangers to be used in off-road machines.

Radiator charge experiments

A significant effort was spent studying the effects of heat exchanger electrical charge on debris fouling. When we consider that the inorganic debris used for our test medium is typically less than 50 microns, it is doubtful that much of the fouling is the result of a large piece of debris trying to move through a small passage.

The first experiment involved grounding the core, to insure that there was no electrical charge on the surface of the core to attract dust. To evaluate the concept, the heat exchanger was cut in half and each side isolated from the test apparatus so that a side by side comparison could be done where one side was connected to earth ground while the other side was isolated as shown in the picture below.

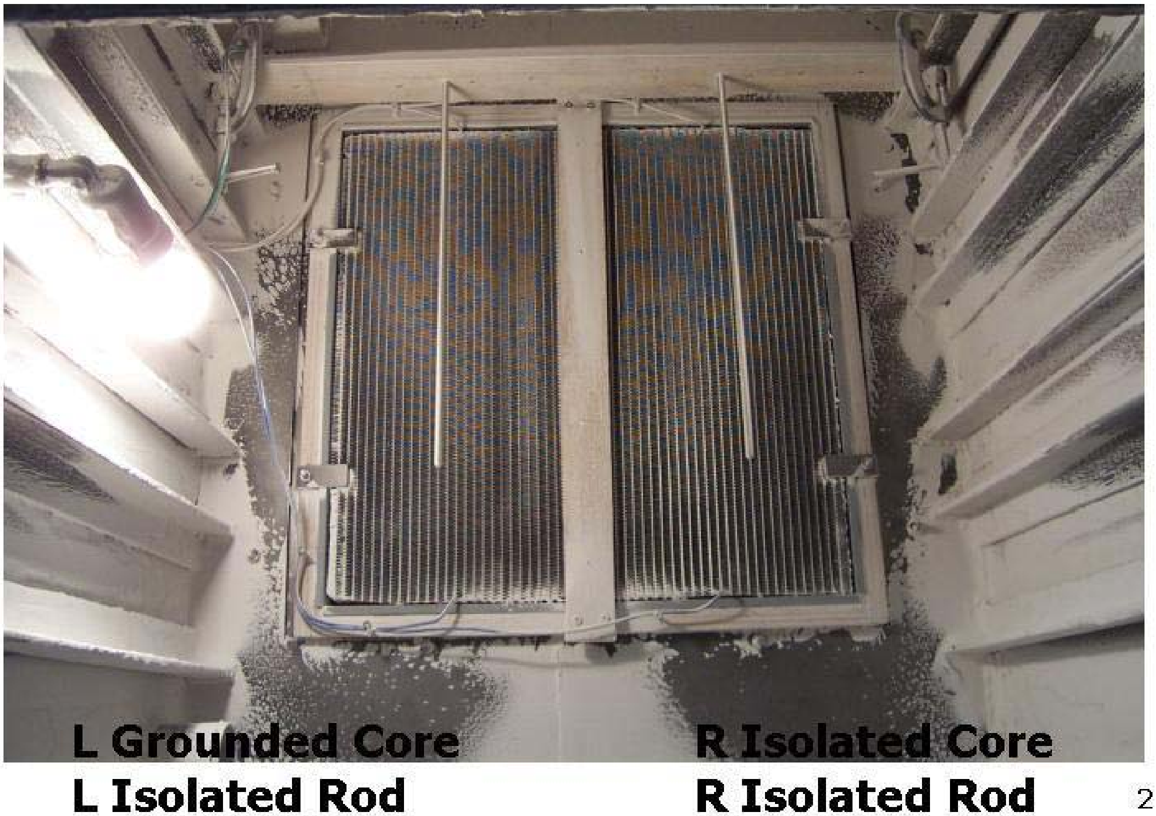

Both sides were wired to a junction box where voltage readings could be taken with a high voltage static meter (ETS model 212). At the same time, steel rods were wired in a similar fashion and suspended in front of the radiator cores. This was done to give a better view and a more controlled surface for a comparison of dust accumulation. This setup was run for 30 minutes and the voltages recorded during that time. Initially when the airflow was started, high voltages were observed on the core that was not grounded. When the debris was introduced into the system, the voltages started to drop quickly. After 30 minutes the charge on the core was significantly less than the initial charge as shown in the table below.

Time (minutes)	Top Right kvolts	Bottom Rt kv	Left Core kv
0	0	0	0
Turn on air circulation			
1	2.8	2.7	0
2	2.6	2.6	0
3	2.6	2.6	0
4	2.6	2.6	0
5	2.6	2.6	0

Add debris to airstream			
7	2.55	2.57	0
8	2.51	2.51	0
9	2.43	2.47	0
10	2.51	2.51	0
15	1.92	1.96	0
20	1.41	1.36	0
22	1.10	1.09	0
24	0.86	0.86	0
26	0.70	0.70	0
28	0.57	0.61	0
30	0.46	0.46	0

There was no observable difference of dust accumulation on the left isolated core and the right grounded core after 30 minutes of operation. Our conclusion is that grounding the cores has no value in controlling dust accumulation on the surface of the heat transfer surfaces.

The same set up that was used for the grounded effects was then used to observe the effects of an applied 24 V DC to the core. One side of the core was left grounded, while the voltage was applied to the other side. The right side of the core was wired in series with a 1 K Ohm resistor and then hooked up to a 24 V DC power supply. This was run for approximately 1 hour and 40 min without showing any observable difference in accumulation of dust on the left or right side of the core. Our conclusion is that the application of low voltage DC to the cores has no value in controlling dust accumulation on the surface of the heat transfer surfaces.

The same set up that was then used to observe the effects of an applied 24 V AC to the core. One side of the core was left grounded, while the voltage was applied to the other side. The right side of the core was wired in series with a 1 K Ohm resistor and then hooked up to a 24 V AC power supply. This test was run for approximately 1 hour and 40 minutes with no observable difference between the grounded side and the applied voltage side. Our conclusion is that applying low voltage AC the cores has no value in controlling dust accumulation on the surface of the heat transfer surfaces.

High pressure air knives with ionization

Two air knives were installed 200 mm in front of the radiator cores. They were fed by shop air regulated to 400 kPa . One of the air knives was equipped with an ion emitter so that its air stream carried the ions to the core face as shown in the photo below.

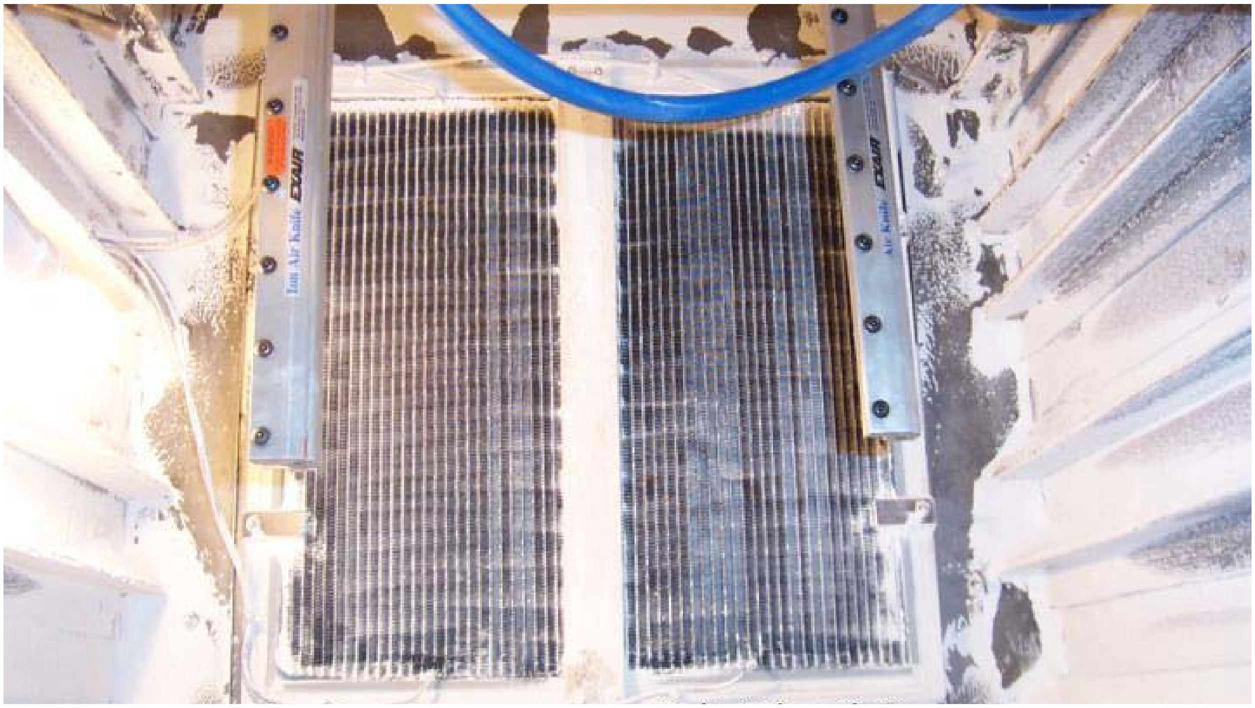

Left – Air knife + ions; Right – Air knife

During the course of this test, a high voltage meter was used to record any charge that was induced on the radiator core. The data in the table below shows that the air knife with the ions did have a neutralizing effect on the induced voltage on the left core. The right core without the ions did have periods throughout the test where high voltages were measured. Regardless of the voltages seen on the core, there was no observable difference in the rate of dust accumulation on the face of the core. However, it was evident that the areas that were being sprayed with high pressure air remained clean and open. This test was terminated after 2 hours and 14 minutes.

Time (min)	Top rt. kV	Top lt kV	Test conditions			
10	1.65	0.48	400kpa air	Ions	Fan on	No dust
11	0.54	0.20	400kpa air	Ions	Fan on	No dust
13	0.60	0.19	400kpa air	Ions	Fan on	No dust
16	0.80	0.20	400kpa air	Ions	Fan on	No dust
20	0.89	0.18	400kpa air	Ions	Fan on	No dust
22	1.07	0.20	400kpa air	Ions	Fan on	No dust
24	0.15	0.05	No air	Ions	Fan on	No dust
28	0.08	0.04	No air	Ions	Fan on	No dust
30	0.07	0.04	No air	Ions	Fan on	No dust
31	0.45	0.11	400kpa air	Ions	Fan on	No dust
32	0.62	0.14	400kpa air	Ions	Fan on	No dust
33	0.60	0.07	400kpa air	No Ions	Fan on	No dust
34	0.74	0.06	400kpa air	No Ions	Fan on	No dust

35	0.35	0.02	400kpa air	No Ions	Fan off	No dust
36	0.05	0.02	400kpa air	No Ions	Fan off	No dust
40	0.04	0.02	400kpa air	No Ions	Fan off	No dust
41	0.09	0.06	400kpa air	Ions	Fan off	No dust
42	0.07	0.06	400kpa air	Ions	Fan off	No dust
43	0.04	0.02	400kpa air	No Ions	Fan off	No dust
44	0.04	0.02	No air	No Ions	Fan off	No dust
45	0.03	0.02	No air	No Ions	Fan off	No dust
46	2.00	0.30	No air	No Ions	Fan on	No dust
47	1.50	0.20	No air	No Ions	Fan on	No dust
48	0.11	0.04	No air	No Ions	Fan on	No dust
49	0.06	0.04	No air	No Ions	Fan on	No dust
50	0.28	0.07	400kpa air	No Ions	Fan on	No dust
52	0.30	0.06	400kpa air	No Ions	Fan on	No dust
54	0.43	0.07	400kpa air	No Ions	Fan on	No dust
56	0.56	0.07	400kpa air	No Ions	Fan on	No dust
58	0.83	0.18	400kpa air	Ions	Fan on	No dust
60	0.79	0.15	400kpa air	Ions	Fan on	No dust
61	1.70	0.26	400kpa air	Ions	Fan on	Dust
62	2.00	0.3	400kpa air	Ions	Fan on	Dust
63	2.00	0.35	400kpa air	Ions	Fan on	Dust
64	1.88	0.33	400kpa air	Ions	Fan on	Dust
65	1.97	0.21	400kpa air	No Ions	Fan on	Dust
66	2.00	0.24	400kpa air	No Ions	Fan on	Dust
67	2.00	0.31	400kpa air	Ions	Fan on	Dust
69	2.04	0.33	400kpa air	Ions	Fan on	Dust
70	1.98	0.24	400kpa air	Ions	Fan on	Dust
110	2.04	0.17	400kpa air	Ions	Fan on	Dust
144	2.00	0.14	400kpa air	Ions	Fan on	Dust

Ultrasonics

An ultrasonic speaker "YardGard" made by Bird-X for repelling small animals, was placed upstream from radiator face. This device was powered during the test to see if it affected the rate of dust accumulation. There was no observable effect of dust accumulation by having this ultrasonic device running (below left). Even the speaker cone of the ultrasonic device was covered with dust (below right).

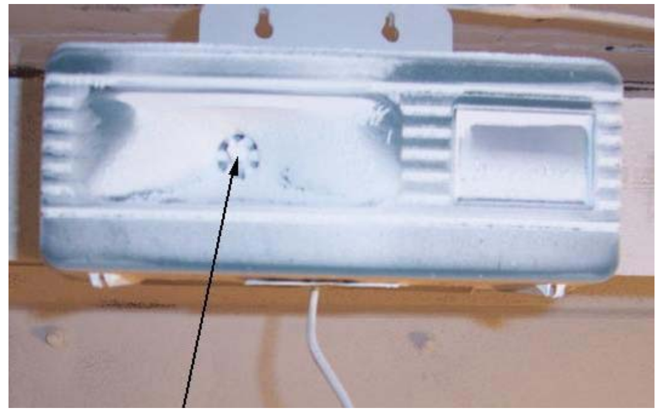

Application of +/- ions

A Milty ZeroStat 3 ion gun was used to apply ions to the face of the core. This device could produce either + ions or – ions. Even though this device could produce ions and achieve a very high voltage, it couldn't be sustained on the face of the core. The charge would dissipate within a second. It was clear that a continuous source of ions would be needed, much like the ion generator on the air knife.

Vibration

A Cleveland Vibra Might pneumatic shaker was mechanically fastened to the face of the radiator core with four bolts that went through the core to a plate and the back side of the core. This pneumatic shaker was run at short bursts over long intervals to see if it would clean the accumulated dust off. After one hour of dust accumulation, the shaker was energized for 10 seconds. Most of the debris was dislodged and worked its way through the core. Even though this method proved effective, it would not be practical because of the structural limitations of the heat exchanger.

High Voltage (Electrostatic Precipitation)

Three grids 300mm by 300mm were built using galvanized wire cloth with a spacing of 6 mm between individual wires. As shown in the schematic below:

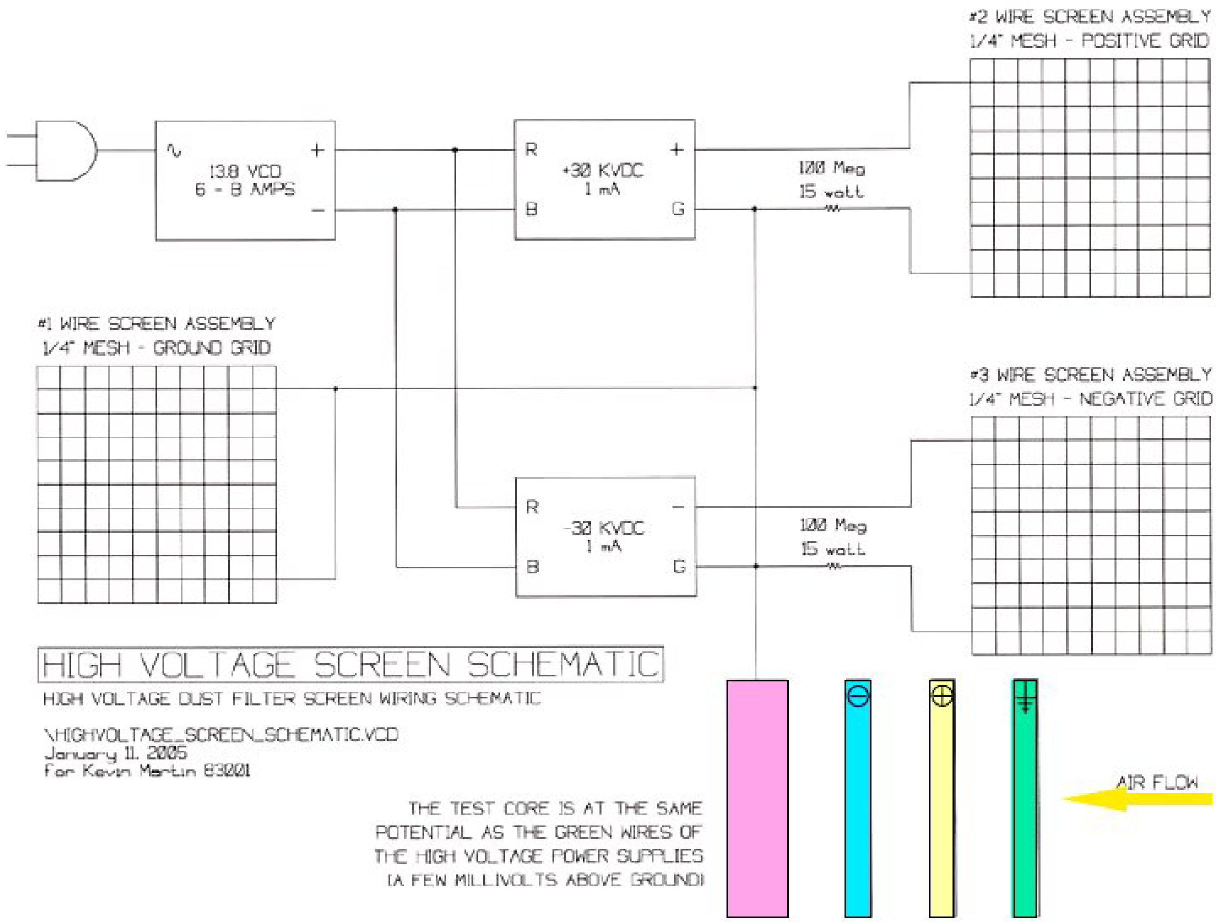

These three grids were suspended in front of the radiator where one was charged with +20,000 volts, one with –20,000 volts and one was grounded. The first order of the grids tried was ground, positive, negative, core. The second order tried was ground, negative, positive, core. It appeared that the high voltage had no effect on the dust accumulation. All three grids, no matter what order they were in, coated evenly with dust. Even when the voltage was increased to the point of arcing, there was no effect on dust accumulation. During the test there was a faint odor of ozone and a faint pink glow at a few nodes on the hardware cloth indicating that a corona had been struck.

One more frame was added. This time instead of using a wire mesh, parallel plates were used as shown in the photo below. This would provide a longer distance that particles would be exposed to the high voltage charges. Even with that, it could be that the density of the particles and the velocity created too much momentum that could not be altered with an electrical charge. A probe was made that could be charged with the power supplies, and this probe could make static particles on the inside surface of the test chamber move/jump, but this effect could not be demonstrated with moving particles.

Moving Media Bed

Two hoppers were installed side by side in front of the radiator core as shown in the drawings below. The front and back faces of these hoppers were made of perforated sheet metal so that the air could pass through them and then through the radiator. This hopper was filled with 8 mm od polypropylene balls that were recirculated from the bottom of the hopper to the top of the hopper by means of an air pump. At the top of the hopper, the balls passed underneath an air jet that cleaned off the polypropylene marble. This process was intended to create a continuously moving and continuously cleaned filter media.

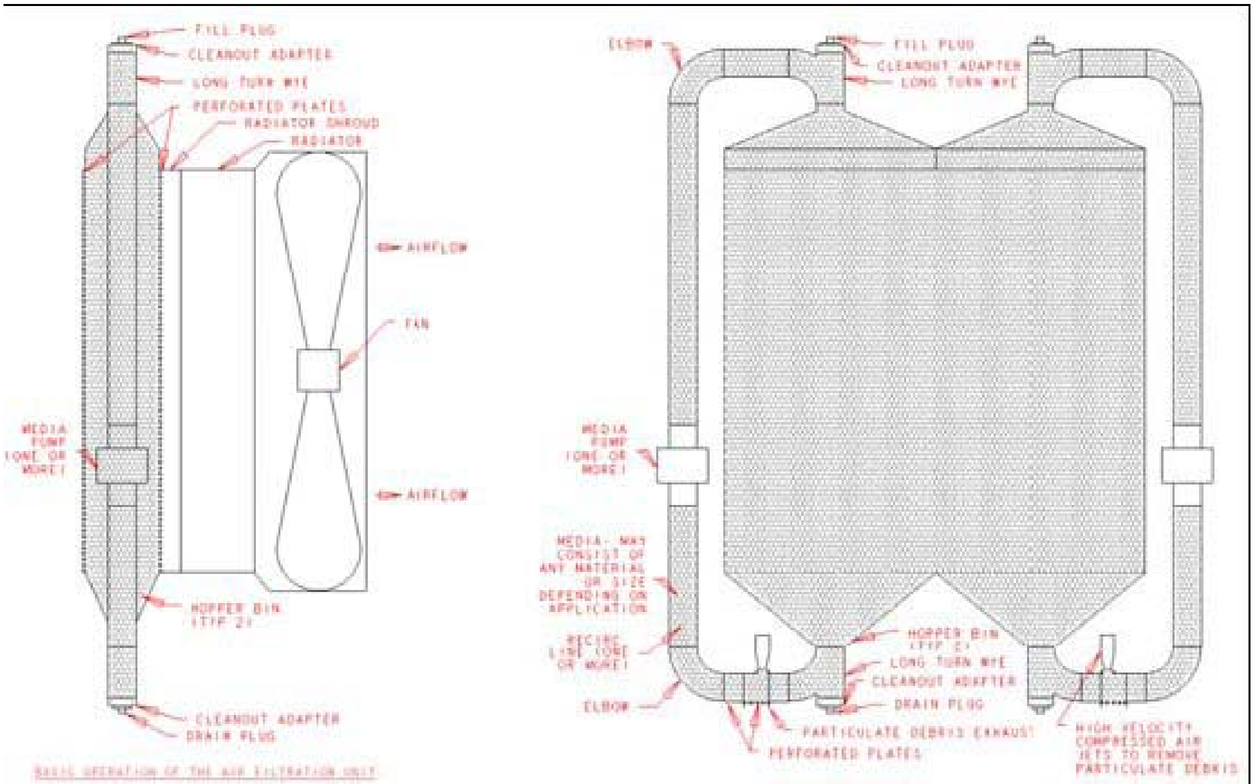

The photo below demonstrates a problem seen with high pressure drop filtration techniques. The hopper system was intended to be sealed against the front face of the radiator. In the case of this installation, the seal across the top of the cores didn't seal very well, which allowed the dust laden air to bypass around the filter system, and enter into the radiator. Any filtration device which adds to the restriction of the fan system will significantly impact the available airflow, and performance of the cooling system. Because of concerns about added pressure drop, not other devices like this were pursued.

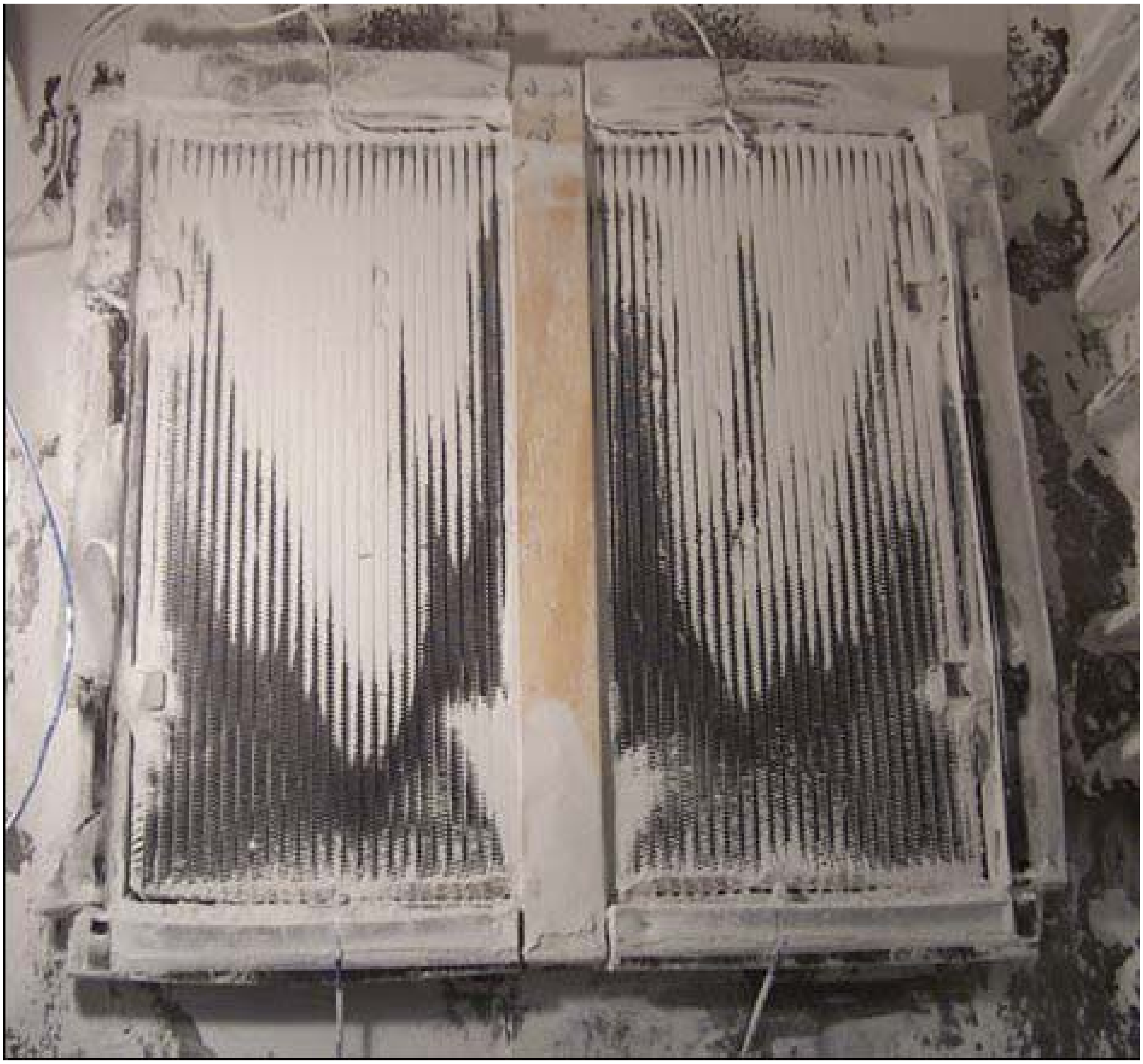

The following photo illustrates a phenomenon seen at several times during the testing. The fine debris is concentrated at the surface, and only a few millimeters into the core. The debris generally does NOT fill the entire depth of the core.

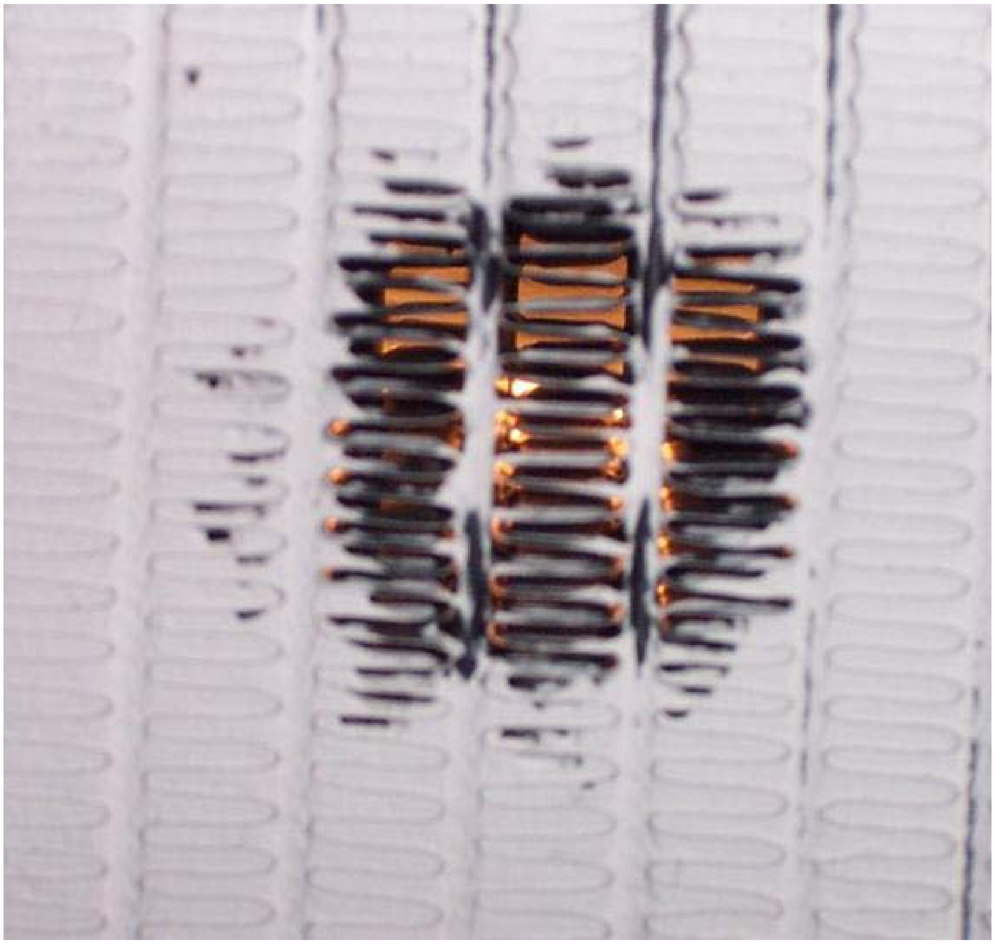

Moving Louvers

Since a number of air *filtration* related methods proved ineffective at reducing radiator debris accumulation, the attention turned to increasing the energy of the incoming air particles to help force them through the heat exchanger, instead of allowing them to accumulate on the entrance face. To increase the air velocity at the face of the core, a louvered wall was built with louvers that move back and forth as shown in the sketch below. The only external energy required for system operation was for an air cylinder to change the angle of the louvers.

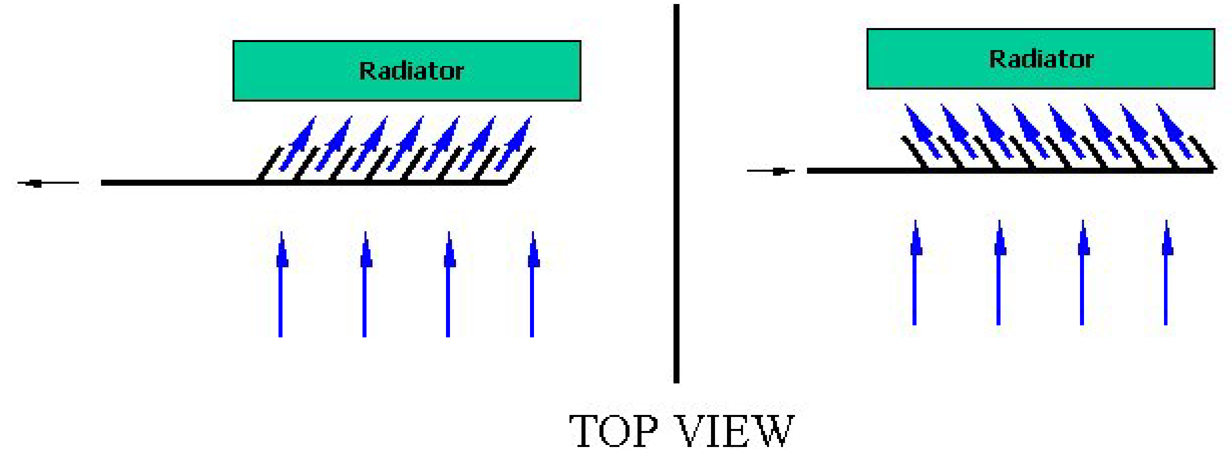

The performance measurand for this testing was the amount of time in the test chamber until the core pressure drop doubled. The photos below show the comparison in fouling between the moving louvers, vs the baseline unprotected core after 44 hours inside the dust chamber. The 44 hour point for the unprotected core is important, because at this time the core pressure drop had reached the point of 2x clean pressure drop. The louvered configuration ran 120 hours before it reached this same pressure drop, for a 3x increase in life to cleanout. This is the first technology to demonstrate a significant improvement in life to cleanout.

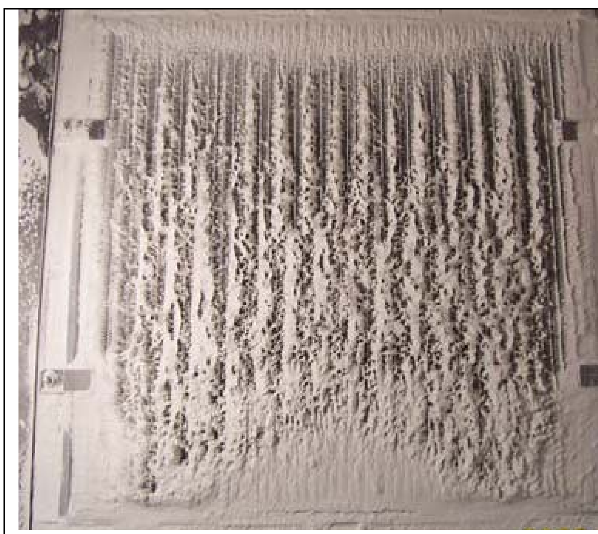	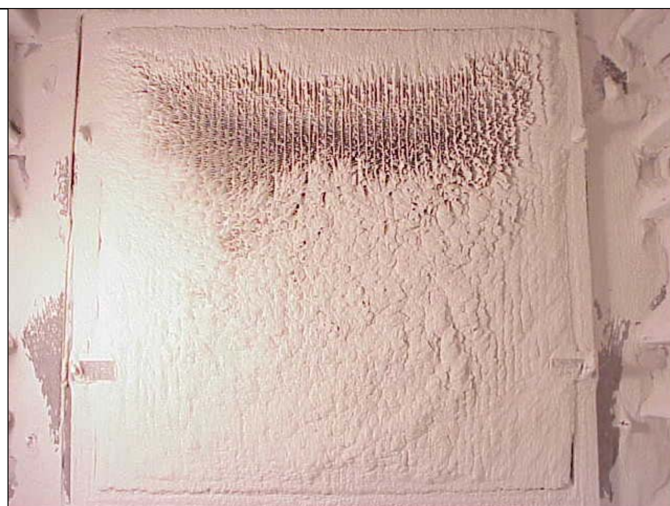
Moving louver fouling after 44 hours	Unprotected core after 44 hours

Free spinning fan

A recently patented concept[8] uses a free spinning fan located in front of the core. This is somewhat akin to the moving louver concept, and would not require any control system or external power. A commercial version of the free spinning fan was purchased and installed in the lab test facility for evaluation. The photo below shows the fan installation at the start of the test:

The photos below show a comparison of the core with free spinning fan vs. the baseline unprotected core after 44 hours in the dust test rig:

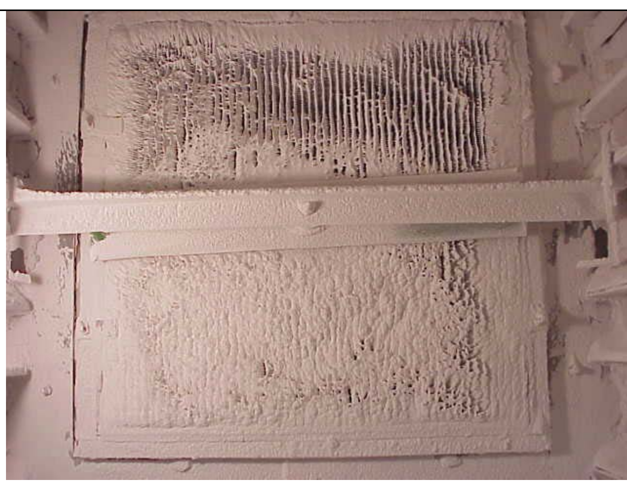	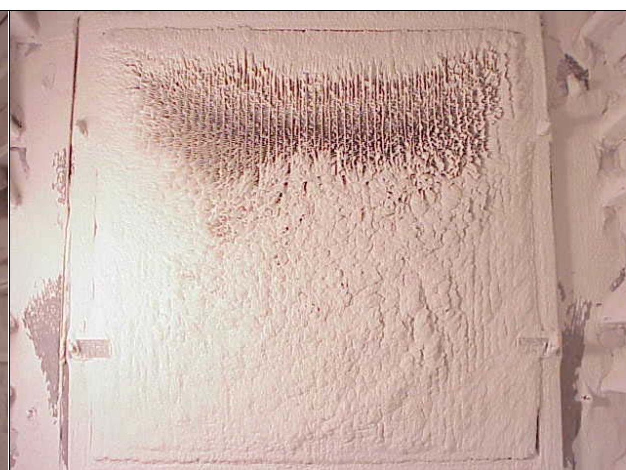
Free Spinning fan after 44 hours	**Unprotected core after 44 hours**

The photos illustrate that the free spinning fan provided virtually no improvement in clogging resistance. The free spinning fan performance is expected to be a function of the speed of the free spinning fan, which would be a function of the primary fan speed! To better evaluate the free spinning fan, the test was repeated at higher fan speeds, but the final results remained that the free spinning fan provided little improvement in clogging rate of the heat exchanger.

High Pressure Air

The moving louvers demonstrated the value of increasing incoming debris velocity as a way to reduce core fouling. The next step was to install an air knife setup to concentrate a high velocity blast to help force the debris through the core. An air knife was mounted to a linear motion track and positioned so that it would blow perpendicular to the face of the radiator core as shown in the drawing and photo below.

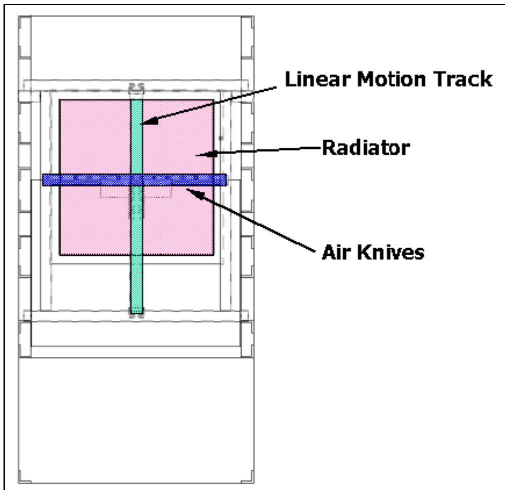

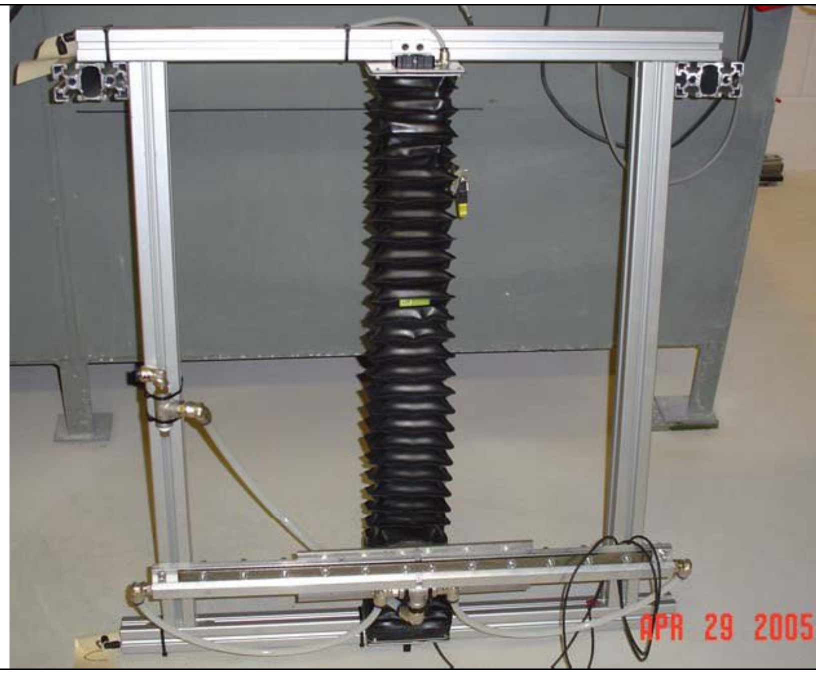

This air knife was timed so that every 15 seconds it would go to the top of the core and then blow while it traveled downward. Once at the bottom the air would be shut off and ready to cycle again. This would blow the debris that accumulated on the face through the radiator core. The air knife provided a 5x improvement in life to plugging in the test chamber as the photo below, taken after 220 hours shows. The buildup of dust in the center of the core represents the area blocked by the linear motion track, otherwise life to plugging may have been longer. This concept is deemed to be the most promising identified in this task. The use of an air knife with a linear motion track may not be feasible for off-road machines, but some form of high velocity air knife that can sweep the surface of the heat exchanger provides the best improvement in life to cleanout. To be effective for both inorganic and organic debris, some form of inlet screen with controlled porosity mounted upstream of the heat exchanger will be needed to form an effective debris filtration system.

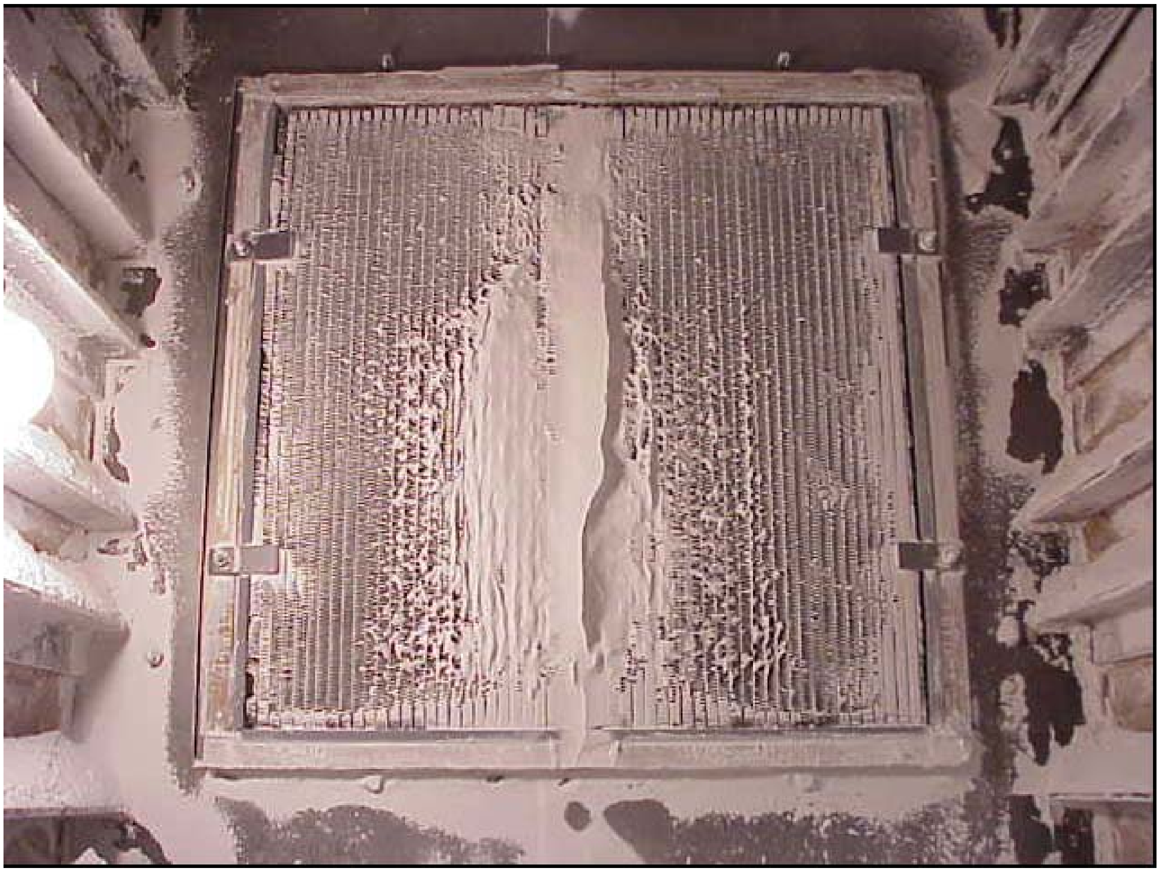

Conclusions

Task 1 - Develop an axial fan that will provide more airflow, with less input power and less noise

1. Genetic Algorithms are not an appropriate method to use for fan design at this time, based on the complexities of automating fan design and CFD analysis to allow the numerous potential designs to be analyzed in a reasonable amount of time.
2. Forward fan sweep as a potential sound reduction design methodology is more than offset by the loss in fan flow and pressure rise performance. Third generation fan design did not include the use of forward sweep.
3. For fans designed to provide identical airflow at the same speed, the number and spacing of blades has minimal effect on fan sound power levels, even with side by side cooling systems, but can have a significant effect on the noise spectrum, and the resulting sound quality.
4. The construction and testing of a prototype remains the best way of determining the noise level of a new fan design.

Task 2 – Develop for machine use, an 'aeroshroud' concept developed at Michigan State University

1. The aeroshroud concept, when used with a tight tip clearance fan shroud, can significantly affect the performance of an axial fan when in the stall region.
2. The aeroshroud concept, when used with a tight tip clearance fan shroud, cannot significantly affect the performance or efficiency of an axial fan when in the axial flow region.
3. The aeroshroud concept will provide a reduction in fan sound power level in the fan performance regions where the fan would have been in stall without the aeroshroud. In the axial flow region, the aeroshroud increases fan noise levels.

Task 3 – Improve the axial fan system modeling process accuracy to accommodate the numbers of cooling systems to be redesigned to meet lower emissions requirements

FIFO modeling

1. External dimensions of the multiple reference frame rotating fluid volume in the Fluent model is critical to accurate solutions.
2. The CFD model's pressure and flow simulation results under FIFO conditions generally correlated well with both Caterpillar and MSU measured data.
3. The CFD model's input torque results correlated favorably with Caterpillar and MSU measured data in the axial-flow regime of the fan performance curve. Simulated torques were higher than measured for flow rates below the stall point.
4. Overall efficiency as calculated from the CFD model's results compared favorably with those measured by MSU.
5. The current model does not produce flow or torque results that are within 3% of measured values when the pressure rise is at or above the fan's stall point.

System modeling

1. CFD generally underpredicted flow and pressure.
2. Model accuracy was most influenced by only a very few modeling factors.
3. The modeling guidelines for axial fans in installed conditions should improve solution accuracy and consistency between models.
4. Models created in accordance with the guidelines accurately predicted the MSU measured data for overall flowrate and pressure rise in the region of interest within the accuracy limits specified by CDC analysts.
5. Prediction accuracy can be improved somewhat by modeling the fan speed at 5% higher than the nominal value. This accounts for unmodeled losses in the system and incomplete modeling of the tip/shroud interface.
6. Not all factors that can affect a model's solution, including, specifically, fan projection and fan shroud design, were addressed by the design of experiments that was used.

Task 4 - Demonstrate the performance and design versatility of a high performance fan

Machine related test results

1. Fan Noise vs Fan Speed results, for the SBMF fan, was lower than the axial flow fans
2. Fan Noise vs Airflow results, for the SBMF Fan, was higher than the axial flow fans

Lab test results

1. The baseline Kysor fan performance is 5.9% greater than the SBMF in the basic FIFO configuration, assuming that both fans could both be built to the same diameter.
2. The diameter difference between the Kysor and SBMF fans (caused by the need for a seal assembly with the SBMF fan) increased the performance difference to 11.7%
3. With downstream wall spacing comparable to in-chassis fan-to-engine (and AC-compressor) spacing, SBMF performance degrades by ~16% while the baseline Kysor fan performance only degrades by ~3%.
4. Generally, a conventional axial fan allows for radial airflow in the presence of a nearby downstream obstruction while the tapered hub and rotating shroud of the SBMF prevent air from exiting the fan radially. The net result is that SBMF fan performance degrades much more than a typical axial fan in the presence of nearby downstream obstructions.
5. The combined effects of 1) a downstream wall in close proximity to the fan and 2) an enclosure with similar dimensions to the test machine resulted in SBMF fan performance somewhat comparable to that measured on the machine.
6. Kysor fan performance only suffers minimal additional degradation by adding the simulated enclosure. The measured level of performance in-chassis was slightly less than what was measured in the simulated configuration.

Task 5 - Develop a high efficiency variable speed fan drive to replace existing slipping clutch style fan drives.

1. The combination of fan speed vs. ambient temperature curves, plus fan system input power curves can be used along with ambient temperature data from the DOE Energy+ website to predict the fuel savings of any fan/fan drive combination for any machine at virtually any location in the world.
2. A DCVS fan drive was designed that could fit within the allowable envelope on a mobile machine.
3. The use of a single ratio variable speed slipping clutch fan drive would reduce machine fuel consumption by between 5% and 6% compared to a fixed ratio fan drive, and the DCVS drive would reduce fuel consumption by another approximately 1%.
4. Comparison between the fuel savings potential available relative to current fan designs, when compared to the fuel savings potential of variable speed fan drives, suggests that effort still needs to be spent on improving fan efficiency *even if the fan is to be driven by a temperature controlled variable speed fan drive.*
5. Further development of the DCVS was halted at a mid-program gate review because:
    a. Demonstrated fuel savings did not meet the requirements established for this task

b. Incremental fuel savings above a single ratio clutch were small, while the complexity of the DCVS was significantly greater than a commercially available single ratio clutch
c. The design and operation of the DCVS depended upon the availability of 2100kPa oil pressure for clutch operation. This would limit applicability of the DCVS to a limited range of mobile machines. To be applicable to all mobile machines, as well as stationary engine applications, the clutch must function over its entire operating range with a control pressure of approximately 400kPa

Task 6 – Develop a cooling system air filtration device to allow the use of automotive style high performance heat exchangers currently in off road machines

Baseline Measurement of Susceptibility to Inorganic Debris Clogging

1. Tube/fin geometry had a significant effect on heat exchanger susceptibility to inorganic debris clogging.
2. Airside face velocity also had a significant effect on heat exchanger susceptibility to inorganic debris clogging. Generally, segments of cores with higher face velocities were less susceptible to clogging than segments of cores with lower face velocities.

Radiator Filtration Developments

1. Eleven phenomena were identified and evaluated for their ability to reduce or eliminate debris accumulation on the face of heat exchangers. They were:
    a. Electrical grounding of cores to prevent static buildup
    b. Application of 24V DC to cores
    c. Application of 24V AC to cores
    d. High pressure air and ionization blown on cores
    e. Ultrasonic source in airstream
    f. (+)ions and (-)ions introduced in airstream
    g. Vibration applied to core
    h. High Voltage 20,000 V applied to core
    i. Moving media bed filter upstream of core
    j. Moving Louvers upstream of core
    k. High pressure air blown on core
2. Moving louvers (j) improved the time to plugging by a factor of 3
3. High pressure air (k) improved the time to plugging by over a factor of 5
4. The phenomena that produced the best results were those that created turbulence in
5. front of the radiator core.

References

[1] ORNL/TM-2004/92 'OFF-HIGHWAY TRANSPORTATION RELATED FUEL USE' April 2004 by Stacy C. Davis and Lorena F. Truett
[2] Morris, S.C., (1997), "Experimental Investigation of an Aerodynamic Shroud for Cooling

Fan Applications," M.S. thesis, Department of Mechanical Engineering, Michigan State University, East Lansing.
[3] Morris, S.C., Foss, J.F., (2001), "An Aerodynamic Shroud for Automotive Cooling Fans," ASME J. Fluids Eng., 123, 287-292.
[4] Morris, S.C., Good, J.J., Foss, J.F., (1998), "Velocity Measurements in the Wake of an Automotive Cooling Fan," Exp. Thermal and Fluid Sci., 17, 100-106.
[5] Air Movement and Control Association Publication 211-94 "Certified Ratings Program-Air Performance"
[6] Dawabata and Saitoh, (1986), "Application of a Mixed Flow Fan for Quiet Heavy-Duty Vehicles", SAE Technical Paper 861945
[7] Glassey, S.F. (1978), "Cooling the Woods Tractor", SAE Technical Paper 780454
[8] US patent number 6,817,414 "Cooling Package for Agricultural Combine", assignee Deere & Company, Moline, Il.
[9] Masters Thesis, Dusel, Michael D "An Experimental Investigation of the Aerodynamic Shroud with an Off-Highway Engine Cooling Fan" Michiagan State university, 2005

<u>List of Acronyms and Abbreviations</u>

ATAAC – Air to Air Aftercooling
CFD – Computational Fluid Dynamics
CVT – Continuously Variable speed Transmission
Fan Specific Diameter - Ds = D * (P/q)0.25/√Q where Q is flow in m3/sec, Kp is compressibility coefficient and assumed to be 1, q is density in kg/m3 (1.2 kg/m3), P is total pressure in Pa, and D is fan diameter in meters
DCVS fan drive – Dual Clutch Variable Speed fan drive
DofE – Design of Experiments
FIFO – Free Inlet Free Outlet fan performance test. A fan performance test where the fan is mounted in a shroud in a fan test facility and evaluated for performance with no heat exchangers or other obstructions either upstream of downstream of the fan.
GA – Genetic Algorithm
MSU – Michigan State University
PW – Projected width of an axial fan
SBMF – Swept Blade Mixed Flow Fan
Specific Noise = $ks = Lw_{(a)} - 20\log(P) - 10\log(Q)$ where Lw is the measured sound power in dB(a), P is the pressure rise, and Q is the volumetric flow rate through the fan.
Task 1 - Develop an axial fan shroud that will provide more airflow, with less input power and less noise
Task 2 – Develop for machine use, an 'aeroshroud' concept developed at Michigan State University
Task 3 – Improve the axial fan system modeling process accuracy to accommodate the numbers of cooling systems to be redesigned to meet lower emissions requirements
Task 4 - Demonstrate the performance and design versatility of a high performance fan
Task 5 - Develop a high efficiency variable speed fan drive to replace existing slipping clutch style fan drives

Task 6 – Develop a cooling system air filtration device to allow the use of automotive style high performance heat exchangers currently in off road machines.